

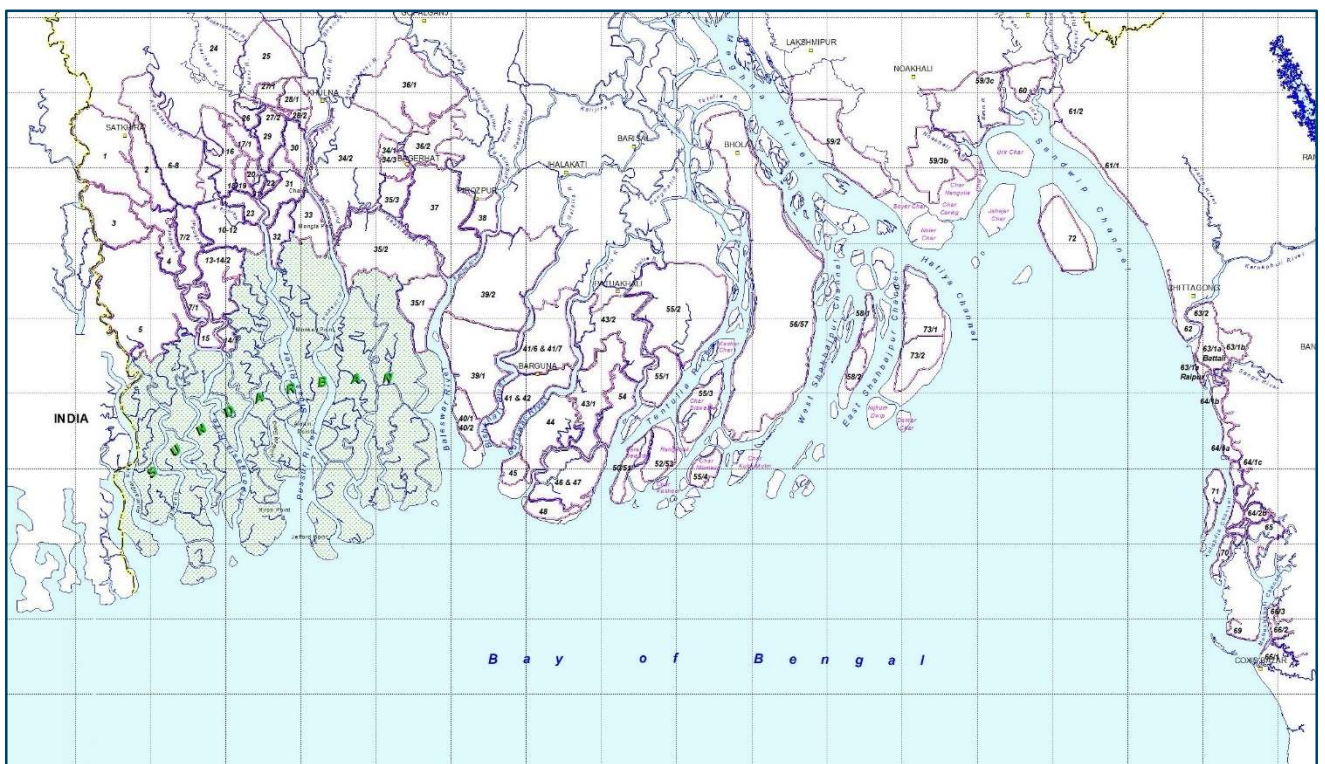
Ministry of Water Resources



Bangladesh Water Development Board

Coastal Embankment Improvement Project, Phase-I (CEIP-I)

Long Term Monitoring, Research and Analysis of Bangladesh Coastal Zone (Sustainable Polders Adapted to Coastal Dynamics)



Micro-Scale Modelling Modelling of TRM Operation at East Beel Khuksia and future conditions

April 2022







Ministry of Water Resources



Bangladesh Water Development Board

Coastal Embankment Improvement Project, Phase-I (CEIP-I)

Long Term Monitoring, Research and Analysis of Bangladesh Coastal Zone (Sustainable Polders Adapted to Coastal Dynamics)

**Micro-Scale Modelling
Modelling of TRM Operation at East Beel Khuksia and
future conditions**

April 2022





Contents

1	INTRODUCTION	1
1.1	Background	1
1.2	Objectives of TRM Modelling	4
2	East Beel Khuksia TRM Operation and Data Available	7
2.1	Pre TRM Situation	7
2.2	TRM Operation	8
2.3	Data Available	9
3	Model Development (MIKE 11) historical/present conditions.....	11
3.1	Introduction.....	11
3.2	Model Adjustments.....	12
3.3	Model Calibration	13
3.4	Erosion and Deposition Before and During TRM Operation	20
4	Model Development (MIKE 21) historical/present conditions.....	24
4.1	Introduction.....	24
4.2	Construction of Model Mesh and Bathymetry	24
4.3	Hydrodynamic Boundary Conditions.....	28
4.4	Measurements, Model Parameters and Calibration.....	28
4.5	Model Results.....	33
4.5.1	The Hari River without TRM.....	34
4.5.2	TRM with an Opening in the Southern End of the Beel	41
4.5.3	TRM with an Opening in the Eastern Side of the Beel	53
5	Model Development (MIKE 21) future conditions	66
5.1	Introduction.....	66
5.2	Future conditions.....	66
5.2.1	Subsidence rates	66
5.2.2	Sea level rise.....	67
5.3	Hari River bathymetry present and future	69
5.4	Model results and scenarios for Hari River year 2050 and 2100.....	71
5.4.1	Hari River discharges	71
5.4.2	Hari River mean gross discharges	76
5.4.3	Hari River net sediment transport	79
5.4.4	Siltation of the Hari River	84
5.4.5	Drainage congestion and water logging.....	89
6	Conclusions, discussions, and recommendations	99
6.1	Conclusions and discussions	99
6.2	Recommendations	101
7	References	103

FIGURES

Figure 1-1	Average Tidal Range and tidal Limit in the South-West Region of Bangladesh.....	2
Figure 1-2	Coastal Polders of Bangladesh.....	3
Figure 1-3	Example of non-uniform deposition in a polder subjected to TRM	5
Figure 1-4	Rivers, polders and beels in the study area. Note the location of East Beel Khuksia and Beel Kedaria	6
Figure 2-1	Siltation of Hari River after TRM operation of Beel Kedaria was discontinued.....	7
Figure 2-2	East Beel Khuksia with the link canal of TRM at Katakhalı Regulator	8
Figure 2-3	Development of a cross-section in the Hari River. From February 2007 to May 2007 both dredging and erosion take place, while after May 2007 only erosion	9
Figure 2-4	Observed cross-sections in Hari River at Chainage 12412 (location of Chechuri shown on Figure 1.4)	10
Figure 4-1	Left: The original 14 measured cross sections. Right: Cross section information obtained using streamwise interpolation resulting in a total of 59 cross sections	24
Figure 4-2	Left: Interpolated bathymetry based on the 14 measured cross sections. Right: Interpolated bathymetry based on the 59 created cross sections.	25
Figure 4-3	Map showing an example of the established bathymetric basis inside the polder and the peripheral river.	25
Figure 4-4	Bathymetry of the Hari River model.	26
Figure 4-5	Bathymetry of the Hari River and East Beel Khuksia model.....	27
Figure 4-6	Water level time series applied for the downstream boundary condition.	28
Figure 4-7	Discharge time series applied for the upstream boundary condition.	28
Figure 4-8	Water level gauging stations.	29
Figure 4-9	Observed water levels at the six gauging stations in August 2011.....	29
Figure 4-10	Observed water levels at the six gauging stations in December 2011.	30
Figure 4-11	Discharge and water level observations at Ranai 9 th September 2011.....	30
Figure 4-12	Discharge and water level observations at Ranai 14 th September 2011.	30
Figure 4-13	Grain size distribution of bed sediment in the central part of the channel at Bhadra.	31
Figure 4-14	Grain size distribution of bed sediment at the right bank at Bhadra.	31
Figure 4-15	Observed suspended sediment concentrations at Ranai.	32
Figure 4-16	Observed suspended sediment concentrations at Beel Khuksia.....	32
Figure 4-17	Location of cross sections used to analyse the development in tidal discharge and sediment transport.	34
Figure 4-18	Modelled tidal generated flow discharge at Ranai for Year 1-3 (top) and Year 4-6 (bottom) without TRM. Discharge is defined positive for upstream directed flow.	35
Figure 4-19	Modelled tidal generated flow discharge at Katakhalı for Year 1-3 (top) and Year 4-6 (bottom) without TRM. Discharge is defined positive for upstream directed flow.	35
Figure 4-20	Modelled tidal generated flow discharge at Kanaishisa for Year 1-3 (top) and Year 4-6 (bottom) without TRM. Discharge is defined positive for upstream directed flow.	36
Figure 4-21	Bed level development of Hari River without TRM in the consecutive period of 6 years.	37
Figure 4-22	Bed level changes without TRM over a period of 6 years.	38
Figure 4-23	Annual bed level changes without TRM over a period of 6 years.....	39
Figure 4-24	Net sediment transport (upstream directed) at Ranai for each of the 6 consecutive years.....	40
Figure 4-25	Net sediment transport (upstream directed) at Katakhalı for each of the 6 consecutive years.	40
Figure 4-26	Net sediment transport (upstream directed) at Kanaishisa for each of the 6 consecutive years.....	40
Figure 4-27	Area inside Hari River branch below a certain bed level without TRM over a period of 6 years.....	41
Figure 4-28	Modelled tidal generated flow discharge at Ranai for Year 1-3 (top) and Year 4-6 (bottom) with TRM and opening at the southern end. Discharge is defined positive for upstream directed flow.	42
Figure 4-29	Modelled tidal generated flow discharge at Katakhalı for Year 1-3 (top) and Year 4-6 (bottom) with TRM and opening at the southern end. Discharge is defined positive for upstream directed flow.	43
Figure 4-30	Modelled tidal generated flow discharge at Kanaishisa for Year 1-3 (top) and Year 4-6 (bottom) with TRM and opening at the southern end. Discharge is defined positive for upstream directed flow.	43

Figure 4-31	Modelled tidal generated flow discharge at Polder S for Year 1-3 (top) and Year 4-6 (bottom) with TRM and opening at the southern end. Discharge is defined positive for inflow to polder.	44
Figure 4-32	Minimum water level after activation of TRM at the southern end of the polder in the consecutive period of 6 years.	45
Figure 4-33	Maximum water level after activation of TRM at the southern end of the polder in the consecutive period of 6 years.	46
Figure 4-34	Tidal envelope after activation of TRM at the southern end of the polder in the consecutive period of 6 years.	47
Figure 4-35	Tidal variation in Hari River near the polder opening after activation of TRM.	47
Figure 4-36	Bed level development after activation of TRM at the southern end of the polder in the consecutive period of 6 years.	48
Figure 4-37	Bed level changes after activation of TRM at the southern end of the polder in the consecutive period of 6 years.	49
Figure 4-38	Annual bed level changes after activation of TRM at the southern end of the polder in the consecutive 6 years.	50
Figure 4-39	Net sediment transport at Ranai for each of the 6 consecutive years.	51
Figure 4-40	Net sediment transport at Katakhalı for each of the 6 consecutive years.	51
Figure 4-41	Net sediment transport at Kanaishisa for each of the 6 consecutive years.	51
Figure 4-42	Net sediment transport at Polder S for each of the 6 consecutive years.	52
Figure 4-43	Area inside polder above a certain bed level during TRM operation.	53
Figure 4-44	Area inside Hari River branch (downstream polder opening) below a certain bed level during TRM operation.	53
Figure 4-45	Modelled tidal generated flow discharge at Ranai for Year 1-3 (top) and Year 4-6 (bottom) with TRM and opening at the southern end. Discharge is defined positive for inflow to polder.	54
Figure 4-46	Modelled tidal generated flow discharge at Katakhalı for Year 1-3 (top) and Year 4-6 (bottom) with TRM and opening at the southern end. Discharge is defined positive for inflow to polder.	54
Figure 4-47	Modelled tidal generated flow discharge at Kanaishisa for Year 1-3 (top) and Year 4-6 (bottom) with TRM and opening at the southern end. Discharge is defined positive for inflow to polder.	55
Figure 4-48	Modelled tidal generated flow discharge at Polder E for Year 1-3 (top) and Year 4-6 (bottom) with TRM and opening at the southern end. Discharge is defined positive for inflow to polder.	55
Figure 4-49	Minimum water level after activation of TRM at the eastern side of the polder in the consecutive period of 6 years.	57
Figure 4-50	Maximum water level after activation of TRM at the eastern side of the polder in the consecutive period of 6 years.	58
Figure 4-51	Tidal envelope after activation of TRM at the eastern side of the polder in the consecutive period of 6 years.	59
Figure 4-52	Tidal variation in Hari River near the polder opening after activation of TRM.	59
Figure 4-53	Bed level development after activation of TRM at the eastern side of the polder in the consecutive period of 6 years.	60
Figure 4-54	Bed level changes after activation of TRM at the eastern side of the polder in the consecutive period of 6 years.	61
Figure 4-55	Annual bed level changes after activation of TRM at the eastern end of the polder in the consecutive 6 years.	62
Figure 4-56	Net sediment transport at Ranai for each of the 6 consecutive years.	63
Figure 4-57	Net sediment transport at Katakhalı for each of the 6 consecutive years.	63
Figure 4-58	Net sediment transport at Kanaishisa for each of the 6 consecutive years.	64
Figure 4-59	Net sediment transport at Polder E for each of the 6 consecutive years.	64
Figure 4-60	Area inside polder above a certain bed level during TRM operation.	65
Figure 4-61	Area inside Hari River branch (downstream polder opening) below a certain bed level during TRM operation.	65
Figure 5-1	Subsidence rates at Polder 24.	67
Figure 5-2	Sea level rise graph of the 95 th percentile related to the RCP8.5 scenario. (Source: Climate Change Scenarios, 2021).	68
Figure 5-3	Hari River model bathymetry for present conditions (2019), and future conditions (2050 and 2100).	70
Figure 5-4	Discharge time series applied for the upstream boundary condition.	71

Figure 5-5	Development of tidal generated discharges at Ranai.	72
Figure 5-6	Development of tidal generated discharges at Katakhal.	73
Figure 5-7	Development of tidal generated discharges at Kanaishisa.	74
Figure 5-8	Tidal generated discharges in 2019, 2050 and 2100 at Ranai. Top: First morphological cycle. Bottom: Sixth morphological cycle.	75
Figure 5-9	Tidal generated discharges in 2019, 2050 and 2100 at Katakhal. Top: First morphological cycle. Bottom: Sixth morphological cycle.	75
Figure 5-10	Tidal generated discharges in 2019, 2050 and 2100 at Kanaishisa Top: First morphological cycle. Bottom: Sixth morphological cycle.	76
Figure 5-11	The impact of siltation on the mean gross discharge at Ranai.	78
Figure 5-12	The impact of siltation on the mean gross discharge at Katakhal.	78
Figure 5-13	The impact of siltation on the mean gross discharge at Kanaishisa.	79
Figure 5-14	Net sediment transport (upstream directed) at Ranai for each of the 6 (9) consecutive years.	80
Figure 5-15	Net sediment transport (upstream directed) at Katakhal for each of the 6 (9) consecutive years.	81
Figure 5-16	Net sediment transport (upstream directed) at Kanaishisa for each of the 6 (9) consecutive years.	82
Figure 5-17	Area inside Hari River branch below a certain bed level without TRM operation over a period of 6 years for present conditions (2019).	84
Figure 5-18	Area inside Hari River branch below a certain bed level without TRM operation over a period of 6 years for future conditions (2050).	84
Figure 5-19	Area inside Hari River branch below a certain bed level without TRM operation over a period of 6 years for future conditions (2100).	85
Figure 5-20	Area inside Hari River branch below a certain bed level without TRM operation over a period of 6 years for future conditions in 2100 with 50% increase of runoff.	85
Figure 5-21	Area inside Hari River branch below a certain bed level without TRM operation over a period of 6 years for future conditions in 2100 with 100% increase of runoff.	86
Figure 5-22	Future bed level development of Hari River.	87
Figure 5-23	Future bed level development of Hari River. Predicted bed level changes after 6 years.	88
Figure 5-24	2019, 2050 and 2100 polder bathymetry.	89
Figure 5-25	Water level extraction points used for calculation of drainage potential.	90
Figure 5-26	Tidal variation in Hari River 2050 at extraction point mid and south.	91
Figure 5-27	Tidal variation in Hari River 2100 at extraction point mid and south.	92
Figure 5-28	Polder water logging volume – annual average.	95
Figure 5-29	Potential polder drainage volume - annual average.	96
Figure 5-30	Potential polder storage volume – annual average.	96
Figure 5-31	Polder drainage potential – annual average.	97
Figure 5-32	Polder water logging volume – monsoon average (August)	97
Figure 5-33	Potential polder drainage volume – monsoon average (August)	97
Figure 5-34	Potential polder storage volume – monsoon average (August)	98
Figure 5-35	Polder drainage potential – monsoon average (August).	98

TABLES

Table 3-1	Sediment parameters applied for the MIKE 11 model.	14
Table 4-1	Applied MIKE 21 model parameters.	33
Table 4-2	Development of annual time-averaged gross discharge at Ranai, Katakhal, and Kanaishisa without TRM.	36
Table 4-3	Net sediment transport per cyclic period at Ranai, Katakhal, and Kanaishisa.	41
Table 4-4	Development of annual time-averaged gross discharge at Ranai, Katakhal, and Kanaishisa with TRM and opening at the southern end.	44
Table 4-5	Net sediment transport per cyclic period at Ranai, Katakhal, Kanaishisa, and Polder S.	52
Table 4-6	Development of annual time-averaged gross discharge at Ranai, Katakhal, and Kanaishisa with TRM and opening at the eastern side.	56
Table 4-7	Net sediment transport per cyclic period at Ranai, Katakhal, Kanaishisa, and Polder E.	64
Table 5-1	Impact of subsidence on the present bed levels of Hari River in 2050 and 2100.	66

Table 5-2	RCP-scenarios and their meaning.	68
Table 5-3	Sea level rise estimates for the Bay of Bengal.	69
Table 5-4	Mean water level increase at Ranai (Hari River) relative to 2019.....	69
Table 5-5	Development of annual time-averaged gross discharge at Ranai, Katakhal, and Kanaishisa with year 2050 conditions.....	76
Table 5-6	Development of annual time-averaged gross discharge at Ranai, Katakhal, and Kanaishisa with year 2100 conditions.....	77
Table 5-7	Development of annual time-averaged gross discharge at Ranai, Katakhal, and Kanaishisa with year 2100 conditions and 50% increase of upstream discharges.	77
Table 5-8	Development of annual time-averaged gross discharge at Ranai, Katakhal, and Kanaishisa with year 2100 conditions and 100% increase of upstream discharges.	77
Table 5-9	Net sediment transport in kilotons per cyclic period at Ranai.	83
Table 5-10	Net sediment transport in kilotons per cyclic period at Katakhal.....	83
Table 5-11	Net sediment transport in kilotons per cyclic period at Kanaishisa.	83
Table 5-12	Statistical parameters for the annual tide at extraction point south.	92
Table 5-13	Statistical parameters for the annual tide at extraction point mid.	93
Table 5-14	Statistical parameters for the monsoon tide (August) at extraction point south.	93
Table 5-15	Statistical parameters for the monsoon tide (August) at extraction point mid.	93
Table 5-16	Annual mean and drainage water level of the polder	94
Table 5-17	Monsoon mean and drainage level of the polder.....	95

ACRONYMS AND ABBREVIATIONS

BoB	Bay of Bengal
BWDB	Bangladesh Water Development Board
CEIP-	Coastal Embankment Improvement Project
DEM-	Digital Elevation Model
FM-	Flexible Mesh
GBM	Ganges, Brahmaputra and Meghna
HD-	Hydrodynamic
IWM-	Institute of Water Modelling
KJDRP	Khulna-Jessore Drainage Rehabilitation Project
PDV	Polder Drainage Volume
PSV	Polder Storage Volume
SLR-	Sea Level Rise
SSC-	Suspended Sediment Concentration
SWRM-	Southwest Region Model
TRM	Tidal River Management
WL	Water Level
WLV	Water logging Volume

1 INTRODUCTION

1.1 Background

Bangladesh is situated at the confluence of three great trans-Himalayan rivers the Ganges, the Brahmaputra or Jamuna, and the Meghna which forms the Bengal (or GBM) Delta. While over 90 percent of the catchment of the GBM system lies outside of Bangladesh, more than 200 rivers and tributaries and distributaries of the GBM system drain through the country via a constantly changing network of channels, tidal inlets and creeks, forming the most active large deltas on the planet. The coastal land mass is formed by the interaction of large volumes of sediment laden water with the moderate to high tides of the Bay of Bengal. Figure 1-1 shows the tidal limits in the Bengal Delta.

Land in the coastal zone is built up by the deposition of river sediments among the mangroves in one of the largest mangrove forests in the world. The deposits of sand, silt, clay and peat form the land mass, which despite subsidence due to continuous consolidation of layers many kilometres deep, is kept just below the level of the highest tides by the continuing deposition of sediments that are trapped among the mangroves.

The coastal zone of Bangladesh spans over 710 km of coastline and is subject to multiple threats. 62 % of the coastal land has an elevation less than 3 meters above mean sea level. With a sediment supply of the order of 1 billion tons per year, this is the delta with the largest sediment supply in the world. This leads to accretion of the land area in the coastal zone (5-10 km²/year, mainly in the Meghna Estuary). It has been observed that the land subsidence rate may vary from place to place due to anthropogenic factors such as drainage and ground water extraction as well as the properties and depth of underlying strata. On top of this there are tectonic plate movements in the deepest strata that give rise to other changes in ground level.

The coastal lands, being subject to regular flooding by saline water during high tides, could not be used for normal agricultural production in a country with a very high demand for land. The Coastal Embankment Project (CEP) was initiated in the 1950s and 1960s to build polders surrounded by embankments preventing the spilling of saline water onto the land at high tides. These embankments were built along the larger rivers and across the smaller rivers and creeks, which then formed the drainage system within each polder and connected to the peripheral rivers via appropriately sized flap gate regulators, that open at low tide to let the drainage water out.

The Coastal Embankment Project made possible the reclamation of large tracts of land for agriculture from 1960 onwards. Polder building proceeded continuously until today. We now have 1.2 million hectares reclaimed in 139 active polders in the coastal zone of Bangladesh, see Figure 1-2.

In over half a century of its existence, number of challenges have surfaced that threaten the long-term safety and even the very existence of the polder system as a viable and sustainable resource. These are:

- Sea level rise and changes in precipitation and water discharge due to climate change
- Threats of damming and diversion to the delivery of river sediments from upstream
- Subsidence of lands (except where it has been allowed to be rebuilt by tidal flooding) and structures founded on existing land
- Drainage congestion due to accumulation of silt in some peripheral waterways around the polders

- Changes in tidal hydrodynamics and related river erosion and siltation in the peripheral rivers of polders
- Increasing vulnerability to cyclones and storm surges

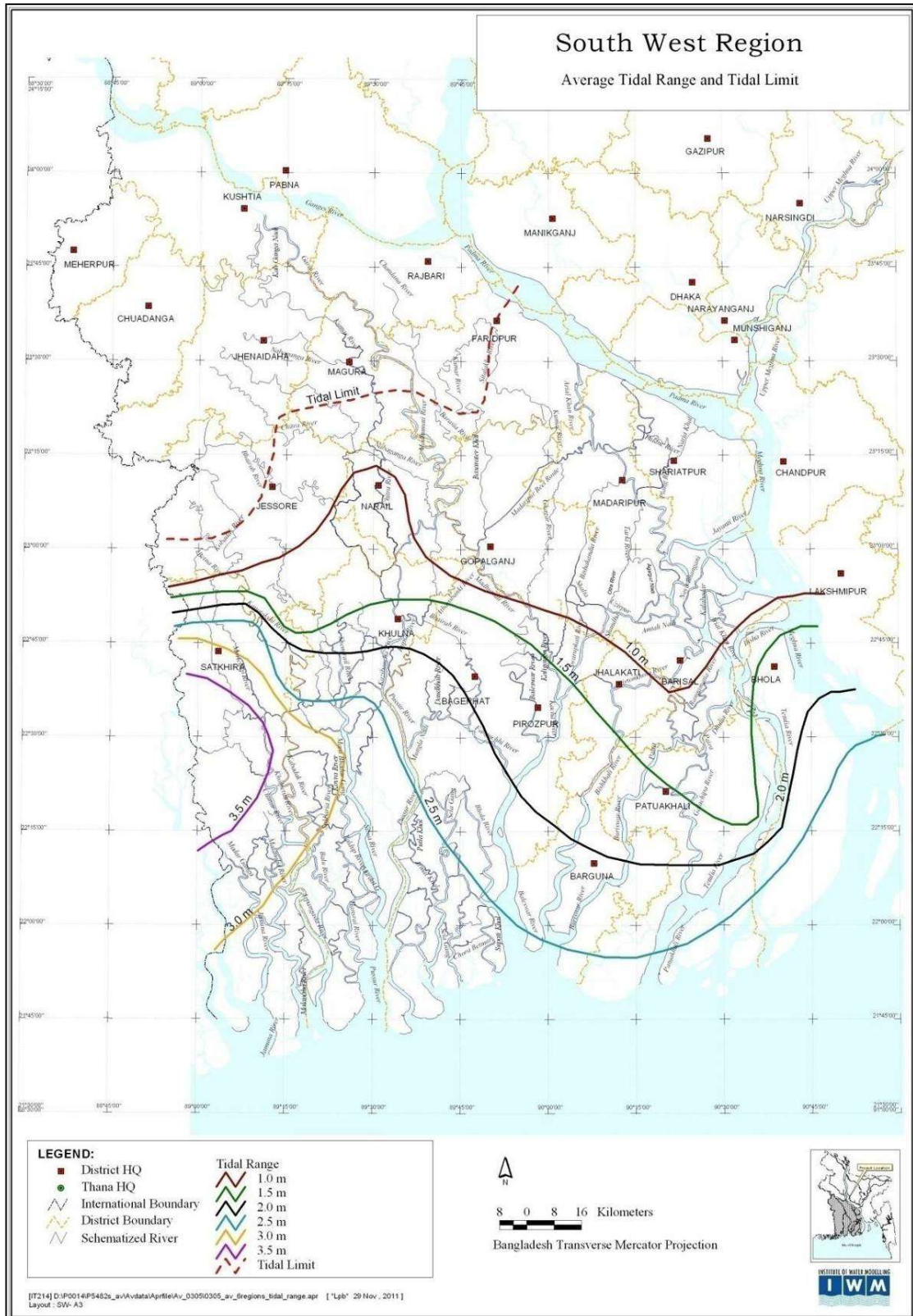


Figure 1-1 Average Tidal Range and tidal Limit in the South-West Region of Bangladesh

The disasters resulting from two major cyclones Sidr (2007) and Aila (2009) and the unexpectedly high value of the damages caused by these, provoked the World Bank and the Government of Bangladesh to initiate the Coastal Embankment Improvement Programme (CEIP-1), which was to redesign and rebuild the entire polder system, in several phases, to resist the long-term challenges of climate change and other natural phenomena such as:

- Storm Surges, wind, and wave attack
- Sea level rise
- Land subsidence
- Changing tidal hydrodynamics and channel network system
- Long term challenges to drainage
- Increasing threats from cyclones and storm surges
- Maintenance and management failures

The objectives of CEIP-1 were:

- *Increase the area protected in selected polders from tidal flooding and frequent storm surges, which are expected to worsen due to climate change and relative sea-level rise*
- *Improve agricultural production by reducing saline water intrusion in selected polders; and*
- *Improve the Government of Bangladesh's capacity to respond promptly and effectively to an eligible crisis or emergency*

The implementation of the first 17 polders of CEIP-1 (see Figure 1-2) brought into stark relief several shortcomings and gaps in our knowledge and understanding of many of the physical phenomena that govern major processes in and the evolution of the Bengal Delta. Recognition of these lacunae resulted in the inclusion of this research study as a component project to support the phased Coastal Embankment Improvement Programme, which was to bring in massive investments over many decades.

1.2 Objectives of TRM Modelling

Tidal River Management (TRM) involves breaching the embankments surrounding the polders allowing tidal flooding of the polders and the associated sediment deposition within the polders as well as erosion of the peripheral rivers due to the increased tidal volume. TRM has for many years been considered a viable way to maintain the drainage capacity of the peripheral rivers and for compensating the impact of subsidence by increasing land level inside the polders through deposition of silt. The key problem with TRM is that the areas inside the polders, which are subjected to tidal flooding cannot be used for the intended purpose of the polders (viz. agriculture), while TRM is ongoing hence the population of the polders must be paid compensation, and likewise alternative livelihood created. An issue with TRM operation is that deposition inside the polders is highly non-uniform (see example in Figure 1-3), hence not the entire area inside the polders may benefit from deposition.

There is thus much to win if TRM operation can be optimised, i.e. accelerate erosion in the peripheral rivers, accelerated deposition within the polders and by ensuring a more uniform deposition pattern. The objective of TRM modelling is to establish a modelling approach that can be used to test alternative TRM operations and identify the most effective operations. The purpose of the modelling presented in this first interim report is to explore what will be required in terms of modelling to optimise TRM operation and is based on the application of a state-of-the-art 2D modelling approach.

The TRM operation implemented for East Beel Khuksia will be used as pilot case because ample data are available from the TRM operation of this beel inside Polder 24. The beel and river system of the area is shown in Figure 1-4. In Section 2 of this Report the key data of the TRM operation as well as the available data are described. The key source of data and information used is the reports:

- Monitoring the performance of Beel Kedaria TRM and baseline study for Beel Khuksia. Khulna Jessore Drainage Rehabilitation Project. Final Report. IWM (March 2006), Ref. /1/.
- Monitoring the Effect of East Beel Khuksia TRM Basin and Dredging of Hari River for Drainage Improvement of Bhabodah Area. Khulna Jessore Drainage Rehabilitation Project. Final Report. IWM (July 2007), Ref. /2/.
- Power Point presentation made by Zahirul Haque Khan, Head of Coast, Port and Estuary, IWM at the Dhaka Water Knowledge Days, October 2019.

The first four sections of this report are identical to the report “Micro-Scale Modelling: Interim Report: Modelling of TRM Operation 2D”. Section 5: “Model development future conditions” and Section 6: “Conclusions, discussions and recommendations” are new.

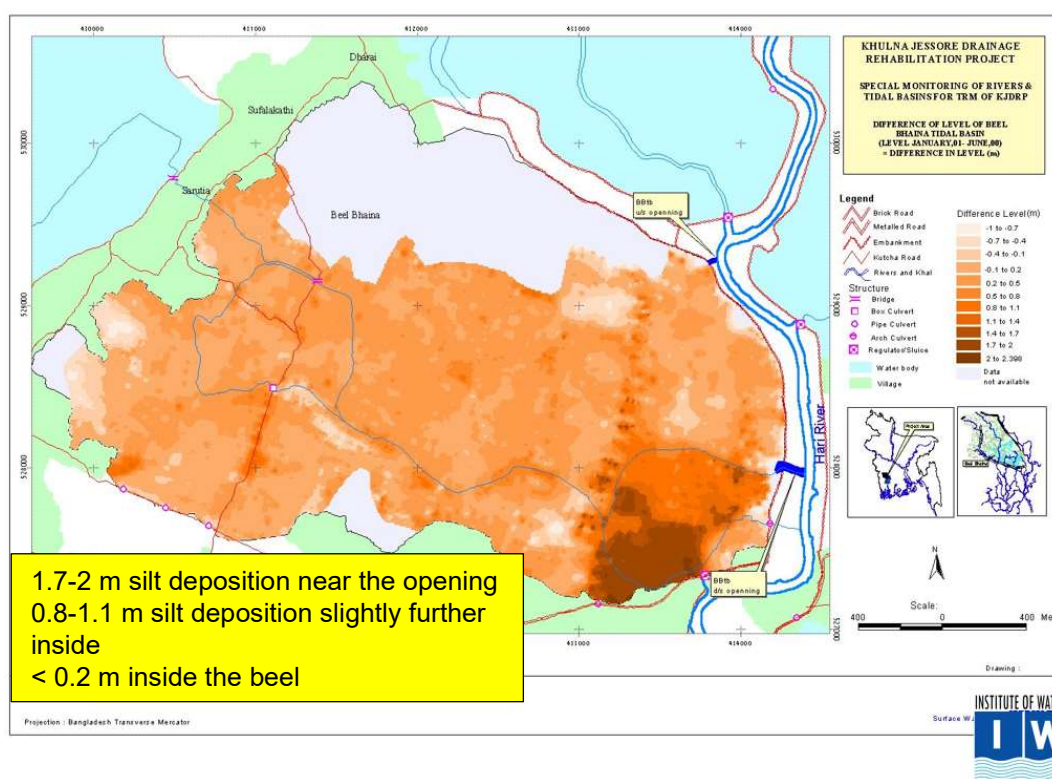


Figure 1-3 Example of non-uniform deposition in a polder subjected to TRM

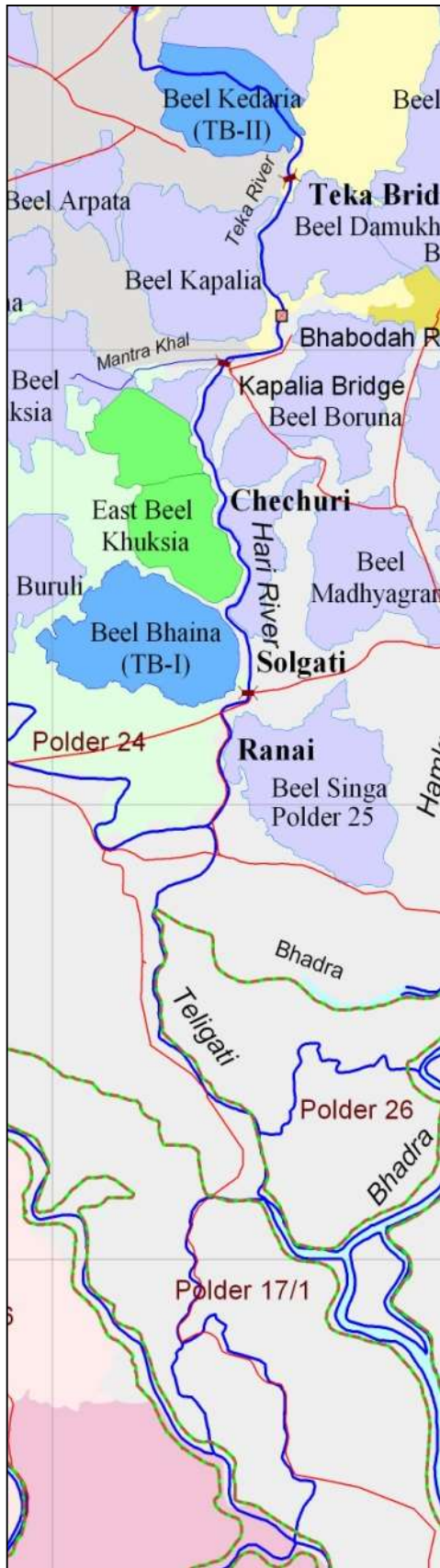


Figure 1-4 Rivers, polders and beels in the study area. Note the location of East Beel Khuksia and Beel Kedaria

2 East Beel Khuksia TRM Operation and Data Available

2.1 Pre TRM Situation

Tidal River Management had been adopted since 1998 in the north-west part of the Khulna-Jessore Drainage Rehabilitation Project (KJDRP) to solve drainage congestion. Beel Bhaina and Beel Kedaria (see Figure 1-4 for location of these polders) were subjected to tidal flooding and created enough tidal volume to maintain the capacity of Teka and Hari Rivers. During the dry season of 2005 TRM operation of Beel Kedaria ceased and the Hari river was rapidly silting up, see Figure 2-1.

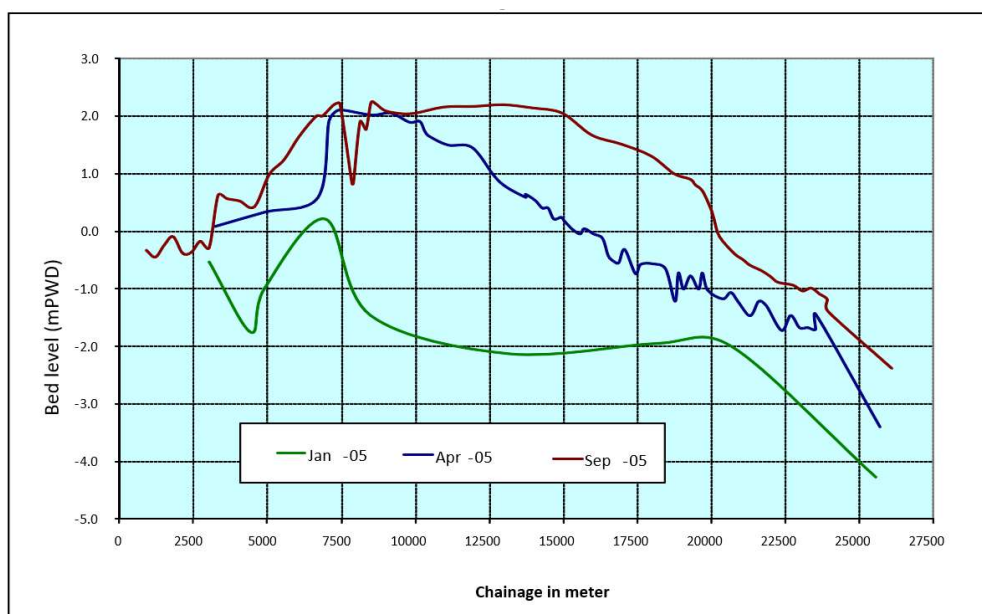


Figure 2-1 Siltation of Hari River after TRM operation of Beel Kedaria was discontinued

The order of magnitude of the deposited sediment from January 2005 to April 2005 can be estimated as follows:

- The average deposition height is about 2 m
- The average width of the river below low water is on average about 20 m, see Figure 2-4
- The length subjected to deposition is about 20 km
- The deposited volume is therefore 800,000 m³

Assuming an average density of the sediment of 1,000 kg/m³ (unconsolidated sediment) the weight of the deposited sediment is 800,000 tons, which corresponds to a deposition of about 4,000 tons per tidal cycle.

2.2 TRM Operation

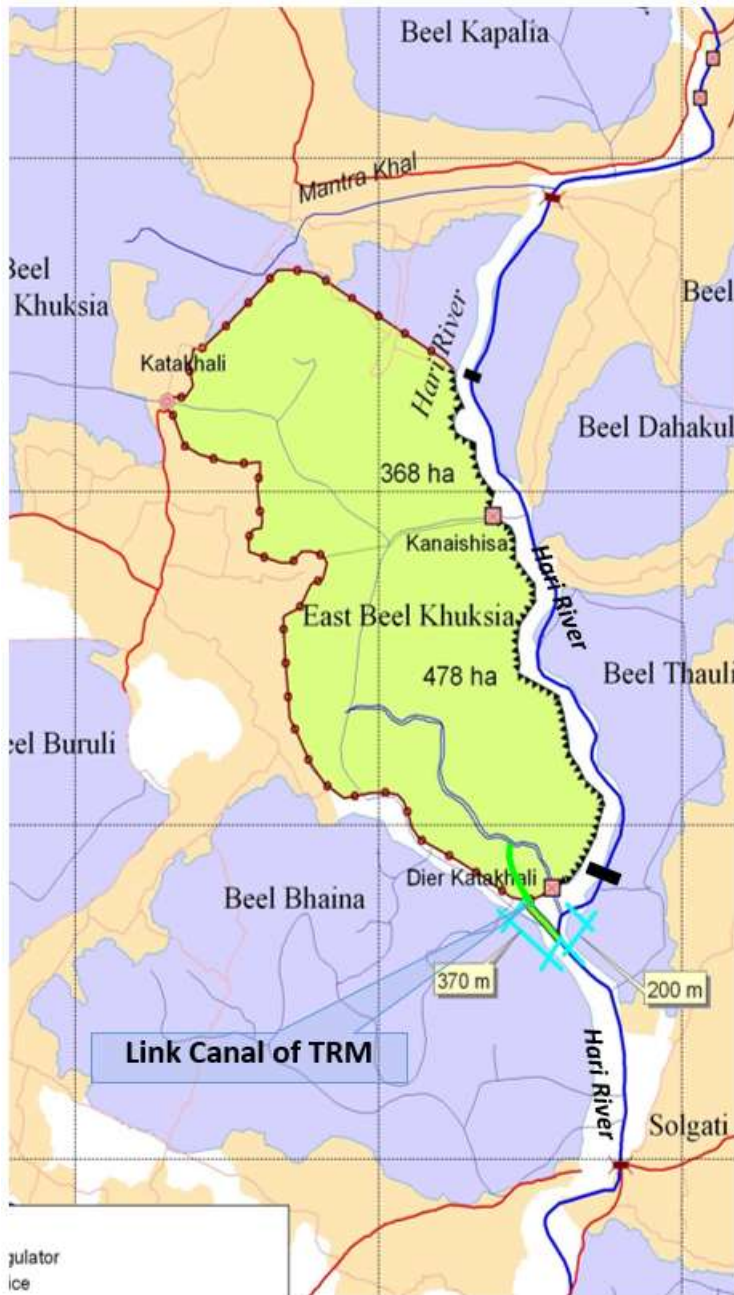


Figure 2-2 East Beel Khuksia with the link canal of TRM at Katakhal Regulator

In response to the lost drainage capacity of the Hari River TRM operation was initiated at the East Beel Khuksia on 30 November 2006 by opening a link channel to the Hari River, see Figure 2-2 for location of the link channel. During the period August 2006 to April 2007 dredging of the Hari River was also undertaken. The TRM operation and dredging led to a significant increase of the drainage capacity of the Hari River as evidenced by the development of a cross-section in the Hari River shown in Figure 2-3. In Figure 2.3, it should be highlighted that major part of the enlargement of the cross-section took place after the dredging operation ceased (i.e. from May 2007 and onwards) thus through natural erosion.

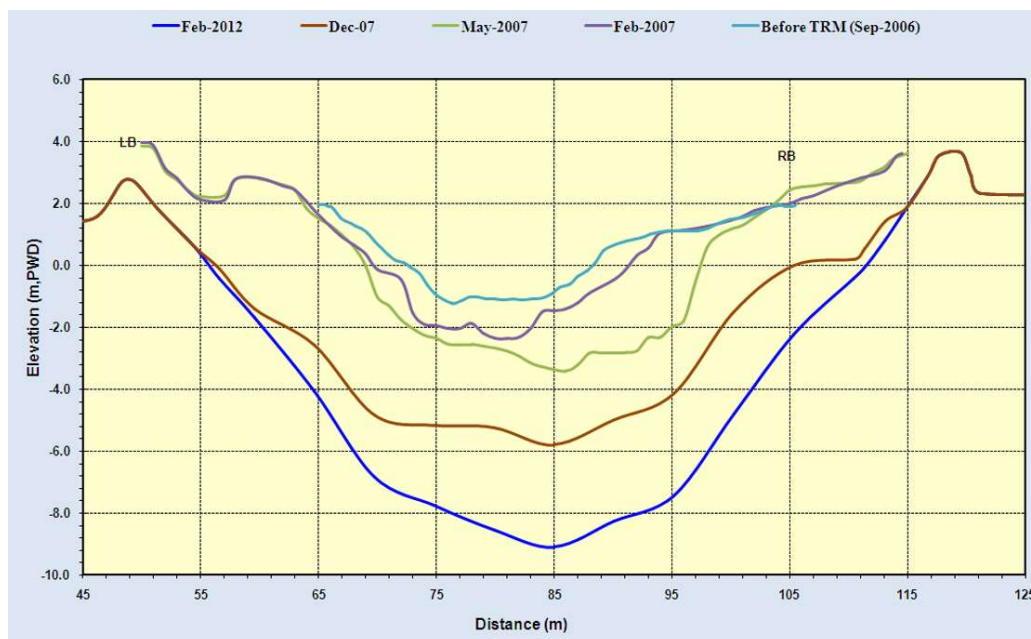


Figure 2-3 Development of a cross-section in the Hari River. From February 2007 to May 2007 both dredging and erosion take place, while after May 2007 only erosion

2.3 Data Available

IWM has made the following data available:

- The cross-section database for the SWRM contains cross-sections from several survey campaigns. For the Hari River cross-sections are available from surveys carried out in 2008 and 2016, where the 2008 cross-sections are generally significant deeper and wider than those surveyed in 2016 (thus there has been deposition from 2008 to 2016).
- Cross-sections in the Hari River at Chainage 11662, 17223 and 24279. All surveyed in February 2004, May 2004 and April 2005. The latter set is after Beel Kedaria TRM operation has ceased. A sample cross-section (at Chechuri – approx. chainage 12412) is shown in Figure 2-4. From February to May 2004 the riverbed is eroding slightly probably due to TRM operation at Beel Kedaria, while significant deposition takes place between May 2004 and April 2005 due to the terminated TRM operation.
- 31 Cross-sections in the Hari River surveyed November 2006 thus immediately before TRM operation of East Beel Khuksia commenced. These data should be processed (and checked) and potentially be included in the model setup.
- Sediment concentration data for a full tidal cycle from two locations inside the East Beel Khuksia during spring tide in May 2007 (thus during TRM operation).
- Sediment concentration data for three full tidal cycles representing spring, neap and spring tides (in May 2007) in Hari River at chainage approx. 19662.
- In connection with the sediment measurements the total depth at the measuring points were recorded: From these data it's possible to derive the tidal range at the measuring points.
- Two full set of topography of East Beel Khuksia from February (pre-TRM operation) and May 2007. We have calculated the accumulated sediment volume to 1.2 mill m³, but this estimate

is somewhat uncertain. In fact, the sample density and quality of data may not be good enough to establish reliable 2D model setups based on these data sets of polder topography.

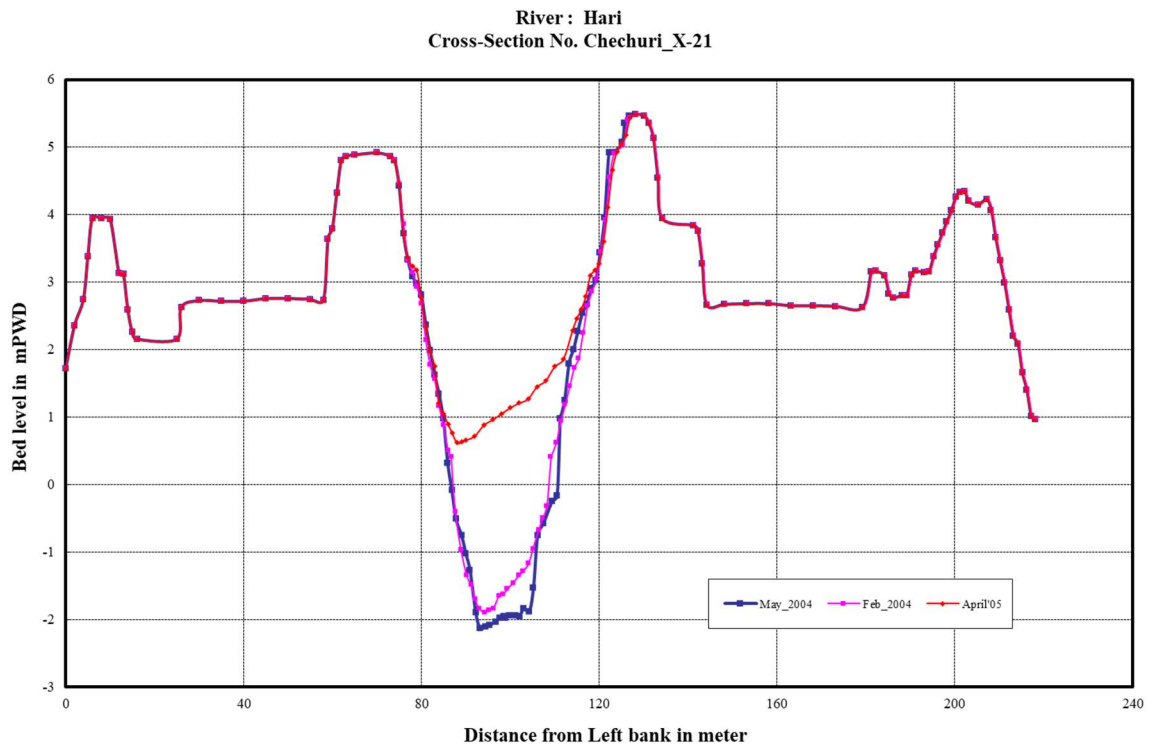


Figure 2-4 Observed cross-sections in Hari River at Chainage 12412 (location of Chechuri shown on Figure 1.4)

3 Model Development (MIKE 11) historical/present conditions

3.1 Introduction

The purpose of modelling presented is to explore what will be required in terms of modelling to optimise TRM operation and is based on the application of a very simple 1D modelling approach. The model simulates hydrodynamics and advection-dispersion of suspended sediment represented by one (representative) size fraction only. Erosion and deposition are defined as sources and sinks in the advection-dispersion model and calculated as simple/standard functions of the cross-sectional average bed shear stress (thus a standard cohesive sediment modelling approach). There are thus no 2D representation, which is likely to be important in the polders/beels, nor morphological feedback (impacts from erosion and deposition on the flow pattern), which may be important in the peripheral rivers.

IWM availed a curtailed version of the South-West Regional Model (SWRM). The layout of the curtailed model is shown in Figure 3.1. East Beel Khuksia is part of Polder 24. Polder 29 is one of the selected polders in this study. The model boundary conditions are the corresponding simulated values from the full SWRM. Boundary conditions are available for the period 4th January 2011 to 31st May 2012, only. For this particular period there are no available observations of neither water levels nor sediment concentration/transport from the study area.

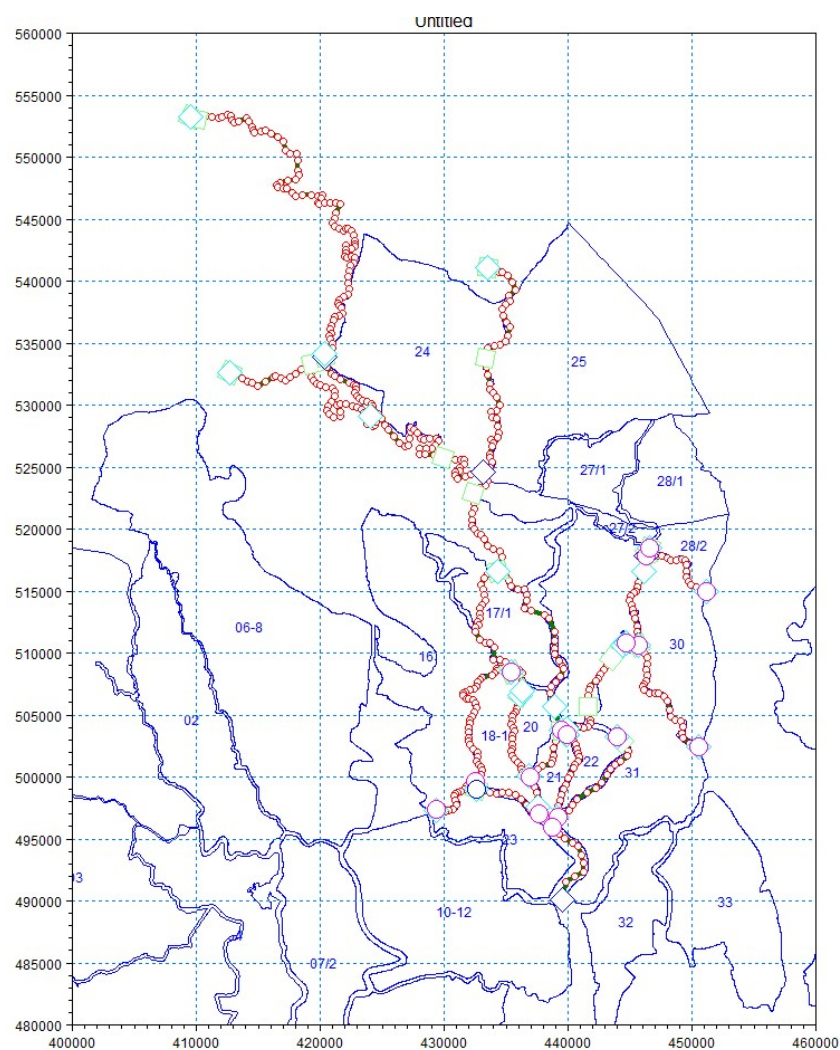


Figure 3.1 Curtailed SWRM setup with polder map.

3.2 Model Adjustments.

For the modelling of the East Beel Khuksia TRM operation the model has been further curtailed. Everything below the junction of Lower Bhadra, Habarkhali and Deluti Rivers has been removed. Implicitly, this implies that it has been assumed that the tidal signal at this junction is not affected by the TRM operation at East Beel Khuksia. The purpose of this further reduction of model extend is to increase the speed of simulations and to avoid having to consider the sediment dynamics below the junction. In addition, the East Beel Khuksia has been added to the model setup through a short (100 m long) link channel with a hydraulic structure in the middle. The hydraulic structure can be adjusted to allow free inflow and outflow (representing TRM operation), only outflow (inserting a flap gate to represent normal polder operation), completely closed or any other operation that could be relevant to investigate for optimisation of TRM operation.

The final model setup is shown in Figure 3.2.

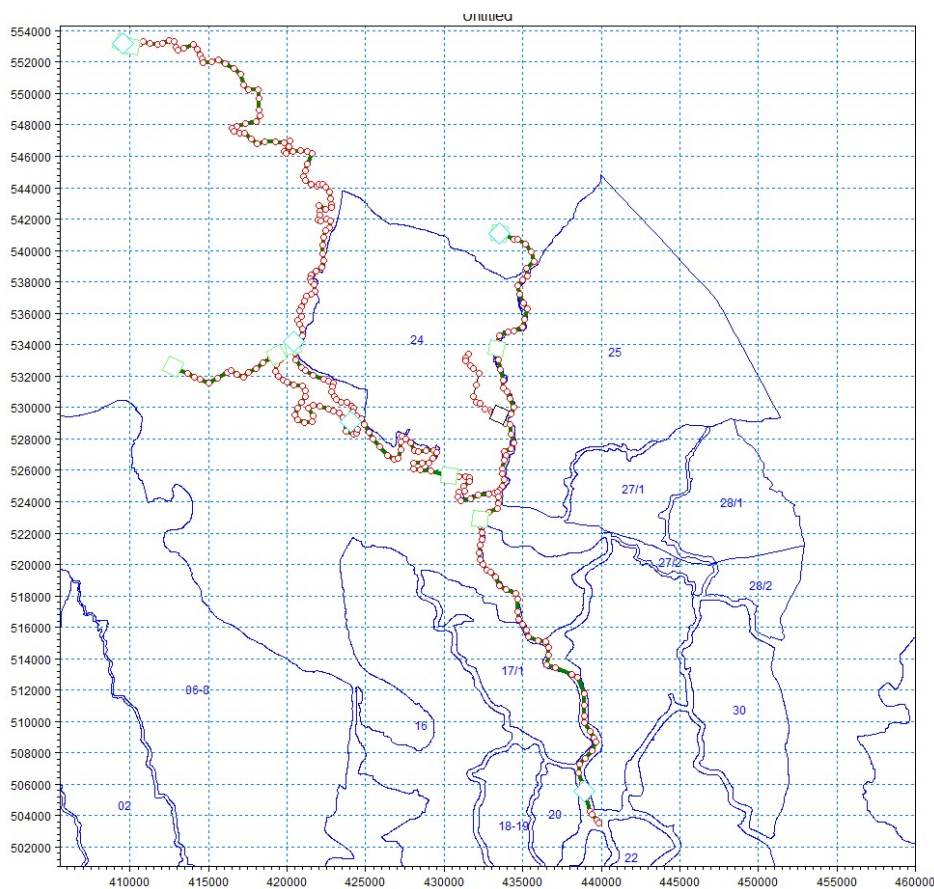


Figure 3.2 The Hari sub-model with East Beel Khuksia included.

MIKE 11 will insert interpolated or extrapolated cross-sections at junctions and external boundaries (cul-de-sac branches) if no (surveyed) cross-section is given at these locations. This can lead to very short space steps between surveyed and interpolated cross-sections, which in turn may require the use of a small timestep. To avoid this type of interpolation/extrapolation of cross-sections the following modifications have been introduced:

- U-BHADRA has been shortened and now starts at first available cross-section at chainage 250 (was chainage 0, where no cross-section is available)
- Move junction from U-BHADRA from Chainage 7050 to 6900
- Move junction from TEKA-HARI-TELI-GENG from Chainage 21350 to 21151

- BURI-BHADRA has been shortened and now starts at first available cross-section at chainage 102 (was chainage 0)
- Cross-sections at TEKA-HARI-TELI-GENG at chainage 6800 and 7000 are identical. Chainage 7000 has been removed from the database
- Cross-sections at TEKA-HARI-TELI-GENG at chainage 42000 and 46800 are identical. Chainage 46800 has been removed from the database
- U-BHADRA has been shortened and now ends at last available cross-section at chainage 25000 (was 25600, where no cross-section is available)

With these changes the model runs smoothly with a time step of 5 min (or larger), which is significantly higher than the 1 min which is the limit in the curtailed model. The listed modifications/changes were implemented one by one and for each change the model was tested whether the modification had impact on the result.

The intention is to simulate the sedimentation taking place after TRM operation of Beel Kedaria was discontinued and the re-erosion when TRM operation of East Beel Khuksia has started. The cross-section survey best representing the situation after TRM operation of Beel Kedaria is the 2008 survey (c.f. Section 2.3), however this survey does not cover the full length of the river. The 2008 survey has therefore been used from chainage 0 to 39588 while the 2016 survey has been used from chainage 40800 to 47292 (ID IWM2008/16 in cross-sectional database). In Figure 3.3 the simulated water level in East Beel Khuksia using these data (black line) is compared with the corresponding result using the 2016 survey (blue line), only. There is a very significant difference in the simulated water levels. This suggests that it is of great importance to have cross-sectional survey data that are concurrent with actual simulation period.

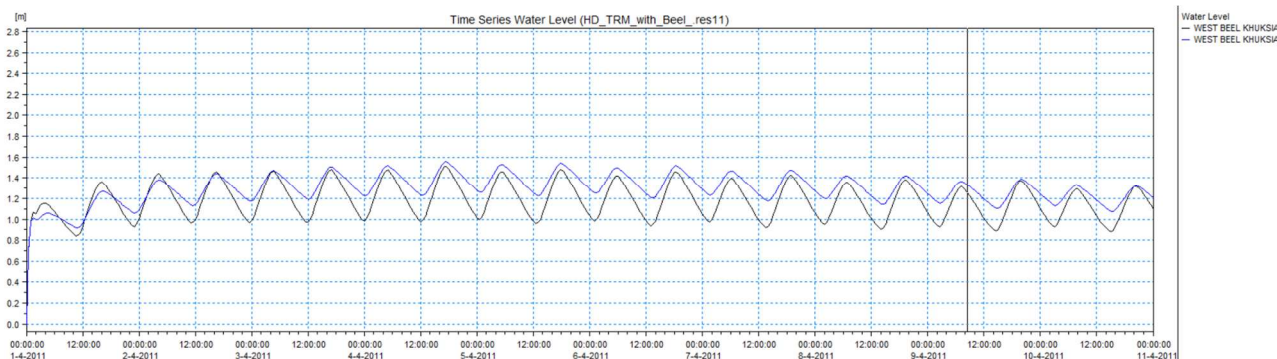


Figure 3.3 Simulated water level for two different sets of cross-sectional survey data.

3.3 Model Calibration

The hydrodynamic component of the SWRM is fully calibrated and verified hence there is no need to repeat this for the curtailed model. Boundary conditions are available for the period 4th January 2011 to 31st May 2012, only, whereas the actual simulation periods are January – April 2005 (Figure 2.1) and (say) February – May 2007 (Figure 2.3). Both of these periods will be represented by the simulation period 4th January to 4th April 2011. The "calibration" strategy will therefore be:

- To identify a simulated tide, where the tidal variation is similar with the observed tidal range (obtained through depth recordings, see Section 2.3).
- Compare observed and simulated sediment concentration for this particular tide and adjust model parameters until a satisfactory agreement with the observed sediment concentration has been achieved.

The model will subsequently be “verified” through

- Comparison of simulated and observed sediment concentrations for the subsequent neap and spring tide as well as spring tide observations within East Beel Khuksia.
- Testing the ability to simulate sediment accumulation/siltation in the Hari River for the period after discontinuation of TRM operation at Beel Kedaria.
- Testing the ability to simulate sediment erosion in the Hari River and sedimentation in East Beel Khuksia following initiation of TRM operation.

The simulation results are presented in Figure 3.4 through 3.11 and give rise to the following observations:

- In Figure 3.4 the observed water level (assuming a bed elevation of -3.2 m PWD) is compared to the simulated water level. The agreement between observed and simulated water level is very good, but this would also have been the case for numerous other tides in the selected simulation period, hence the phase (in the spring-neap-spring cycle is not well-determined).
- Figure 3.5 shows observed and simulated sediment concentrations. Again, the agreement is good. The sediment parameters used are listed in Table 3-1.

Table 3-1 Sediment parameters applied for the MIKE 11 model.

Parameter	Value
Settling velocity	0.5 mm/s
Critical shear stress for deposition	0.2 Pa
Critical shear stress for erosion	0.2 Pa
Erosion coefficient	0.05 g/m ² /s
Dry density of bed sediment	1000 kg/m ³
Sediment concentration downstream at boundaries	5 g/l

All the applied values are quite similar to those used in other model studies in Bangladesh and elsewhere.

- Figure 3.6 shows the water level for a full spring-neap-spring cycle. The simulation shows that the low waters become lower during neap tide, whereas the observations do not show the same behaviour. A possible explanation is that the full impact of the TRM operation has not materialised when the measurements were made during May 2007. Figure 2.3 shows that erosion of the cross-sections has commenced but it’s not fully developed, thus the higher bed elevation keeps the water level at low tide up. The second spring tide is under-simulated by the model.

These discrepancies between observations and model prediction suggest that a better agreement would be achieved by 1) re-run the model with proper boundary conditions and 2) by including morphological feedback in the simulations.

- Figure 3.7 shows simulated and observed sediment concentration in Hari River. The neap tide concentrations are well represented by the model, whereas the second spring tide concentrations are too small in the simulations. This corresponds well with the under-simulation of the tidal range (Figure 3.6). This underscores that the sediment concentration is very sensitive to the tidal range.

- Figure 3.8 and the zoom plot in Figure 3.10 show simulated water level in East Beel Khuksia at two adjacent locations. The tidal range is well predicted while the phase is 2-3 hours off. The phase of the tide in Hari River is well-predicted. Considering the proximity of the Hari River and the two locations within East Beel Khuksia, it is difficult to find a physical explanation for the apparent phase lag. The most likely explanation is therefore that the measurements must have been carried out at a different date or time or at a different location than stated in the data files.
- Figure 3.9 and the zoom plot in Figure 3.11 show simulated and observed sediment concentration in East Beel Khuksia at two the adjacent locations. The figures give rise to the following remarks:
 - The observed concentration is significantly higher than the simulated. In the 1D model setup the drainage canal(s) in the polders and polder surface have been lumped into one cross-section, where simulated flow velocity will be much smaller than in the drainage canals. This means that sediment will deposit quickly inside the polders in the model. In reality the flood flow will carry sediment further into the polders via the drainage canals and deposition first take place when the water spills into the polder. This discrepancy thus suggests that a 2D description is required to represent correctly the conditions within the polders.
 - In the simulation, the ebb flow (the water flowing out from the polder) does not contain any sediment (thus all sediment entering the polder will deposit). The observations do not confirm this at both stations. In fact, some of the highest observed concentrations at Chainage 4485 (red dots) are found during ebb flow. At Chainage 3979 the variation pattern is similar to the simulations except for one outlier. The sediment samples are collected very close to the bed (10-15 cm) especially those around low water, hence it may be that the sampler itself has stirred up sediment from the bottom. Another contributing explanation could be that part of the finer sediment fractions will remain in suspension inside the polder because of the low settling velocity. This could thus advocate for a multi-fraction modelling approach.

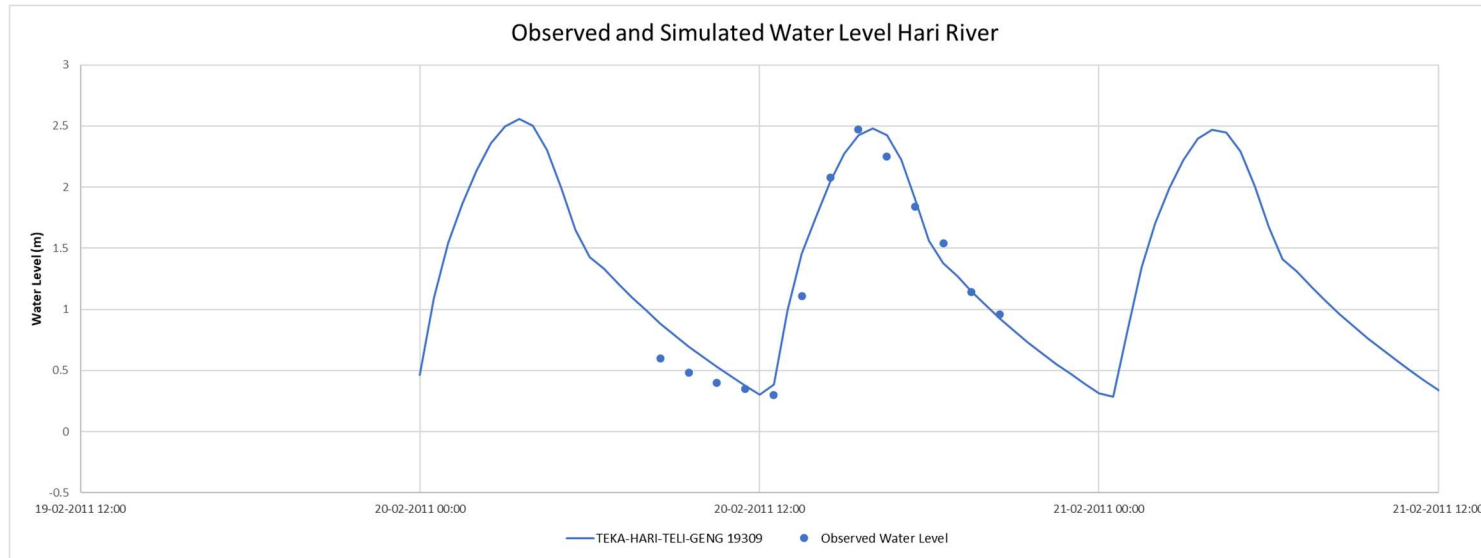


Figure 3.4 Simulated water level in Hari River compared to measured water depth assuming a bed elevation of -3.2 m PWD.

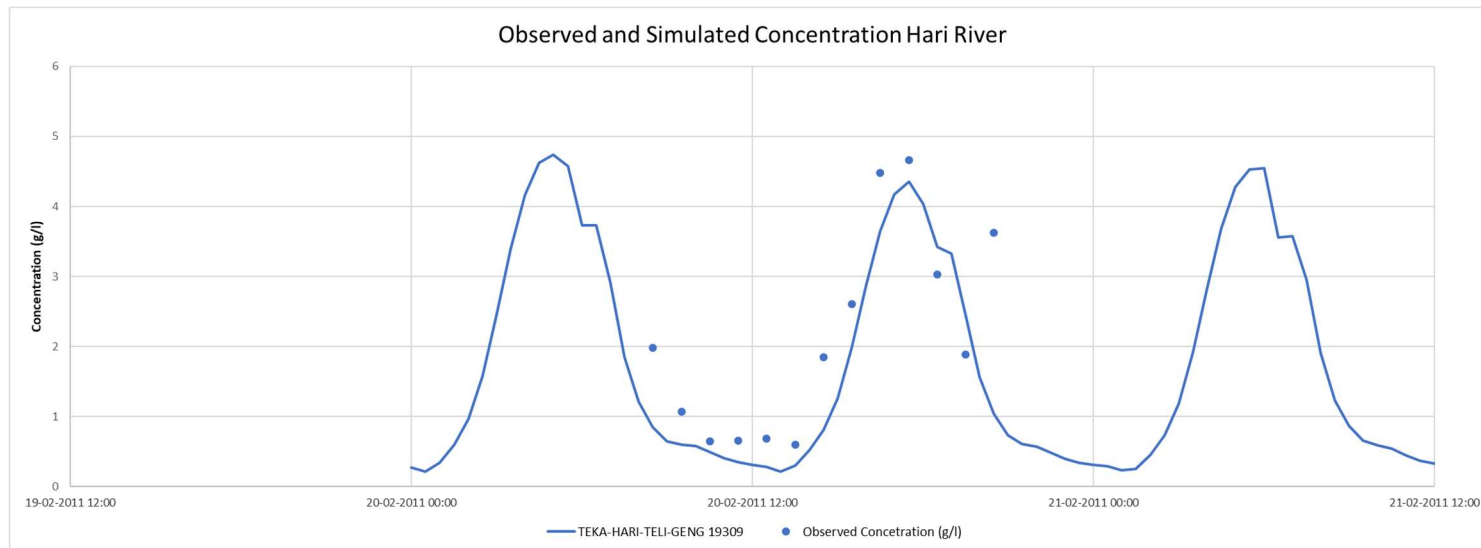


Figure 3.5 Simulated and observed sediment concentration in Hari River – calibrated sediment parameters.

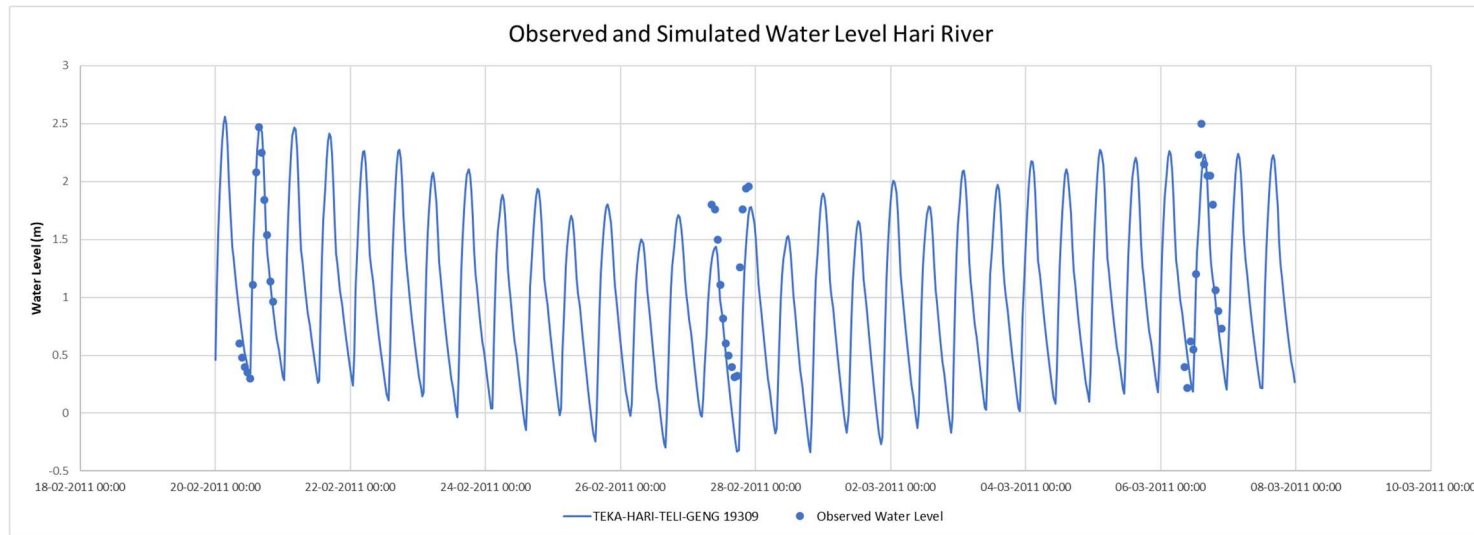


Figure 3.6 Simulated water level in Hari River compared to measured water depth assuming a bed elevation of -3.2 m PWD.

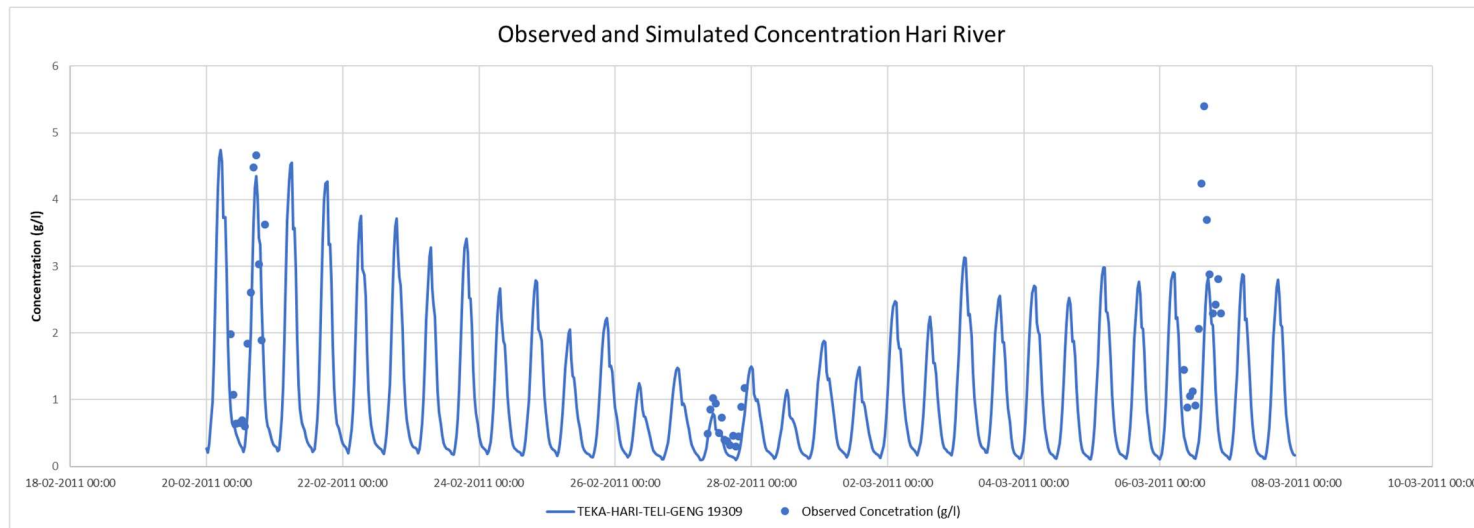


Figure 3.7 Simulated and observed sediment concentration Hari River – calibrated sediment parameters.

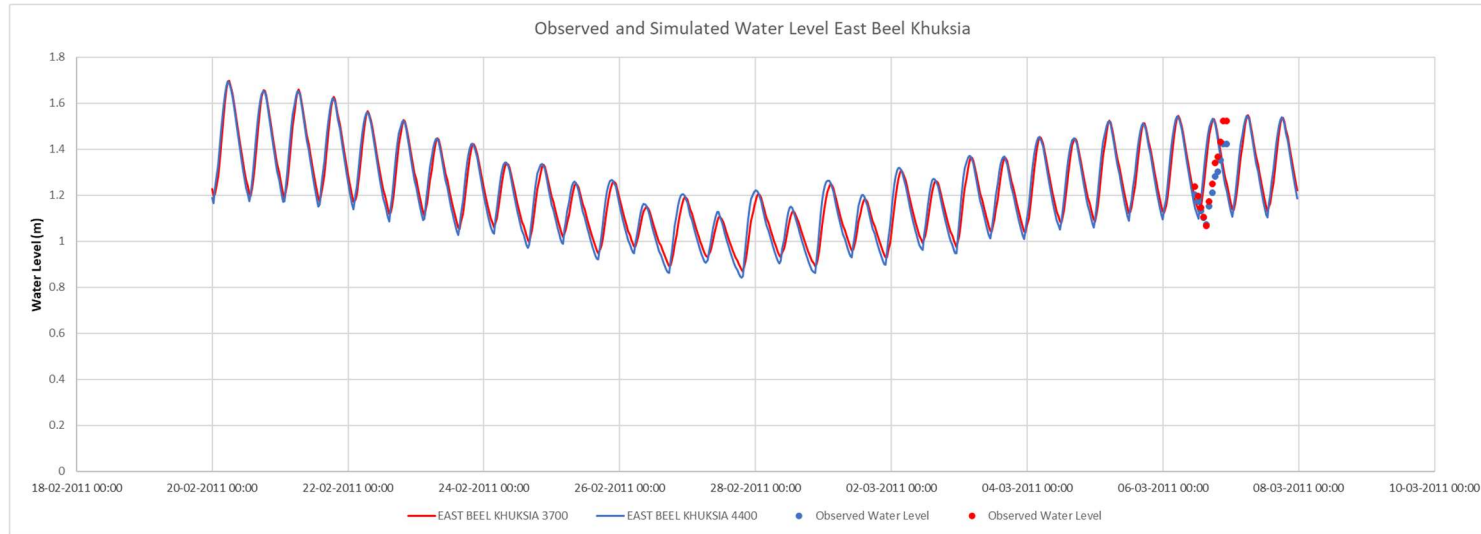


Figure 3.8 Simulated water level in East Bell Khuksia compared to measured water depth assuming a bed elevation of 0.6 m PWD.

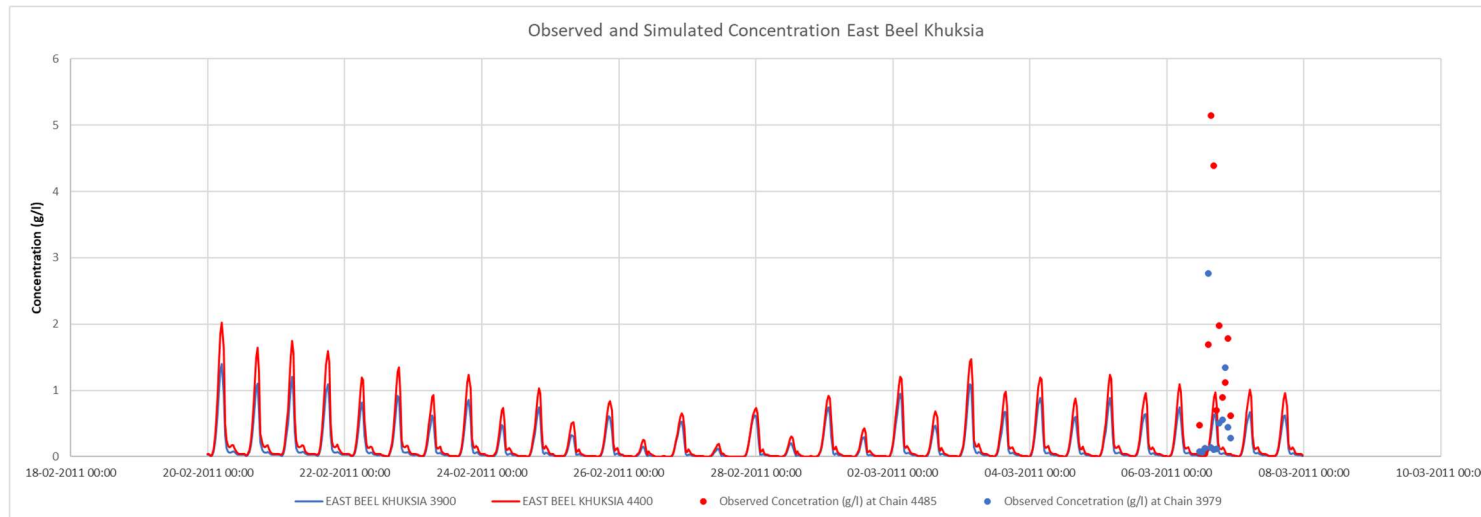


Figure 3.9 Simulated and observed sediment concentration East Beel Khuksia – calibrated sediment parameters.

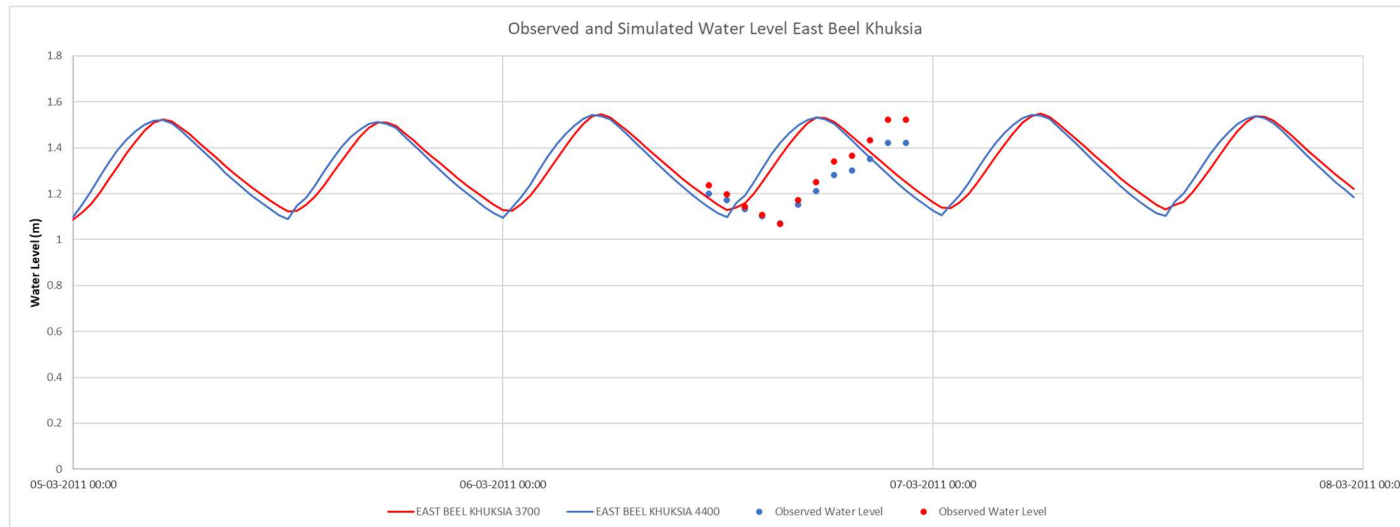


Figure 3.10 Simulated water level in East Bell Khuksia compared to measured water depth assuming a bed elevation of 0.6 PWD.

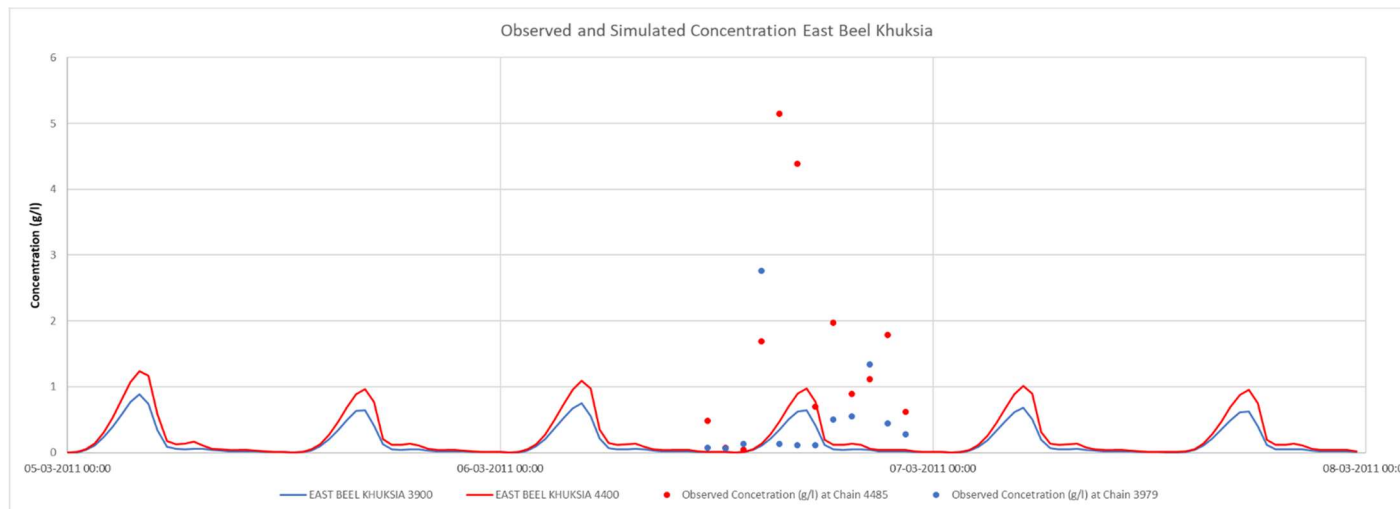


Figure 3.11 Simulated and observed sediment concentration East Beel Khuksia – calibrated sediment parameters.

3.4 Erosion and Deposition Before and During TRM Operation

In this section simulation results representing the erosion and deposition taking place before and during TRM operation at East Beel Khuksia are represented. The simulations are split into two steps:

- Step One: The situation immediately after TRM operation of Beel Kedaria was discontinued. Initial conditions are represented by no sediment at the riverbed and (the large) 2008 cross-sections. East Beel Khuksia is not included in the model setup. The period simulated is three months from 4/1 2011 to 4/4 2011 representing the period January – April 2005 (see Figure 2.1).
- Step Two: The situation after TRM operation of East Beel Khuksia has commenced. Initial condition is the simulated sediment accumulation at the bed in Step One and again the large 2008 cross-sections (the simulation is not (yet) morphological). The period simulated is again the three months from 4/1 2011 to 4/4 2011 but now representing three months during TRM operation (commencing Nov 2006).

However, initially the effect of the East Beel Khuksia on the tidal flow is explored. Figures 3.13 and 3.14 show the simulation result where the Hari River joins the Upper Bhadra River. In Figure 3.14 the tidal volume has been calculated. Without East Beel Khuksia the tidal volume is up to 3.5 mill m³ while East Beel Khuksia adds another 1.5 mill m³ to this. The tidal volume increases thus with about 40%. A similar increase of velocities may be expected while bed shear stresses may increase with about 100%. This is at the junction with the Upper Bhadra River. Further upstream closer to the link channel to East Bell Khuksia the relative impact of East Beel Khuksia will be bigger.

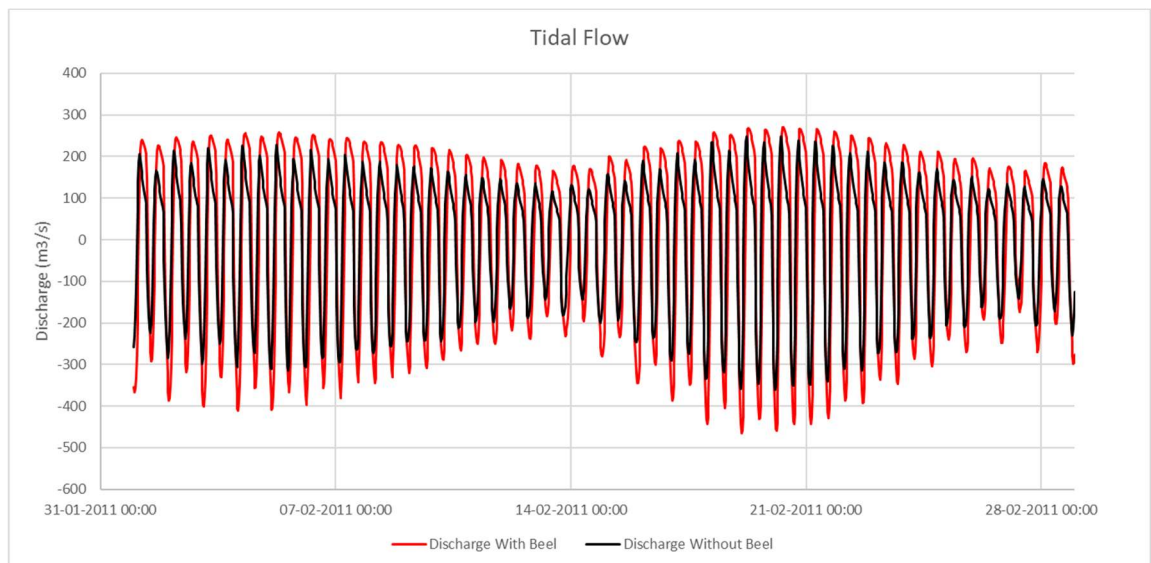


Figure 3.12 Simulated tidal flow with and without East Beel Khuksia included.

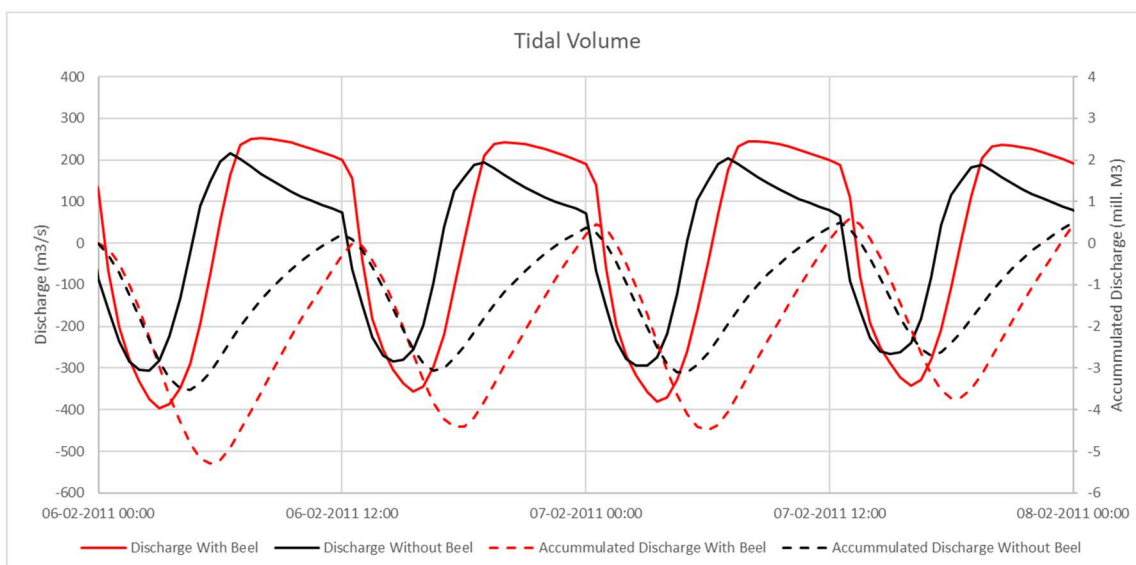


Figure 3.13 Simulated tidal flow and tidal volume with and without East Beel Khuksia included. This is a zoom of Figure 3.12.

In Figure 3.14 the simulated sediment dynamics is shown for the situation after TRM operation at Beel Kedaria has ceased and before TRM operation at East Beel Khuksia commences. The figure shows the strong asymmetry in sediment transport leading to a significant net transport of some 400,000 tons into the Hari River. This should be compared with the net accumulation of 800,000 tons estimated from observed cross-sections for a similar period (see Figure 2.1). The majority of the sediment is accumulated in the lower part of the Hari River (downstream the location of the link channel into East Beel Khuksia).

Figure 3.14 presents the simulated sediment dynamics when East Beel Khuksia is under TRM operation. It is noticed that both the transport during ebb and flood flow has increased due to the increased tidal volume (compared to the simulation presented in Figure 3.14), but surprisingly the net transport is nearly unchanged. It is noticed that only part of the deposited sediment re-erode (viz about 200,000 tons). A closer inspection of the simulation result indicates that the deposited sediment in the lower part of the Hari River does not re-erode. Nearly all of the sediment eroded from the riverbed plus the net sediment transport into Hari River ends up in the East Beel Khuksia, where close to 600,000 tons deposit. For a period of four months, we have calculated the deposited volume to 1.2 mill m³ (an uncertain estimate, see Section 2.3). Assuming a density of 1 tons/m³ this corresponds to 1.2 mill tons, thus twice the simulated deposition.

Considering all uncertainties (e.g. regarding boundary and initial conditions), the very simplistic model approach, few data used for model calibration etc. the agreement between observations and simulation results are remarkably good.

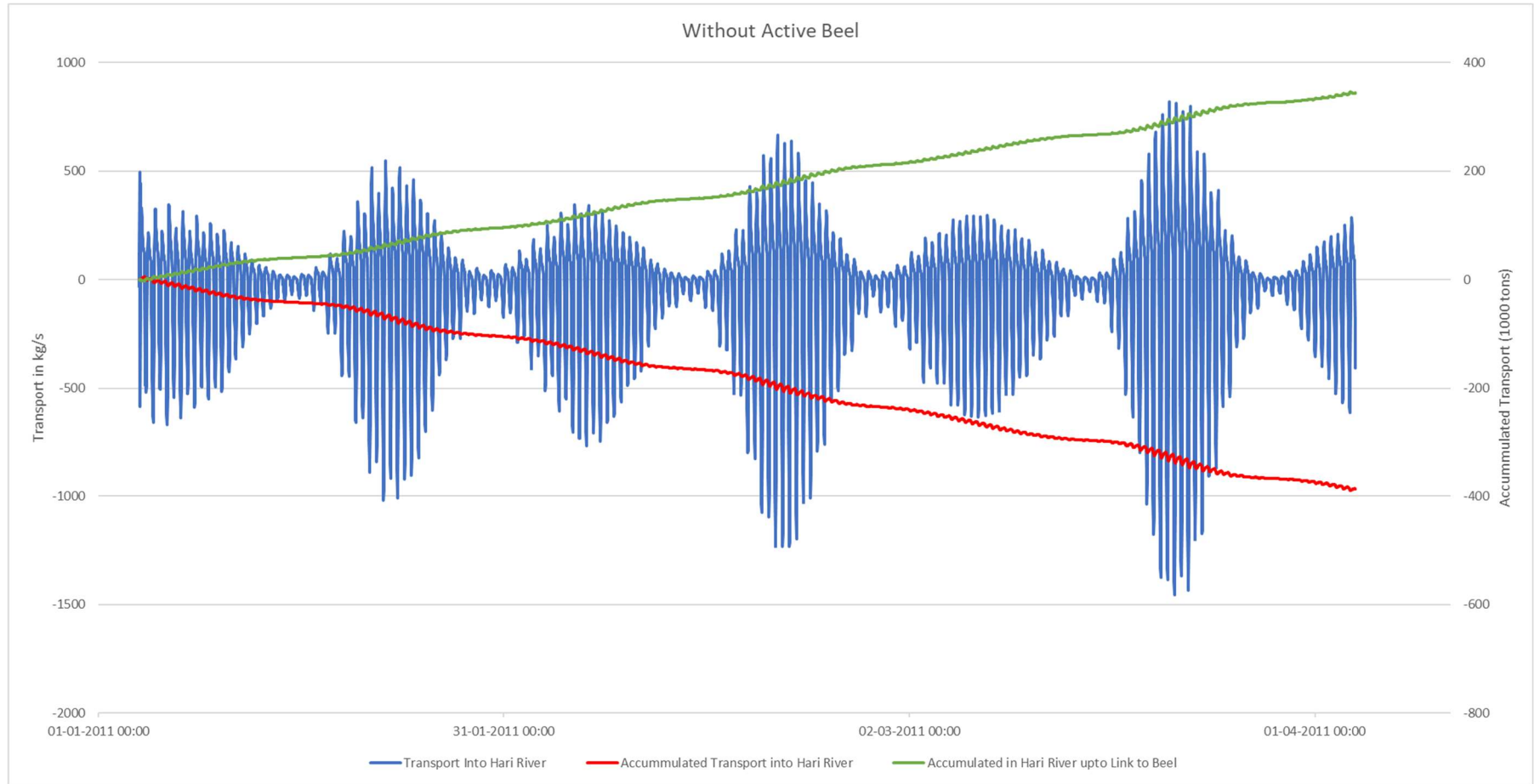


Figure 3.14 Simulated sediment dynamics when East Beel Khuksia is not included. The blue line is the simulated sediment transport (kg/s) in Hari River at the Junction with Upper Bhadra. The red line is the accumulated transport (1000 tons) at the same location while the green line is the accumulation of sediment at the riverbed between the junction and the link channel into East Beel Khuksia.

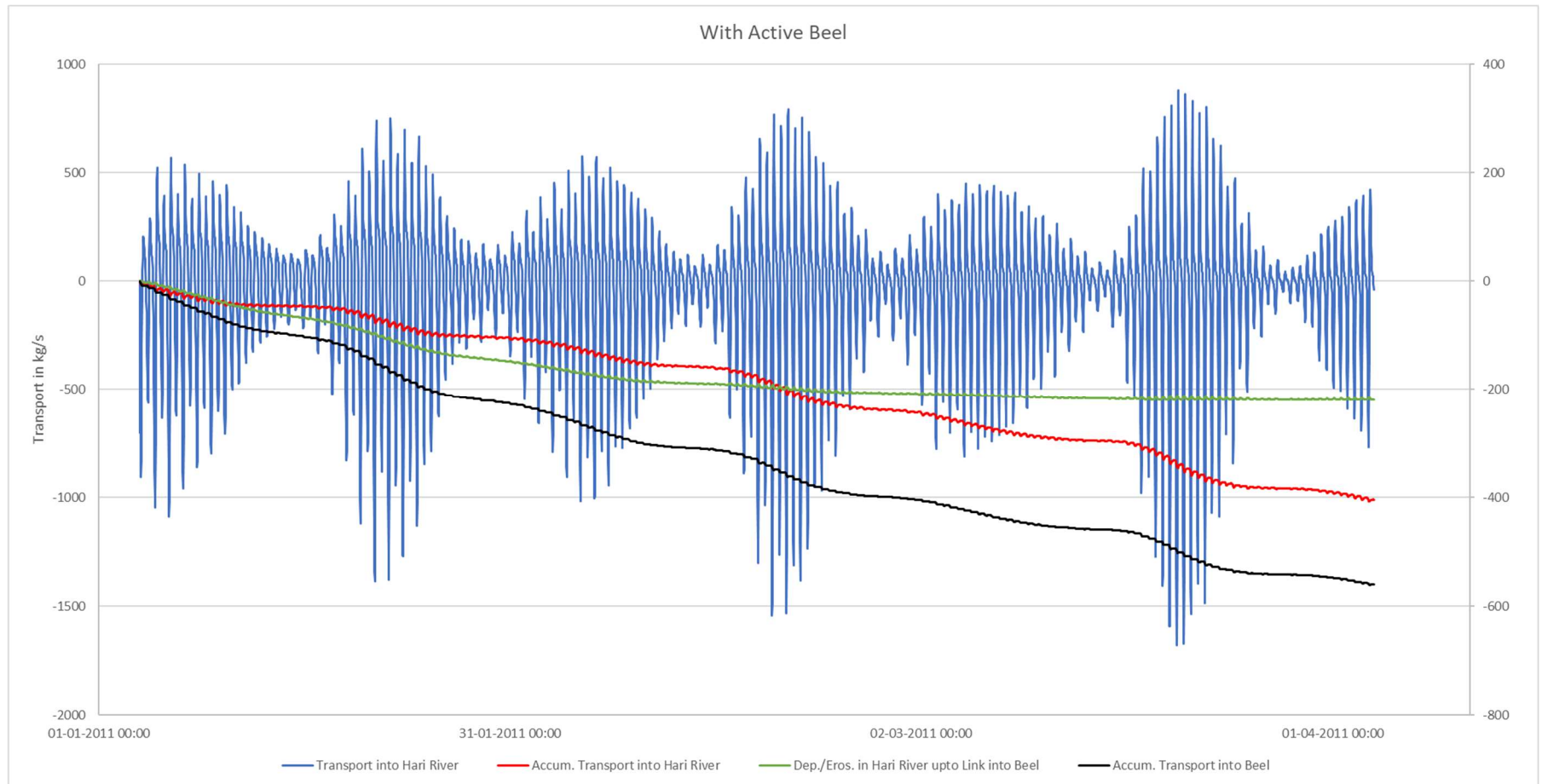


Figure 3.14 Simulated sediment dynamics when East Beel Khuksia is under TRM operation. The blue line is the simulated sediment transport (kg/s) in Hari River at the Junction with Upper Bhadra. Negative value is transport during flood flows. The red line is the accumulated transport (1000 tons) at the same location while the green line is the accumulation of sediment at the riverbed (negative value means erosion/depletion of sediment) between the junction and the link channel into East Beel Khuksia and the Black line represents the simulated deposition (1000 tons) in the East Beel Khuksia.

4 Model Development (MIKE 21) historical/present conditions

4.1 Introduction

Based on boundary conditions derived from the MIKE 11 model a more detailed 2D model (MIKE21 FM) has been developed using the historical topography inside the Polder 24 and 135 cross sections surveyed in 2015 and covering the reach from the Bhabodaho regulator and down to Ranai. The polder bathymetry of East Beel Khuksia is based on topographic survey of the polder from February 2007.

4.2 Construction of Model Mesh and Bathymetry

The distance between the 135 surveyed cross sections is in general too large to ensure a correct description of the thalweg and channel geometry of the Hari River, when generating a flexible mesh and bathymetry using the build-in standard interpolation technique of the mesh generator software tool. When the thalweg is shifting from one bank to the other there is a risk for generation of artificial bars that creates a none-physical flow resistance and in some cases even block for the tidal flow. To avoid this phenomenon a technique to improve the bathymetry basis has been developed taking advantage of the MIKE 21 C curvilinear grid generator tool, which has an option that allows interpolation aligned with the streamwise direction of a curvilinear grid. This technique makes it possible to create additional cross sections and ensure a proper bathymetry interpolation. A comparison of the two methods is illustrated in Figure 4-1 and Figure 4-2. It is seen that the streamwise interpolation or the creation of additional cross section data is required to get a proper channel bathymetry. The technique is applied for the entire reach of the Hari-Teka River in order to develop a suitable bathymetry for the TRM model. Also, the channels routing the tidal flow inside the TRM needs to be resolved to ensure that the model can transport and carry the suspended sediment being brought into the TRM further inside.

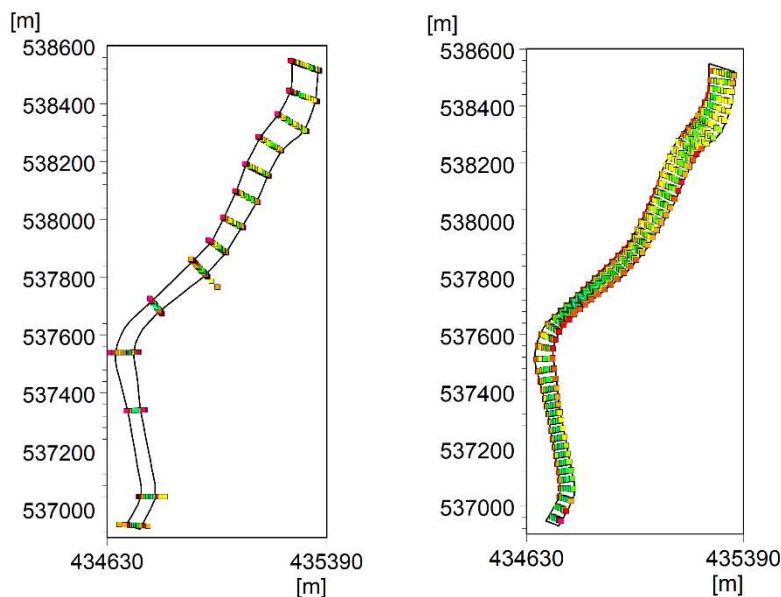


Figure 4-1 Left: The original 14 measured cross sections. Right: Cross section information obtained using streamwise interpolation resulting in a total of 59 cross sections

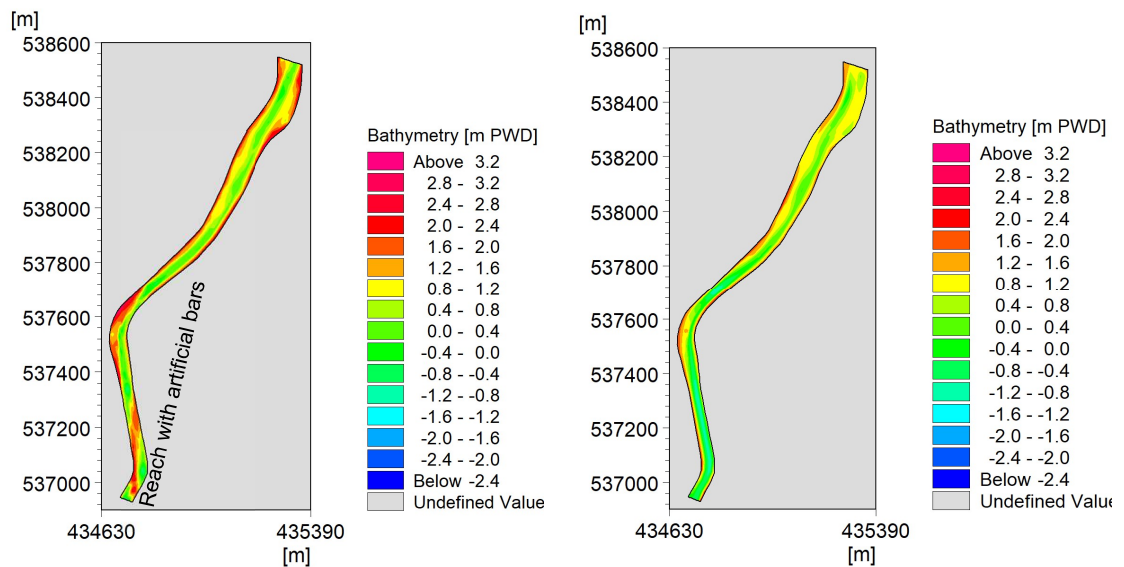


Figure 4-2 Left: Interpolated bathymetry based on the 14 measured cross sections. Right: Interpolated bathymetry based on the 59 created cross sections.

Applying this technique to improve the bathymetric basis a model mesh and bathymetry for the Hari River was established. The model mesh and bathymetry are shown in Figure 4-4. The micro-scale model is constructed so that it covers the reach from the Bhabodaho regulator in the north to Ranai in the south.

The Hari River model was extended into a TRM model that includes the East Beel Khuksia. The basis for that was a topographic survey of the polder from February 2007. The intensity of the survey was too low to generate a proper bathymetry of the polder and resolve the drainage channel network inside the polder. To accommodate for lack of survey data aerial photos were used in combination with the polder surveys from February 2007 and May 2007 to identify the channel network inside the polder and estimate the bed levels. By separating the channels and flood plains additional bathymetric data was constructed to differentiate between the two types of areas and to establish a proper basis for generation of the polder bathymetry. Figure 4-3 shows an example of the established bathymetric basis. The channel network inside the polder can clearly be identified and likewise the floodplains.

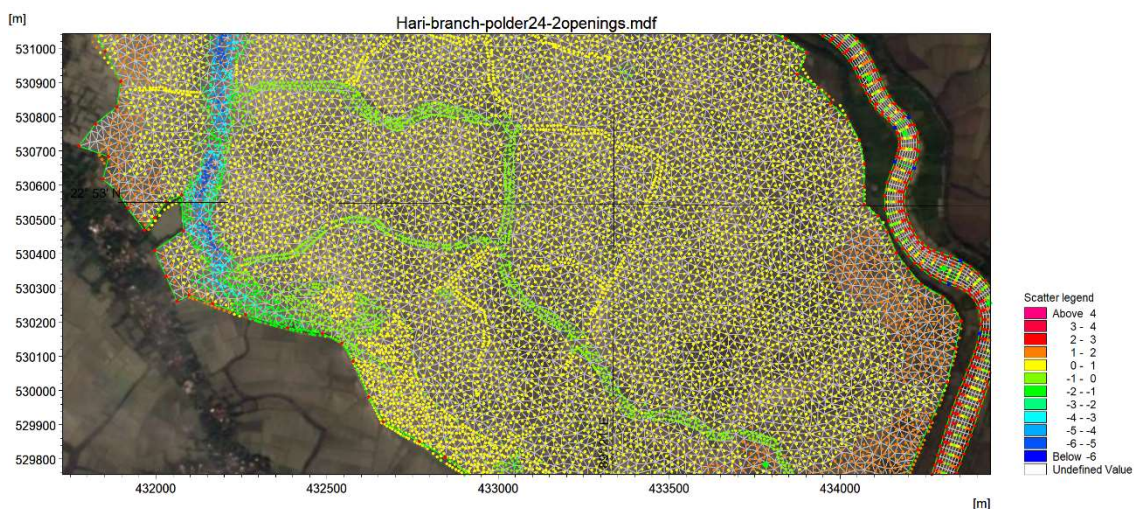


Figure 4-3 Map showing an example of the established bathymetric basis inside the polder and the peripheral river.

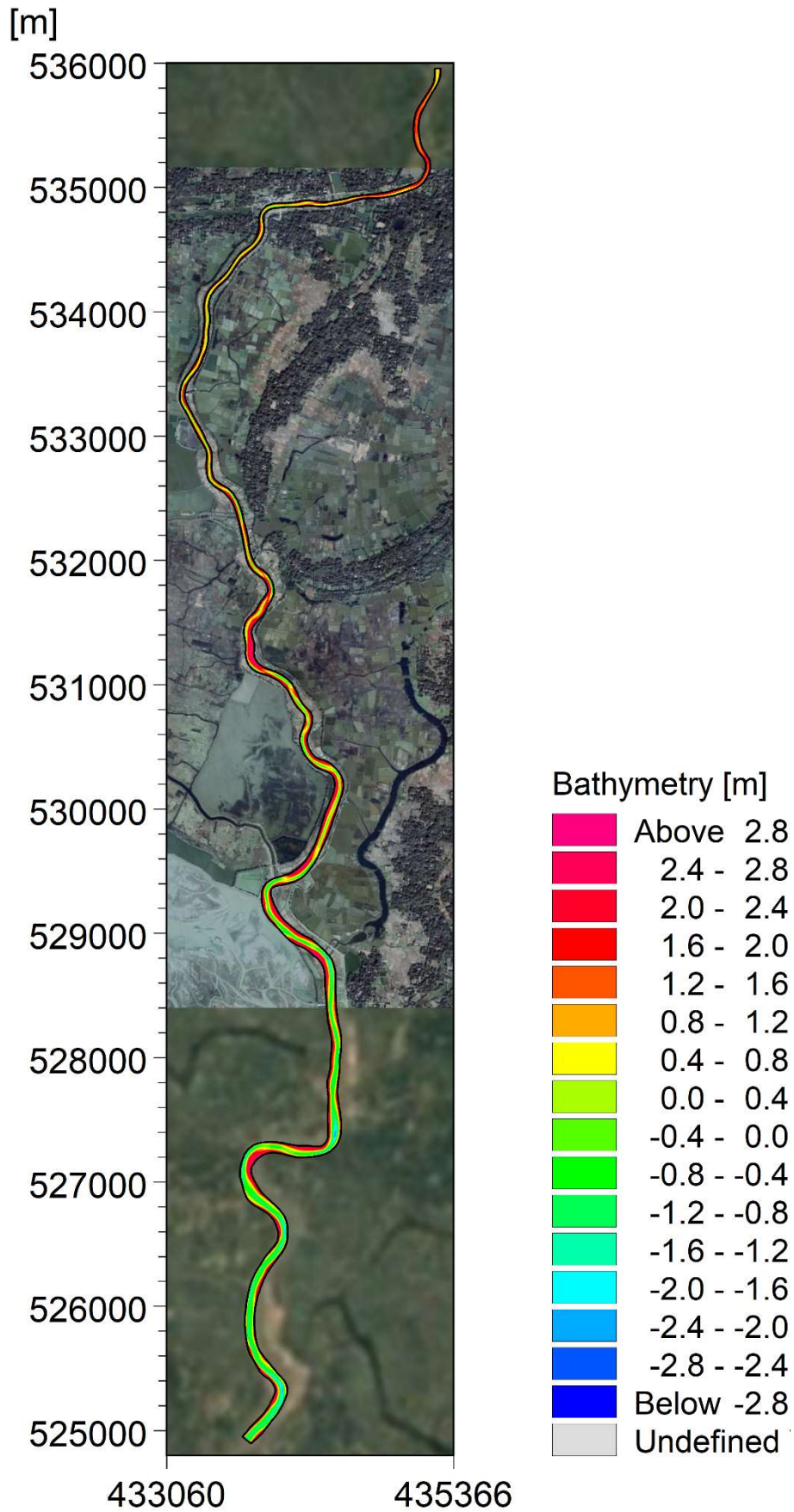


Figure 4-4 Bathymetry of the Hari River model.

The TRM model mesh and bathymetry are constructed with two openings. One in the southern end and one on the eastern side of the polder. By applying the structure module in MIKE 21FM and specifying a closed gate structure at the entrance channel the model mesh and bathymetry can be used to investigate TRM with one opening either to the south or to the east. The TRM model and bathymetry is shown in Figure 4-5.

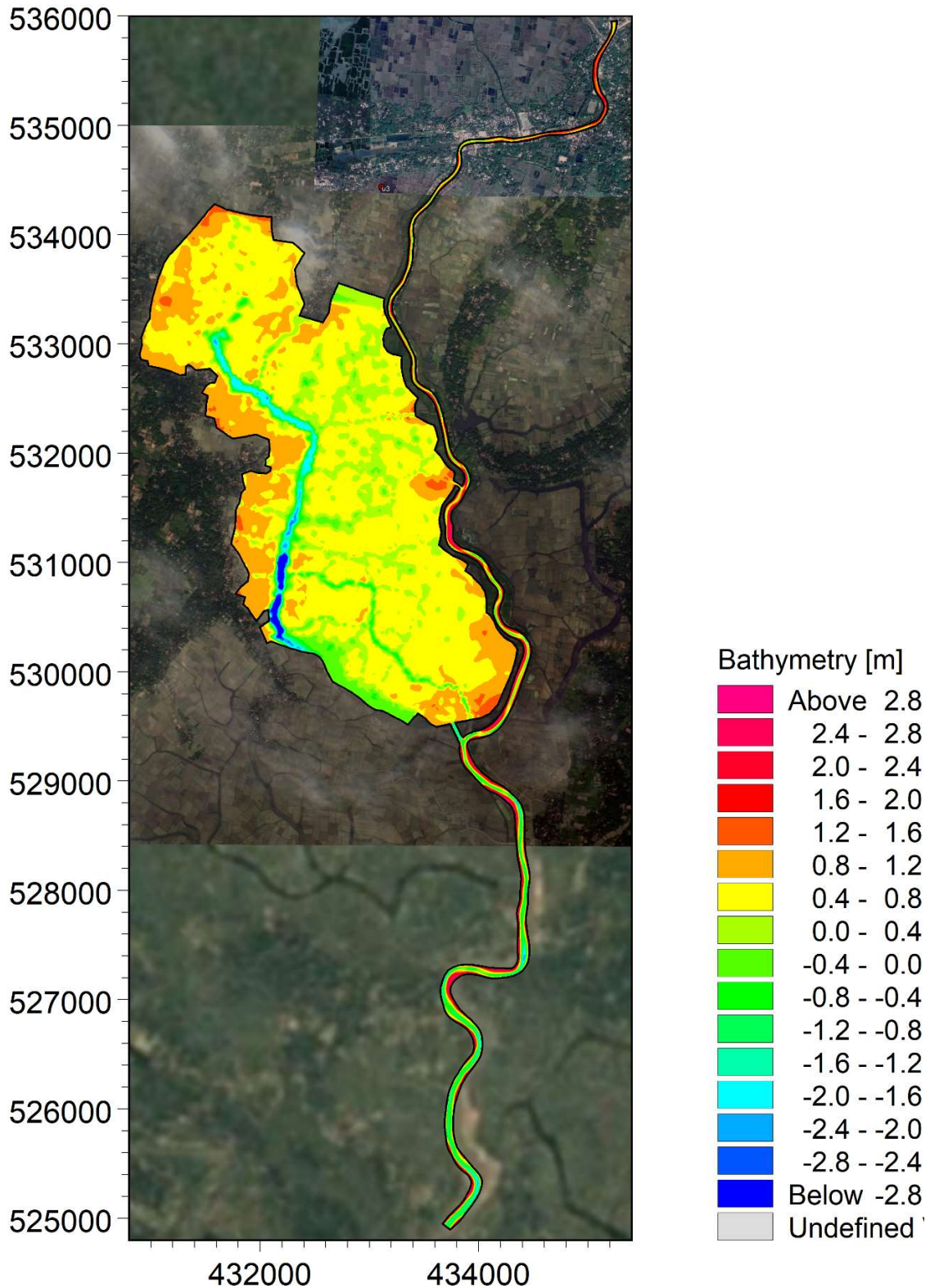


Figure 4-5 Bathymetry of the Hari River and East Beel Khuksia model.

4.3 Hydrodynamic Boundary Conditions

The boundary conditions for the model must be chosen, so that they only will be affected in a minor degree due to the activation of TRM. An opening into the polder will increase the tidal prism significantly and thereby also change the tidal discharge at the downstream boundary. The tidal elevation, however, will not be significantly affected and the model setups are therefore established with a water level time series from the MIKE 11 model extracted at Ranai. The upstream boundary is located at the Bhabodaho regulator. For the upstream boundary condition, it is therefore chosen to use a discharge time series from the MIKE 11 model extracted at the Bhabodaho regulator. The extracted time series was modified, so that the specified discharge represents the running average of 6 hours to avoid spurious fluctuations and uni-directional flow. The downstream water level boundary time series is shown in Figure 4-6 and the upstream discharge time series in Figure 4-7.

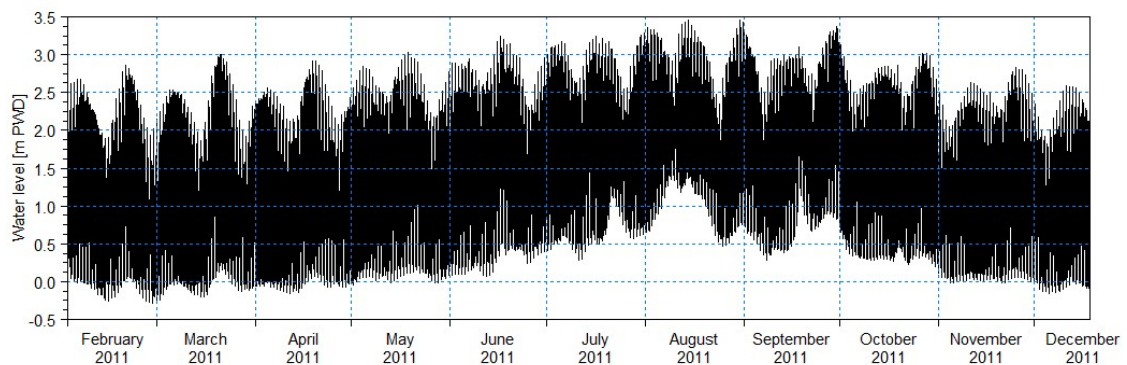


Figure 4-6 Water level time series applied for the downstream boundary condition.

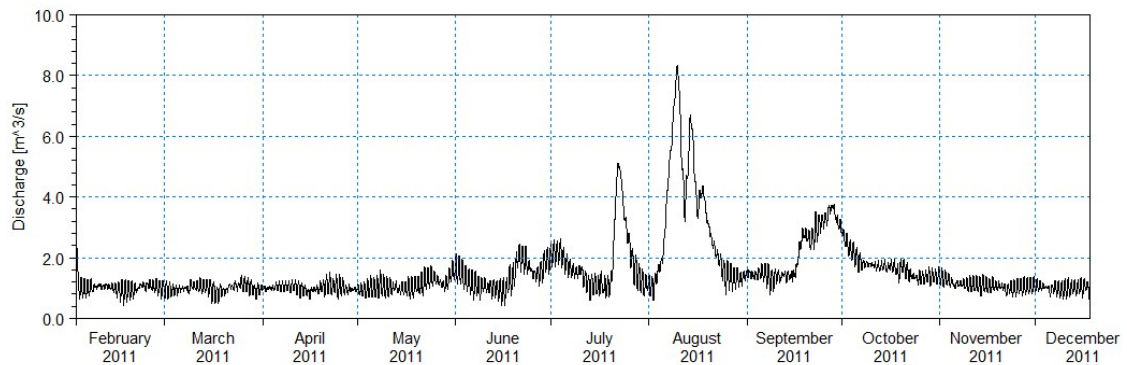


Figure 4-7 Discharge time series applied for the upstream boundary condition.

4.4 Measurements, Model Parameters and Calibration

The fact that the channel bathymetry of the Hari River is based on surveyed cross sections from 2015, the polder bathymetry from 2007 before activation of TRM, and the modelling period covers 2011 conditions makes it impossible to make a meaningful model calibration against observations. Water levels and discharge measurements from 2011-12 are available, but at this point in time the TRM operation has been ongoing for 4-5 years and thereby not comparable. Water levels were observed at six gauging stations during the period August 2011 to April 2012. The location of the gauging stations is indicated in Figure 4-8. Lebugati and Teka are located upstream the Polder 24 TRM basin, while Ranai is located downstream. Kagbandha and Katakhalu are located inside the TRM basin. Kali Charanpur is inside Polder 24, but outside the TRM basin.

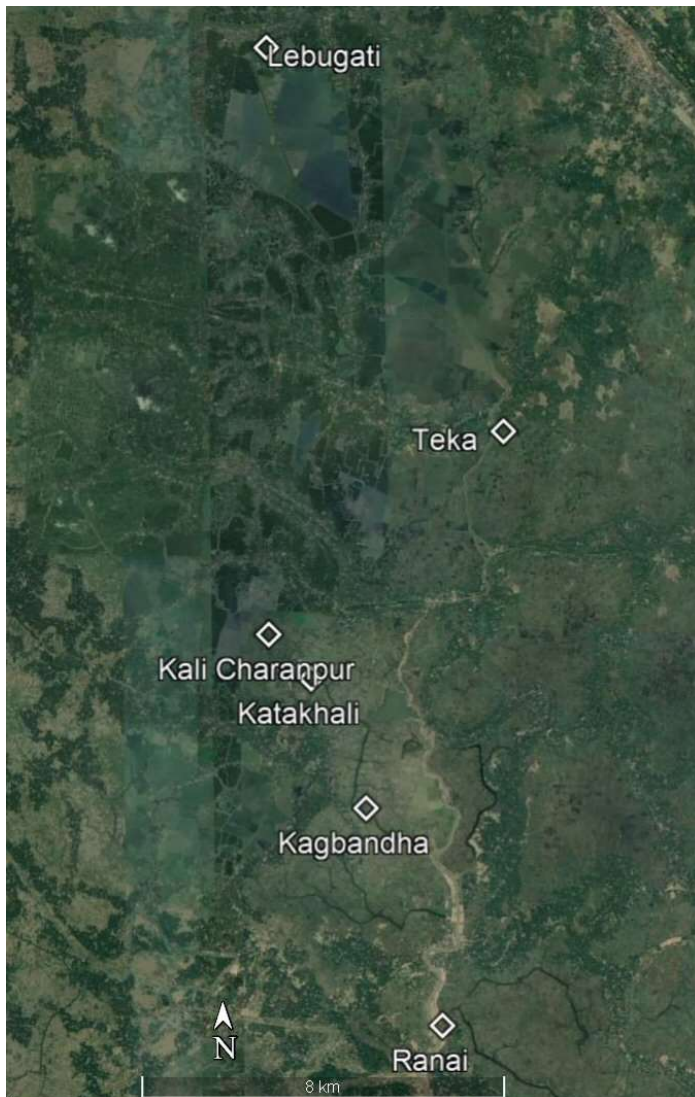


Figure 4-8 Water level gauging stations.

The water level data are based on manually recorded readings. For some periods water levels are recorded hourly, while for other periods every 3 hour. No recordings were made during the night. Examples of the water level recordings are shown in Figure 4-9 and Figure 4-10.

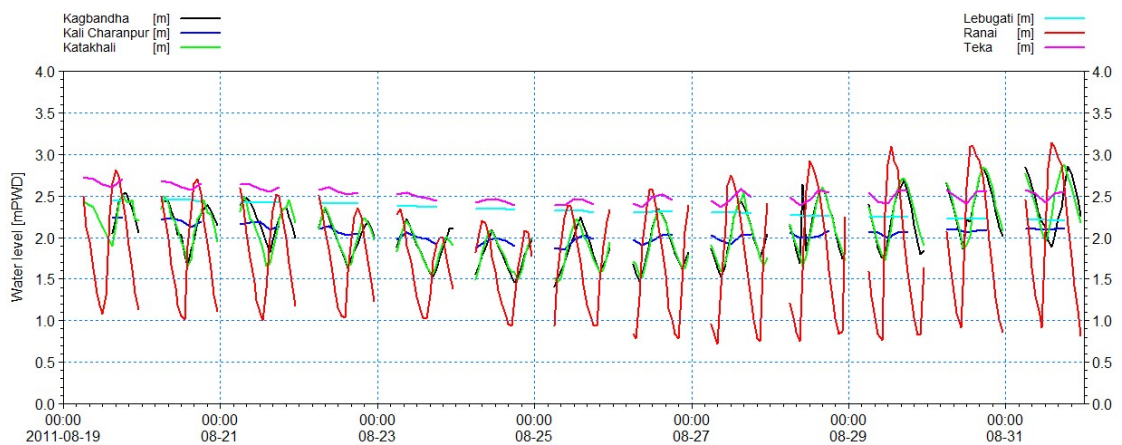


Figure 4-9 Observed water levels at the six gauging stations in August 2011.

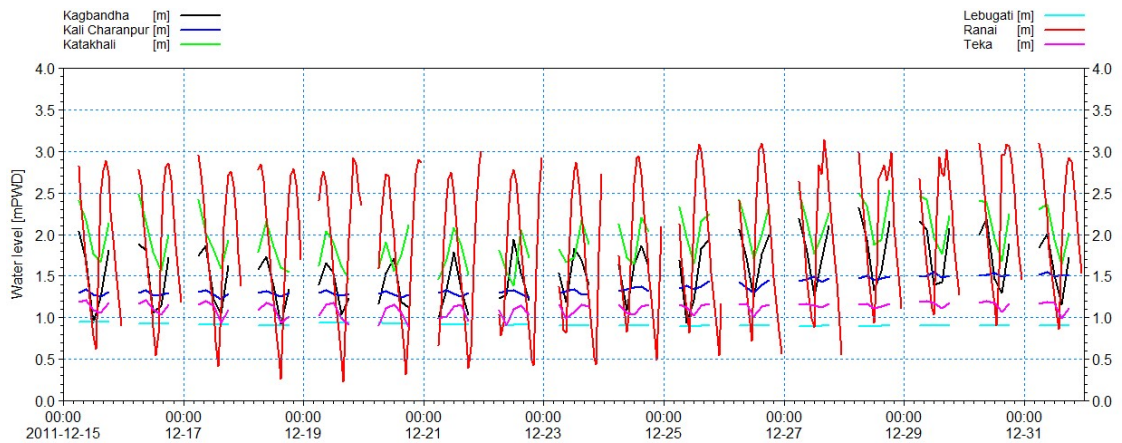


Figure 4-10 Observed water levels at the six gauging stations in December 2011.

It is seen that the observed tidal range at Ranai are in reasonable accordance with the time series shown in Figure 4-6.

Two survey campaigns of the tidal discharge were carried out at Ranai downstream the TRM basin for a tidal cycle on the 9th September 2011 and the 14th September 2011.

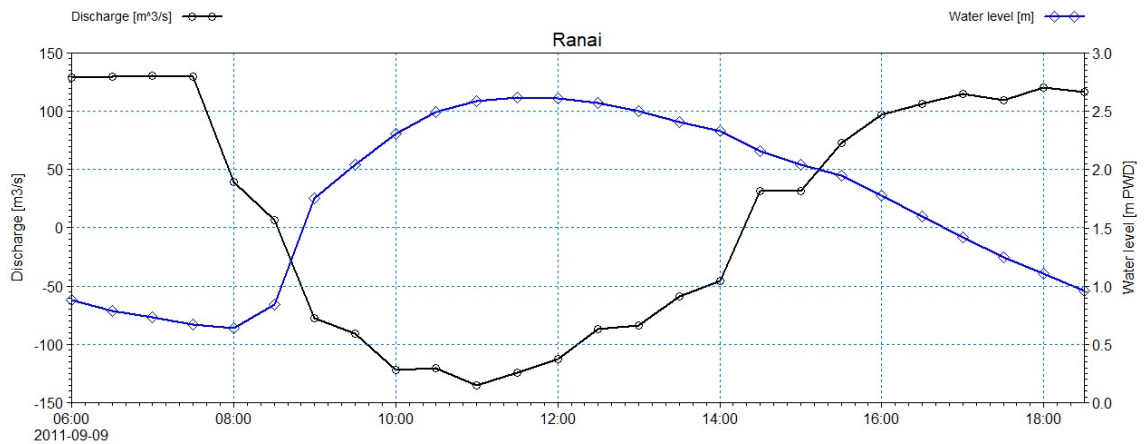


Figure 4-11 Discharge and water level observations at Ranai 9th September 2011.

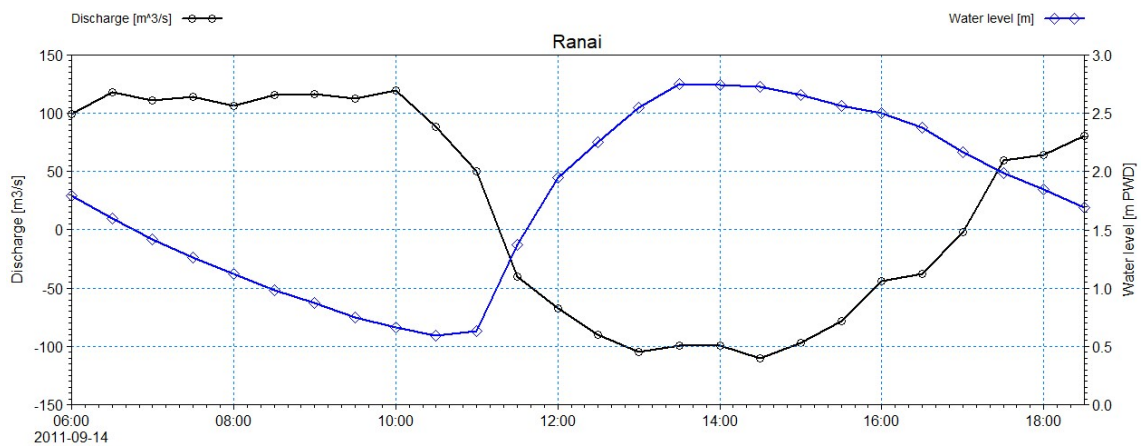


Figure 4-12 Discharge and water level observations at Ranai 14th September 2011.

The surveyed discharges are obtained at a point in time where the TRM has been operated for almost 4,5 years. The continuous deposition of sediment inside the polder reduces gradually the tidal prism over time. It is therefore expected that the tidal generated discharges are larger than the ones indicated in the plots during the first years of TRM operation.

The bed sediments are expected to primarily consist of silt. Samples of grain size distribution is only available at Bhadra located downstream of Ranai. The grain size distributions of the bed sediment in the middle of the channel and at the right bank are shown in Figure 4-13 and Figure 4-14. It is seen that the content of clay and sand is very low.

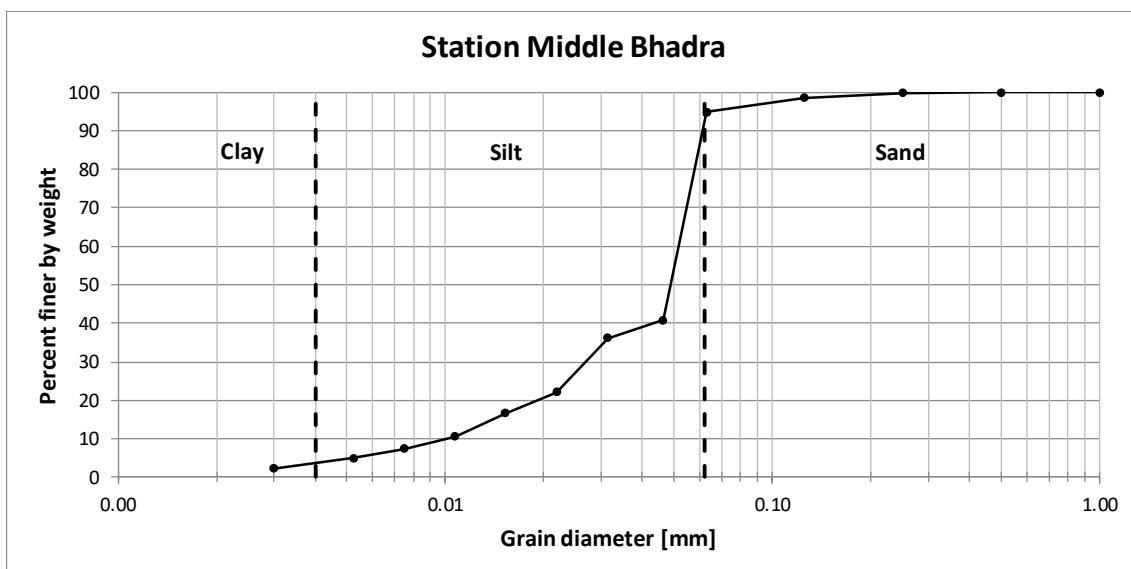


Figure 4-13 Grain size distribution of bed sediment in the central part of the channel at Bhadra.

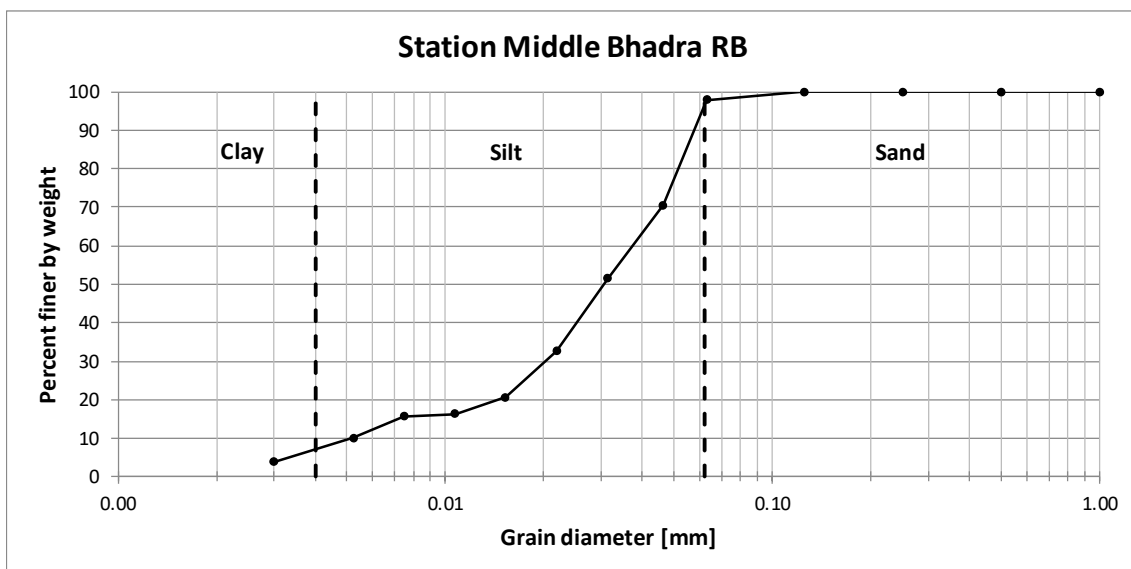


Figure 4-14 Grain size distribution of bed sediment at the right bank at Bhadra.

Suspended sediment samples have been collected at Ranai and near the channel entrance to the eastern side of the polder (Beel Khuksia) during campaigns in 2011 and 2012. The measured sediment concentrations at the two sites are shown in Figure 4-15 and Figure 4-16. From the plots, it is seen that there is a quite large temporal variation with tide and season.

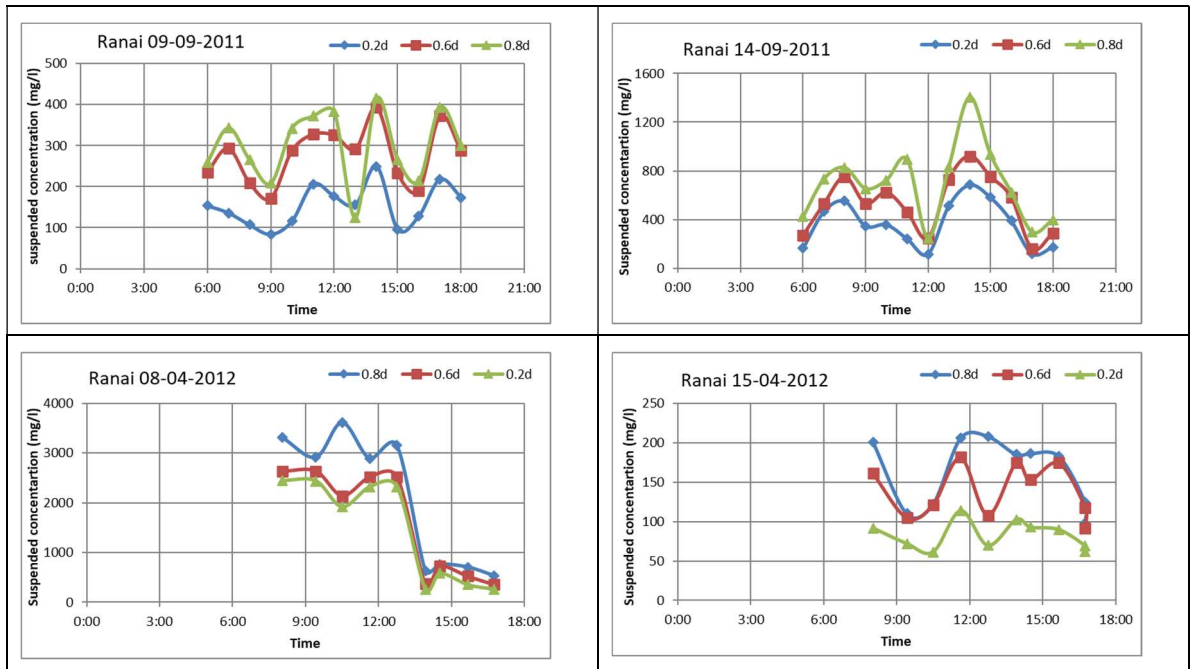


Figure 4-15 Observed suspended sediment concentrations at Ranai.

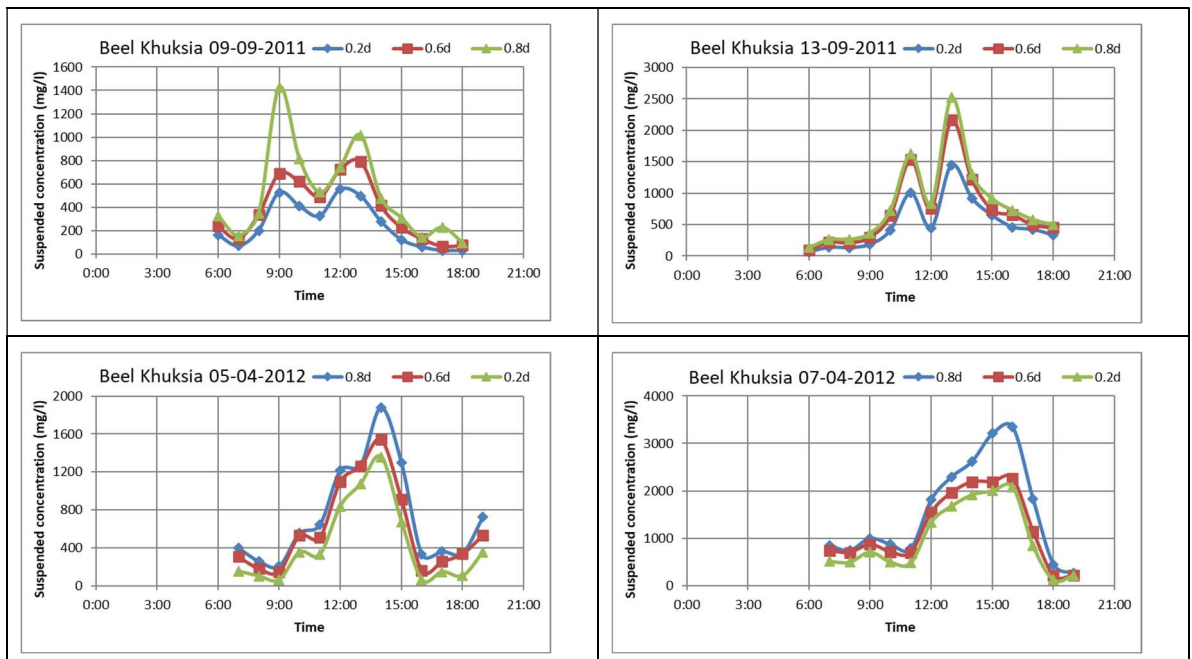


Figure 4-16 Observed suspended sediment concentrations at Beel Khuksia

The TRM model is mainly made as a conceptual model with the purpose of investigating the TRM concept and related dynamics. Table 4-1 contains a list of the model parameters applied for the modelling. The Manning number affects the flow resistance. If lowering the Manning number, the tidal induced discharge will also decrease corresponding to a damping of the dynamics. When specifying a larger settling velocity sediment will drop out of the water column faster, when increasing the critical shear stress for deposition one will allow deposition to take place in a longer time of the tidal cycle and if the critical shear stress is increased erosion will take place in a shorter time of the tidal cycle. The erosion coefficient is affecting the erosion rate and thereby how much sediment is being eroded during one tidal cycle. The dry density is determining the bed volume of the deposited sediment and the downstream sediment concentration will determine how much sediment that enters to the system

with the tide. The suspended sediment boundary condition is only active during inflow. The behaviour of the TRM model will be quite sensitive to model parameters being specified, so it can be quite a challenge to find the right combination of parameters. Especially, because the morphological calculations are quite time-consuming, it is demanding to rerun the model calculations with a modified parameter combination.

Table 4-1 Applied MIKE 21 model parameters.

Parameter	Value
Manning number	65 m ^{1/3} /s
Settling velocity	0.5 mm/s
Critical shear stress for deposition	0.2 Pa
Critical shear stress for erosion	0.2 Pa
Erosion coefficient	0.1 g/m ² /s
Dry density of bed sediment	1000 kg/m ³
Sediment concentration downstream with TRM	1.8 g/l
Sediment concentration downstream without TRM	0.4 g/l
Sediment concentration upstream	0.05 g/l

All the applied values are quite similar to those used in the MIKE 11 model and other model studies in Bangladesh and elsewhere.

4.5 Model Results

Three conceptual model scenarios have been examined and analysed with respect to tidal envelopes, morphological development and tendencies to erosion and siltation. The scenarios are as follows:

- Hari River without TRM
- Hari River and East Beel Khuksia with TRM and open entrance channel at the southern end
- Hari River and East Beel Khuksia with TRM and open entrance channel at the eastern side

Five cross sections as indicated on Figure 4-17 have been defined to keep track on how TRM and the morphological development of the system affect the tidal generated discharge. Furthermore, the predefined cross sections are used to evaluate the sediment budget of the investigated systems. Flow and sediment transport are only taking place through the Polder S and Polder E cross sections when the entrance has been specified as open.

The polder entrance channel is modelled as having an alluvial bed, i.e. the model is allowed to erode the initially predefined cross section and adapt to the capacity of the polder.

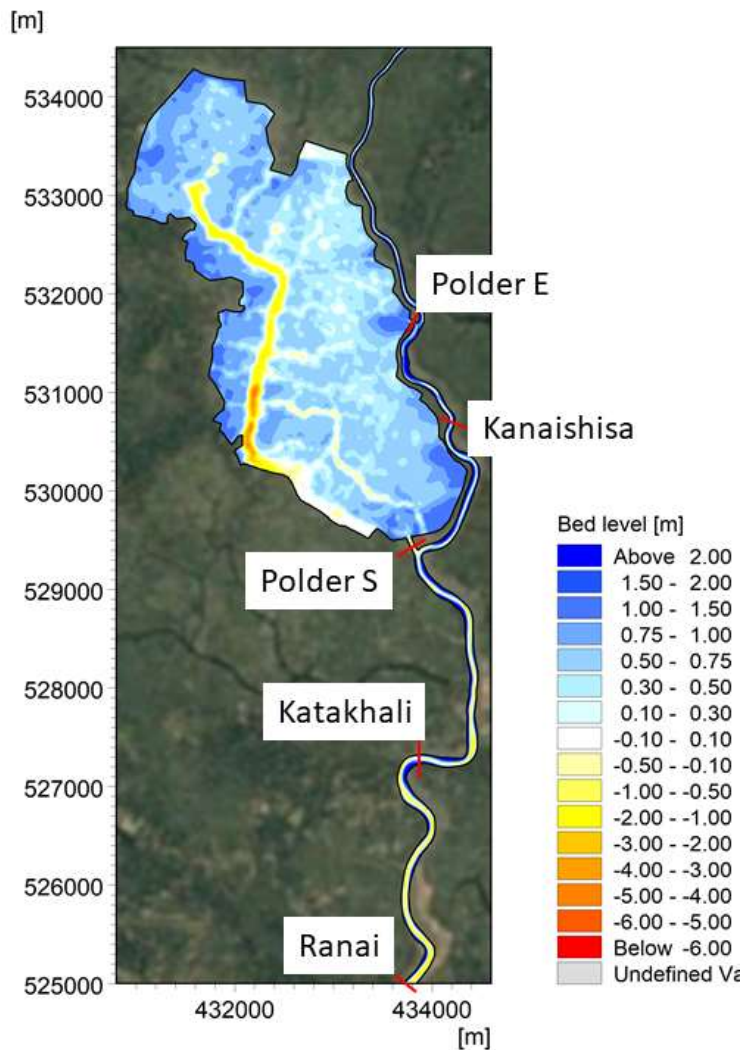


Figure 4-17 Location of cross sections used to analyse the development in tidal discharge and sediment transport.

4.5.1 The Hari River without TRM

The Hari River has a tendency to siltation caused by the tidal asymmetry, which creates an upstream directed net sediment transport that decreases with the tidal prism. First step has therefore been to model the Hari River and try to reproduce the tendency to siltation. For this model a lower value (0.4 g/l) is applied for the suspended sediment concentration at the downstream boundary compared to the TRM models (using 1,8 g/l), due to the much smaller tidal prism.

The morphological model is run cyclic six times, i.e. the modelling period covering almost a year is modelled repeatedly using the end bathymetry of the previous cycle. The modelling is thereby representing a period of almost six years.

For a siltating branch as the Hari River the tidal generated discharge will slightly decrease over time as a consequence of an increased flow resistance and the reduction of the tidal prism. The modelled flow discharges at Ranai, Katakhal and Kanaishisa are plotted in Figure 4-18 to Figure 4-20 for all six cycles. The plots show how the tidal discharge decreases when moving upstream due to the smaller tidal prism and how siltation of the Hari branch over the morphological cycles gradually reduces the tidal generated amplitudes.

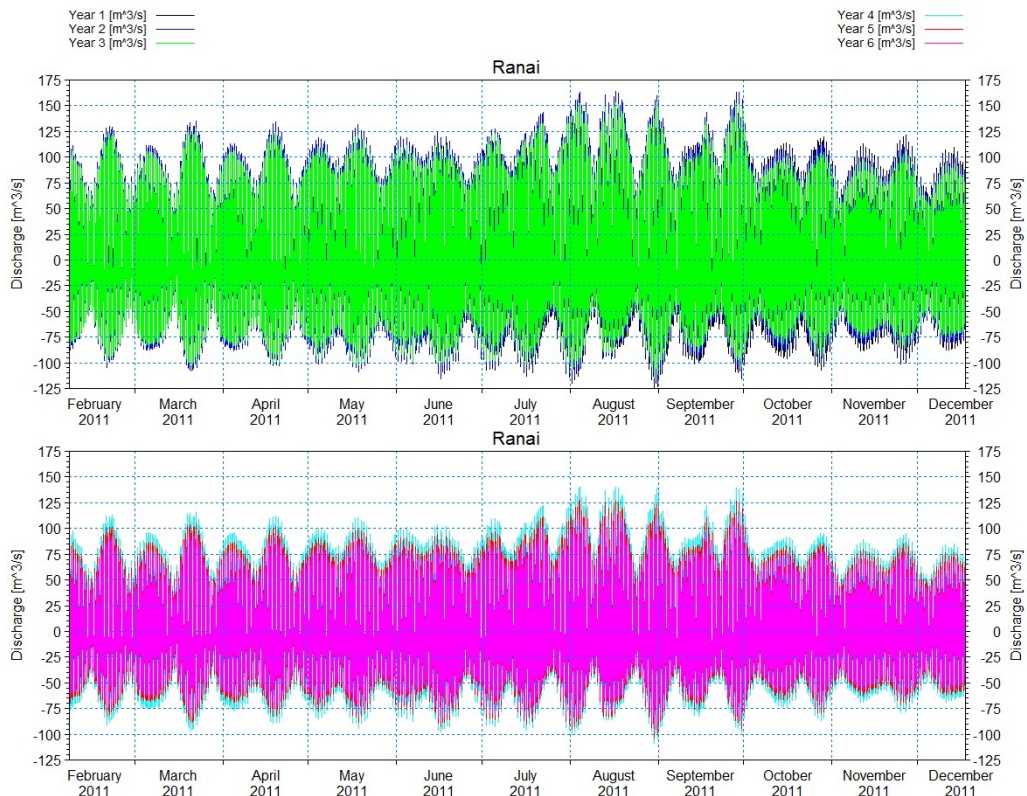


Figure 4-18 Modelled tidal generated flow discharge at Ranai for Year 1-3 (top) and Year 4-6 (bottom) without TRM. Discharge is defined positive for upstream directed flow.

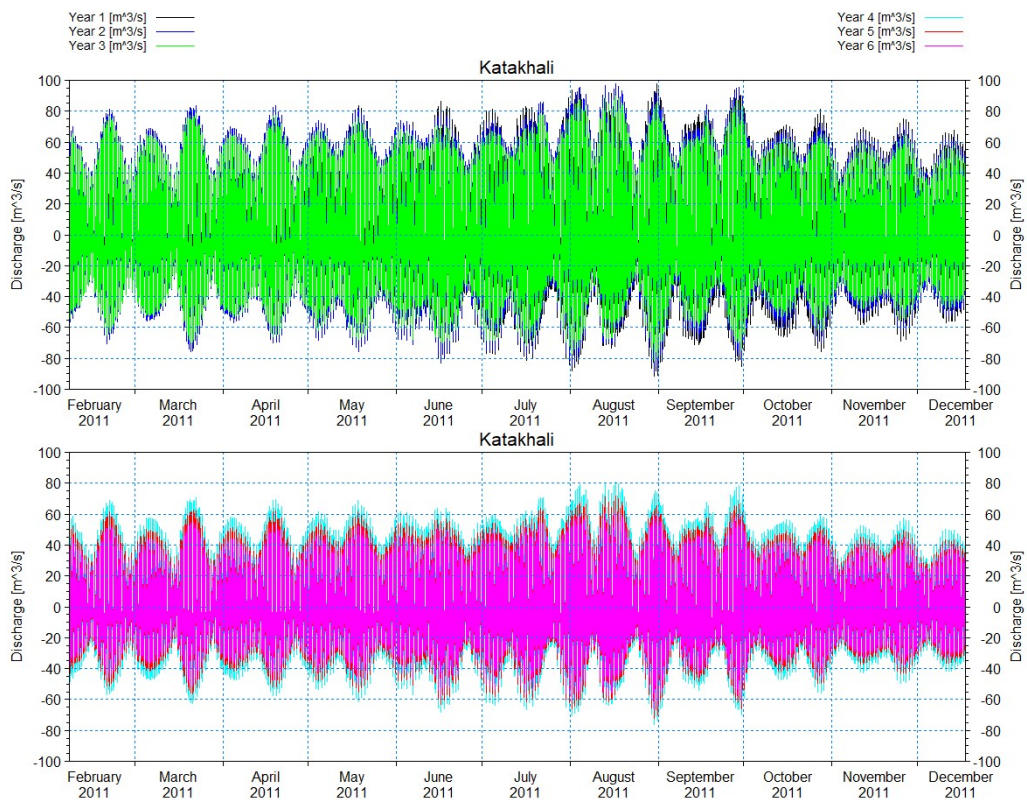


Figure 4-19 Modelled tidal generated flow discharge at Katakhal for Year 1-3 (top) and Year 4-6 (bottom) without TRM. Discharge is defined positive for upstream directed flow.

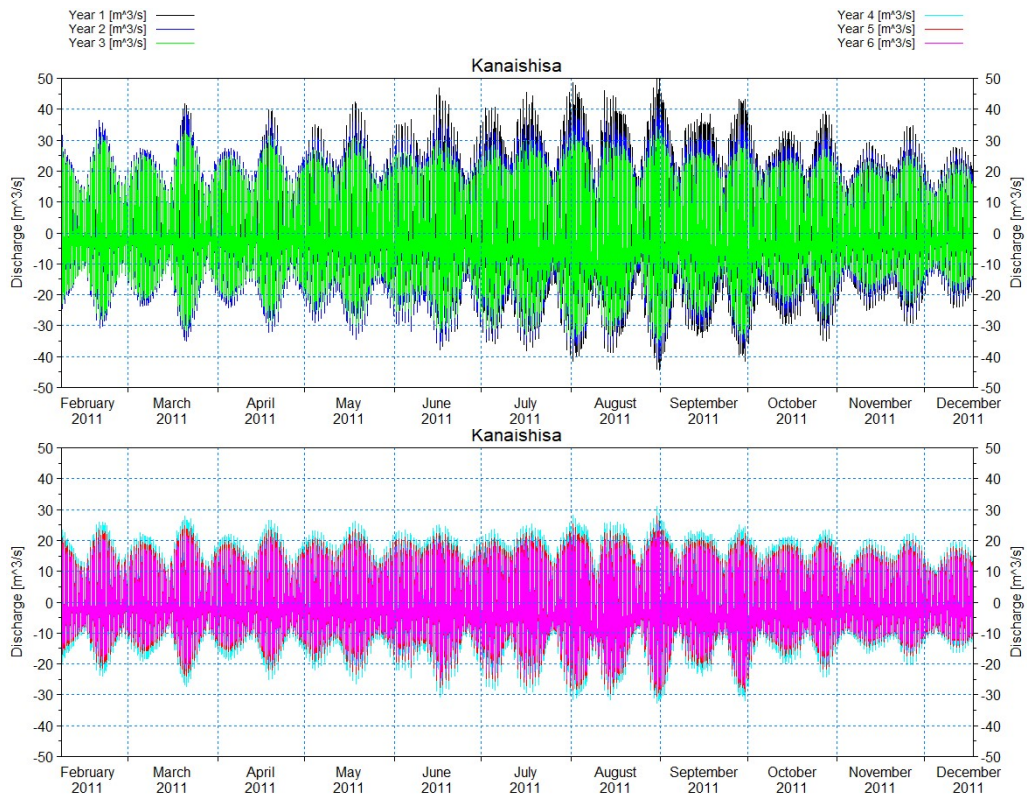


Figure 4-20 Modelled tidal generated flow discharge at Kanaishisa for Year 1-3 (top) and Year 4-6 (bottom) without TRM. Discharge is defined positive for upstream directed flow.

The gradual damping of the tidal generated discharge can also be illustrated and quantified by calculating the annual time-averaged gross discharge, i.e. averaging the absolute value of the flow discharge. Table 4-2 shows how the time-averaged gross discharge decreases over time due to gradual siltation of the branch and increased flow resistance. There is only a slight difference between the numbers for Year 1 and 2. This can be explained by the morphological adjustment of the initial bathymetry, which improves the conveyance of the system and thereby counteracts the impact of siltation. In the following years the decrease in gross discharge is only (mainly) related to the impact of siltation and thereby larger.

Table 4-2 Development of annual time-averaged gross discharge at Ranai, Katakhal, and Kanaishisa without TRM.

Cyclic period	Ranai [m ³ /s]	Katakhal [m ³ /s]	Kanaishisa [m ³ /s]
Year 1	51.1	32.1	12.3
Year 2	50.4	31.3	12.2
Year 3	46.3	28.0	10.5
Year 4	41.8	24.6	9.2
Year 5	37.8	21.7	8.2
Year 6	34.4	19.5	7.5

Figure 4-21 shows the initial bathymetry of the Hari River branch and the morphological development of bed levels the following six years (cycles). The gradual siltation of the branch can be seen from the gradual downstream migration of the blue colour representing the highest bed levels. The presented bed levels are referring to m PWD.

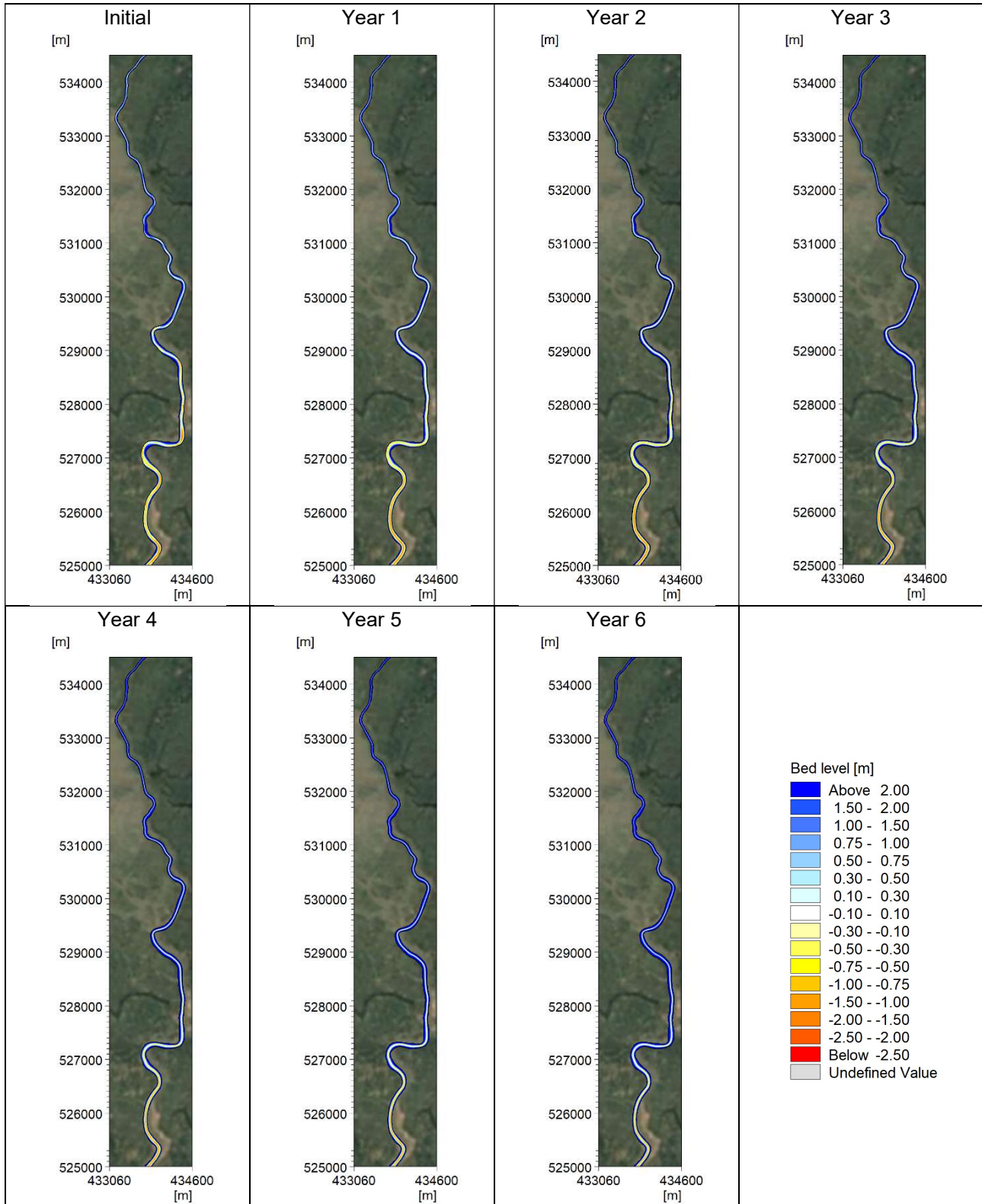


Figure 4-21 Bed level development of Hari River without TRM in the consecutive period of 6 years.

Figure 4-22 shows the bed level changes over time. The blue colours represent areas with deposition, while the red and yellow areas represent erosion. The morphological adjustment of the initial bathymetry is quite easy to identify when looking at the image for Year 1. At some reaches in the southern part erosion is the dominating mechanism to begin with.

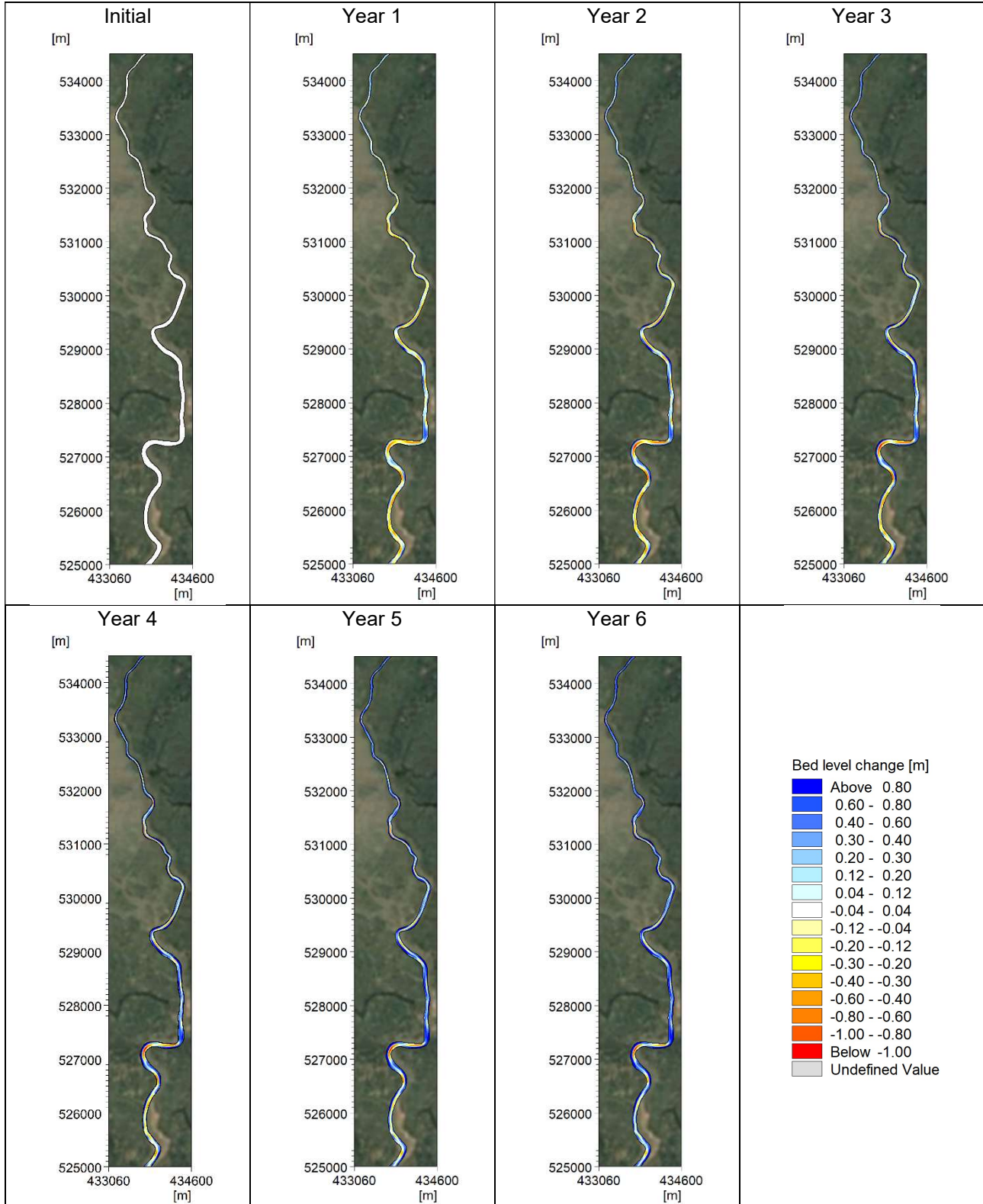


Figure 4-22 Bed level changes without TRM over a period of 6 years.

Figure 4-23 shows the annual sedimentation and erosion in the Hari River branch. The transition into a general siltation area after the morphological adjustment of the initial bathymetry is clearly seen in the plots for Year 3 to Year 6 that only contain the white and light blue colours.

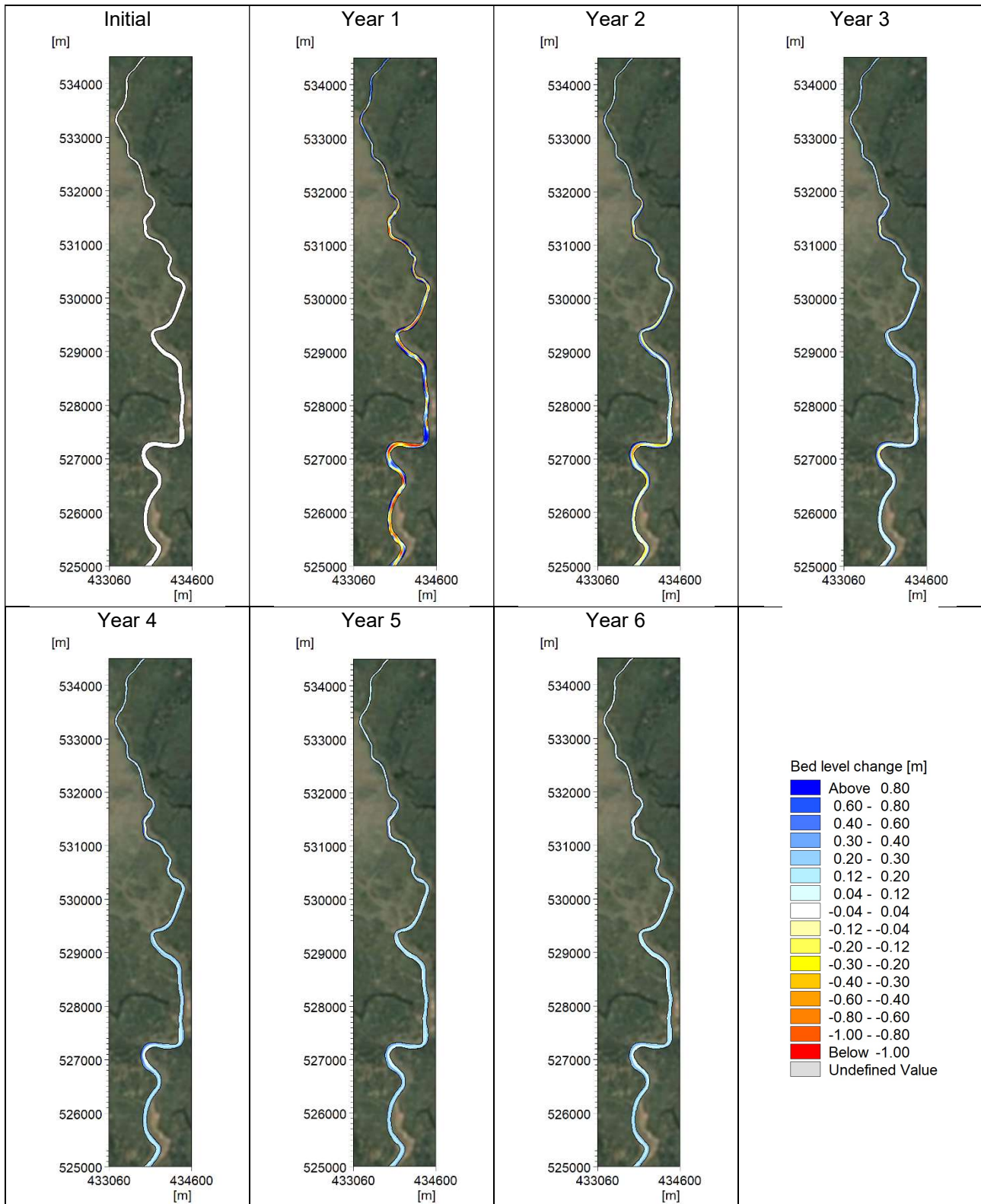


Figure 4-23 Annual bed level changes without TRM over a period of 6 years.

The temporal development of the upstream directed annual net sediment transport is shown in Figure 4-24 to Figure 4-26 for the cross sections at Ranai, Katakhal, and Kanaishisa. It is seen that the largest net sediment transport is obtained for Year 3 at Ranai and Katakhal, and for Year 2 at Kanaishisa. This indicates that the internal adjustment of the initial bathymetry plays a role for a longer period than revealed from the development of the gross discharges.

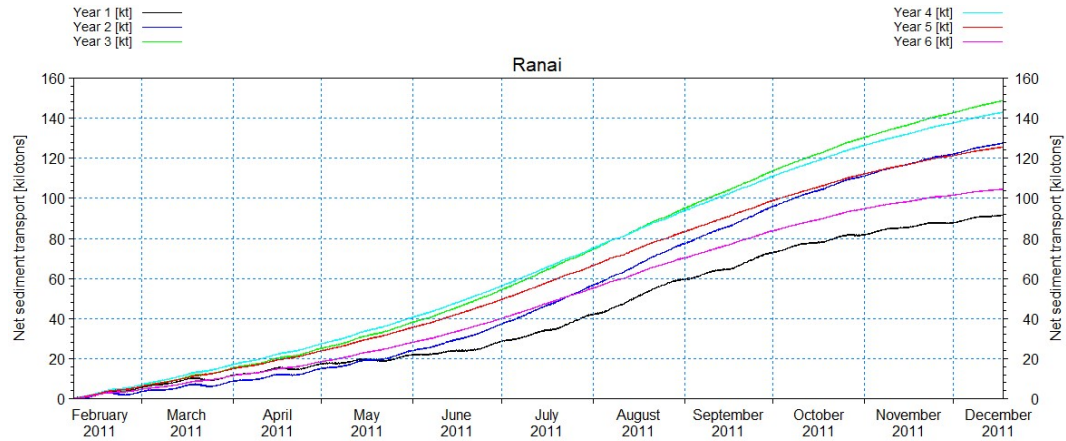


Figure 4-24 Net sediment transport (upstream directed) at Ranai for each of the 6 consecutive years.

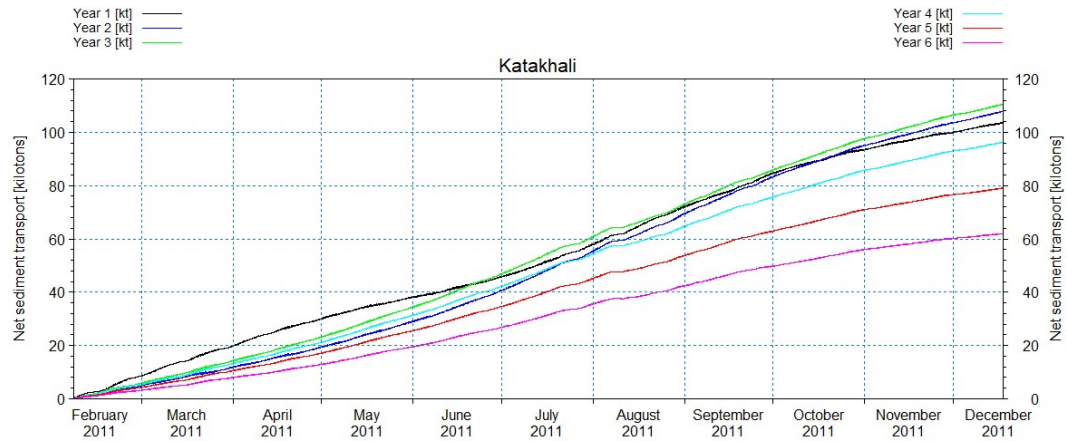


Figure 4-25 Net sediment transport (upstream directed) at Katakhal for each of the 6 consecutive years.

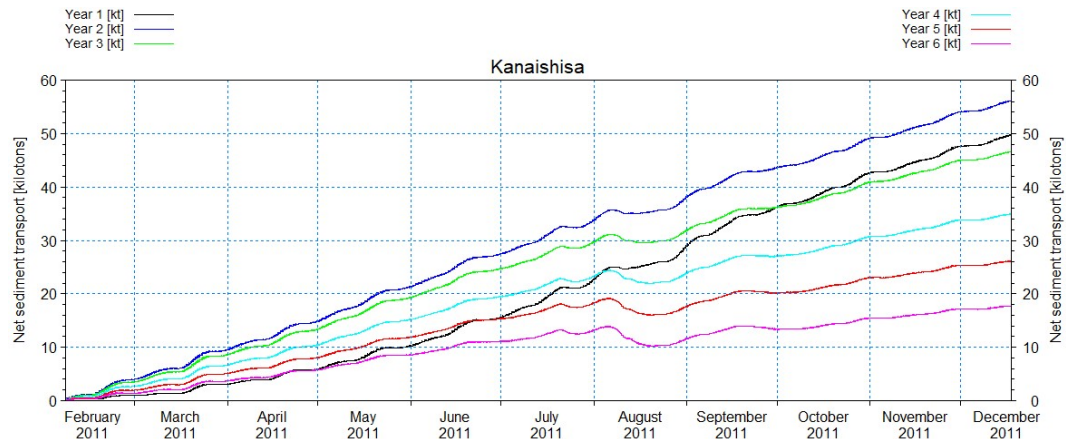


Figure 4-26 Net sediment transport (upstream directed) at Kanaishisa for each of the 6 consecutive years.

The calculated net sediment transport for each of the six cycles is listed in Table 4-3 for the cross sections at Ranai, Katakhal, and Kanaishisa. The net sediment transport at Katakhal is greater than the transport at Ranai in Year 1 even though Katakhal is located further upstream, where the tidal prism is larger. This behaviour can thereby only be explained by an increased transport related to an internal adjustment of the initial bathymetry.

Table 4-3 Net sediment transport per cyclic period at Ranai, Katakhal, and Kanaishisa.

Cyclic period	Ranai [kilotons]	Katakhal [kilotons]	Kanaishisa [kilotons]
Year 1	91.6	103.6	49.7
Year 2	127.6	107.8	56.1
Year 3	148.7	110.4	46.6
Year 4	143.0	96.2	34.9
Year 5	125.6	79.0	26.1
Year 6	104.5	61.9	17.7

The gradual siltation of the river branch can also be illustrated by the diagram (hypso-metric curve) shown in Figure 4-27. The diagram shows the area inside the Hari River branch below a certain bed level for the initial bathymetry and after each of the six morphological cycles. The diagram clearly shows the gradual buildup of the bed caused by the upstream directed net sediment transport induced by tidal asymmetry and modest runoff.

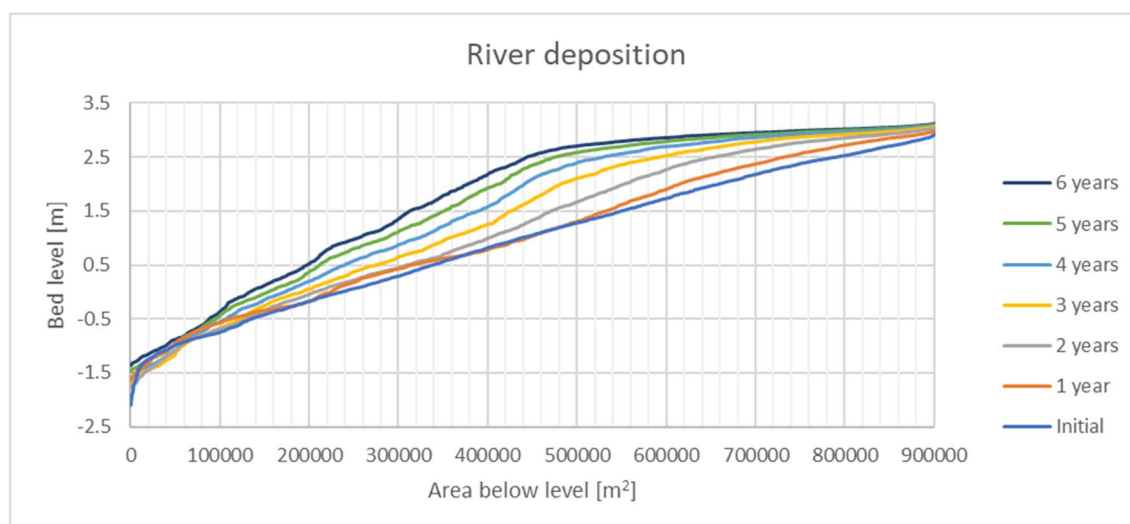


Figure 4-27 Area inside Hari River branch below a certain bed level without TRM over a period of 6 years.

4.5.2 TRM with an Opening in the Southern End of the Beel

The time scales and optimal lifetime for TRM operation have been examined using the TRM basin in Polder 24 (East Beel Khuksia) as conceptual test case. By using the cyclic morphological approach covering a period of almost 6 years annual impact is estimated and identified for both polder and peripheral river branch.

For conditions with TRM the opening into the polder will increase the tidal prism significantly and thereby introduce erosion of the peripheral river and deposition inside the polder due to the inflow of

sediment laden water. The opening into the polder will to a large degree control the exchange of water and sediment between the peripheral river and the polder. The opening and entrance channel cross section geometry and area can be maintained fixed if constructed by concrete blocks able to resist erosion. However, this will not allow the opening to adapt morphologically to the capacity of the polder. For the present modelling the channel width is maintained but allowed to erode.

When running a morphological model, the flow conductivity usually increases due to a smoothing and adaptation of the initial bathymetry compared to running the model with a fixed bed and no adaptation. The morphological development in the first year does thereby both include the morphological changes related to the polder opening dynamics, but also to the internal morphological adjustment of the initial bathymetry of the Hari River branch.

The tidal generated flow discharge at Ranai, Katakhal, Kanaishisa and at the Polder S entrance is shown in Figure 4-28 to Figure 4-31. It is seen how the largest amplification takes place in the first year due to significant erosion of the peripheral Hari River. The tidal generated discharge peaks in Year 2-3, whereafter it decreases due the initiation of siltation in the peripheral river.

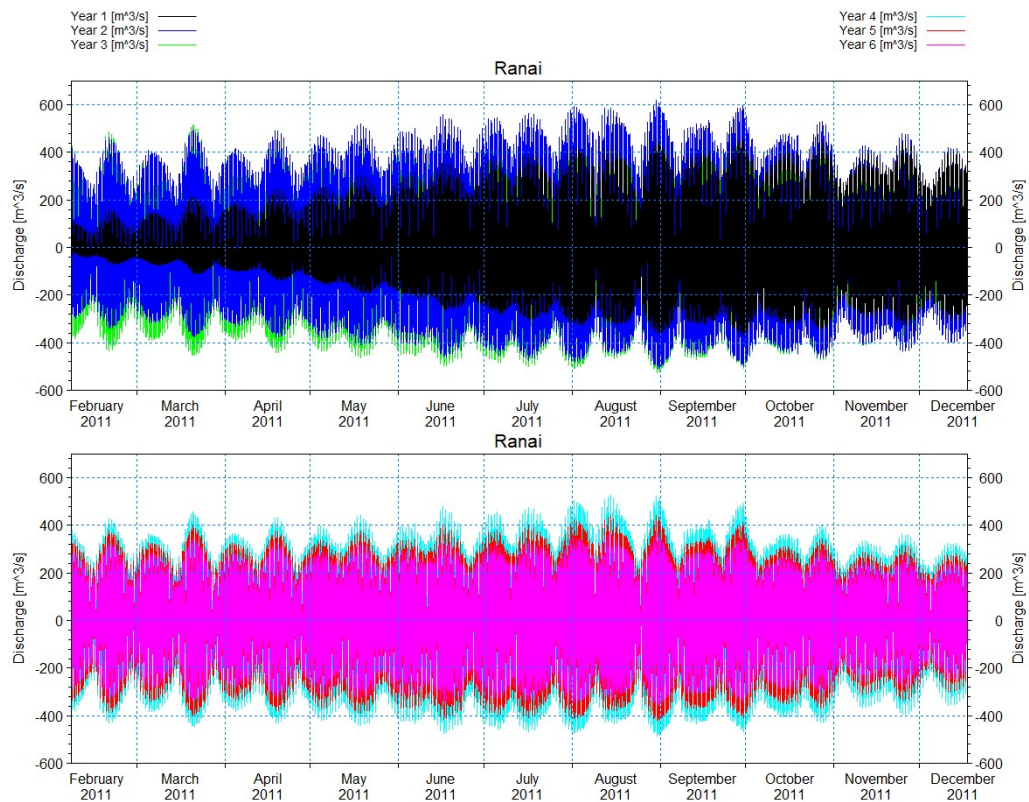


Figure 4-28 Modelled tidal generated flow discharge at Ranai for Year 1-3 (top) and Year 4-6 (bottom) with TRM and opening at the southern end. Discharge is defined positive for upstream directed flow.

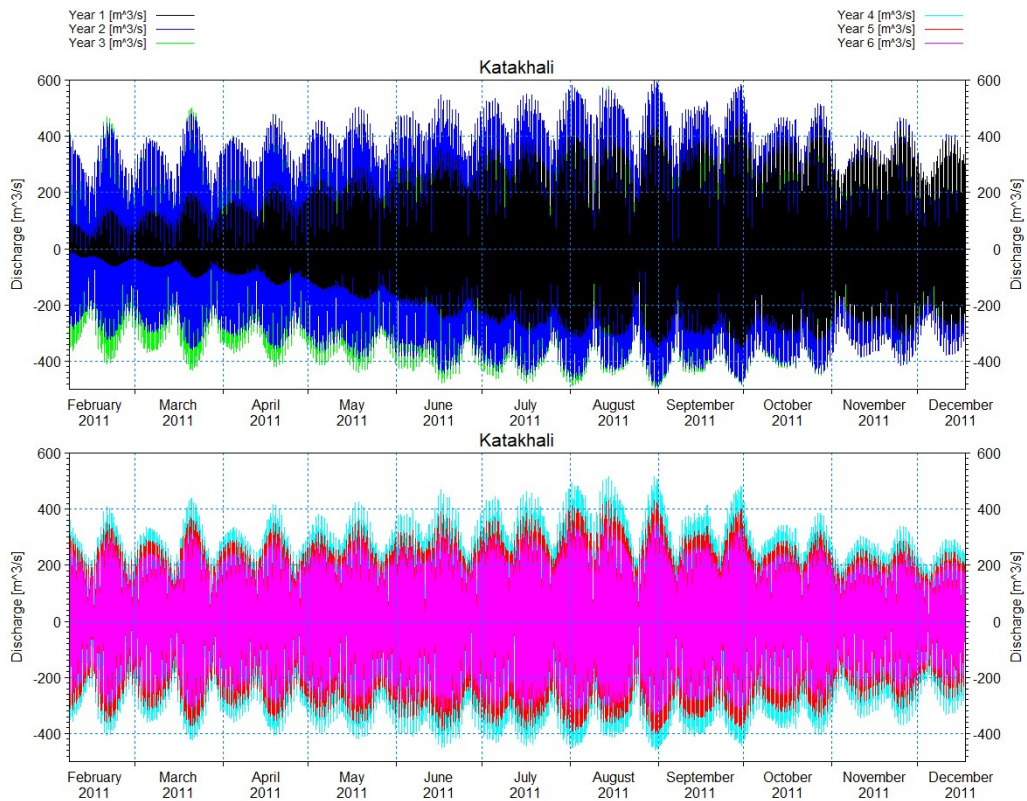


Figure 4-29 Modelled tidal generated flow discharge at Katakali for Year 1-3 (top) and Year 4-6 (bottom) with TRM and opening at the southern end. Discharge is defined positive for upstream directed flow.

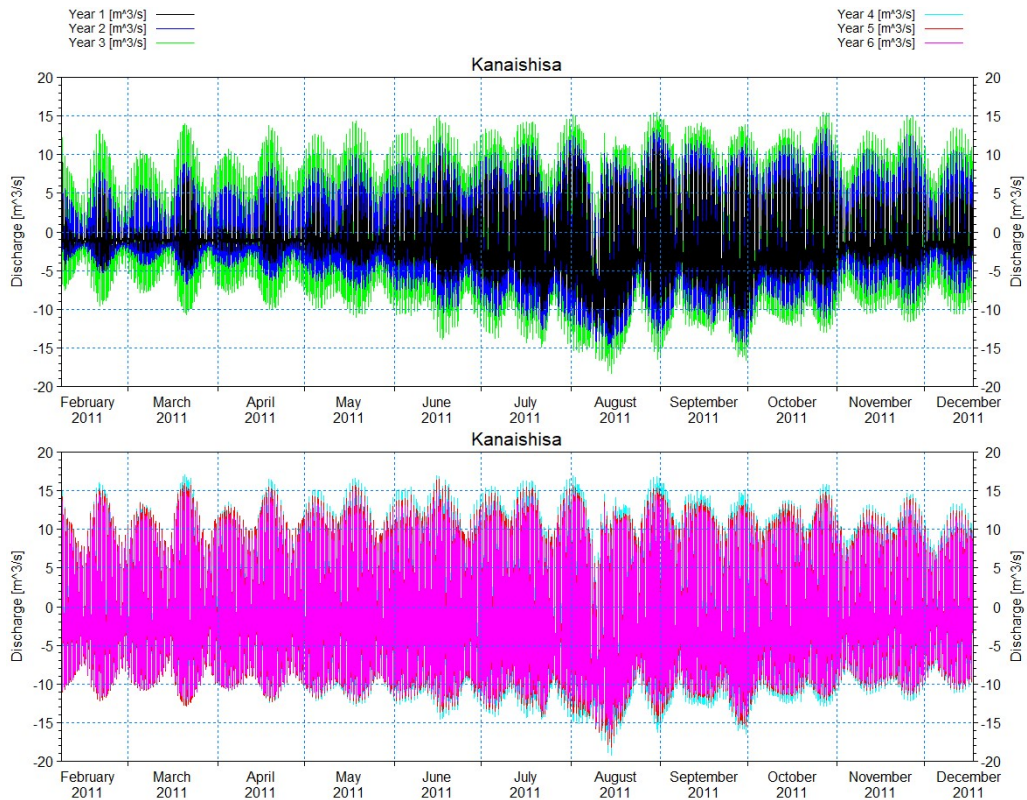


Figure 4-30 Modelled tidal generated flow discharge at Kanaishisa for Year 1-3 (top) and Year 4-6 (bottom) with TRM and opening at the southern end. Discharge is defined positive for upstream directed flow.

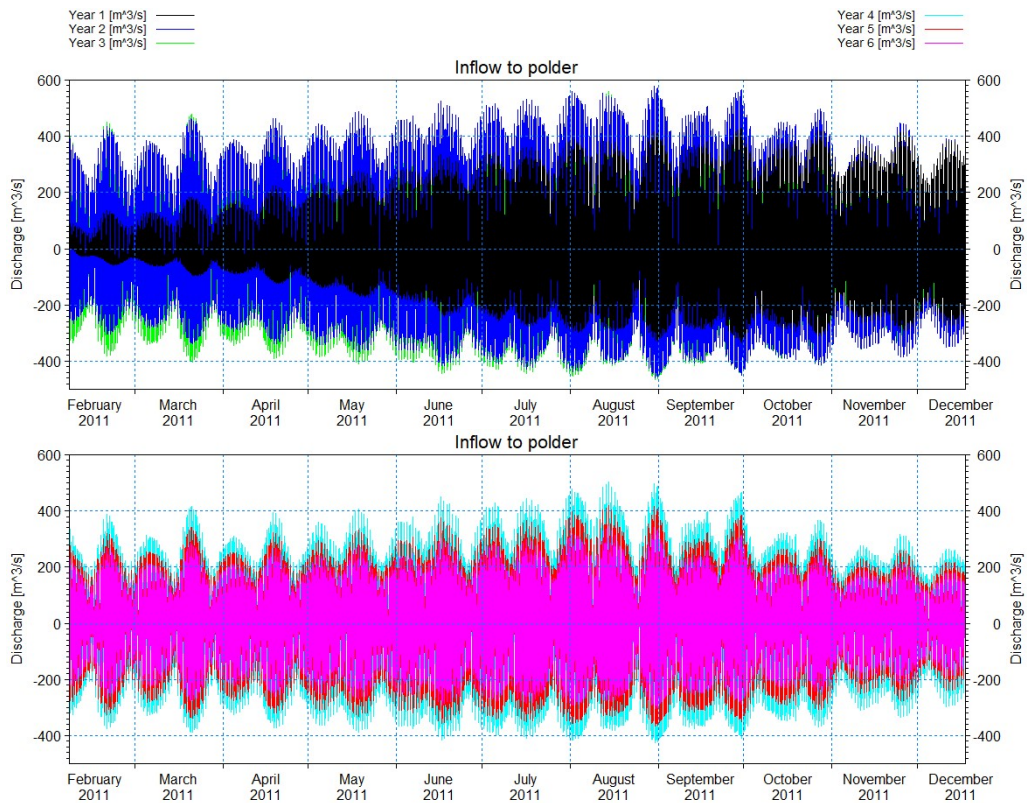


Figure 4-31 Modelled tidal generated flow discharge at Polder S for Year 1-3 (top) and Year 4-6 (bottom) with TRM and opening at the southern end. Discharge is defined positive for inflow to polder.

The significant amplification of the tidal generated discharge due to the increase of the tidal prism when opening into the polder is quantified and illustrated in Table 4-4 by calculating the annual time-averaged gross discharge.

Table 4-4 Development of annual time-averaged gross discharge at Ranai, Katakhal, and Kanaishisa with TRM and opening at the southern end.

Cyclic period	Ranai [m ³ /s]	Katakhal [m ³ /s]	Kanaishisa [m ³ /s]	Polder S [m ³ /s]
Year 1	167.7	162.8	3.2	156.2
Year 2	279.2	267.5	4.8	252.3
Year 3	277.7	261.6	6.3	241.3
Year 4	244.4	227.0	7.4	204.4
Year 5	206.1	188.4	7.2	166.1
Year 6	171.3	153.9	6.7	132.2
Year 1 without TRM	51.1	32.1	12.3	

To clarify the significant amplification of the annual time-averaged gross discharge the numbers for the first year without TRM is inserted in the end row in the table. Kanaishisa is located upstream the southern polder opening. The gross discharge at Kanaishisa is therefore quite low and actually less than obtained for the system without TRM. This indicates that TRM amplifies the tidal generated

discharge downstream the polder opening but reduces it upstream the opening. In the morphological simulations the entrance channel is defined alluvial and able to erode and thereby increase the initially defined cross section area. The gross discharge is therefore found to peak in Year 2 and thereafter slightly decrease due to the siltation inside the polder.

When selecting a beel for TRM, it can be a great advantage that it contains old branches from the time before the polders were established. The connection to old branches will ensure a high tidal envelope inside the polder and long reaches with floodplains where flood tide can enter with sediment laden flow. The opening in the southern end of the beel is located near an old main channel. This opening is therefore found to have favourable conditions for TRM.

The tidal envelope, i.e. maximum water level minus minimum water level is illustrated in the following three figures. Figure 4-32 shows the minimum water level inside the polder and the peripheral river and Figure 4-33 the maximum water level for each of the six morphological cycles. The minimum water level plots show how the main channel and formation of side channels helps to penetrate the different areas of the polder and gradually moves the deposition areas towards north and east.

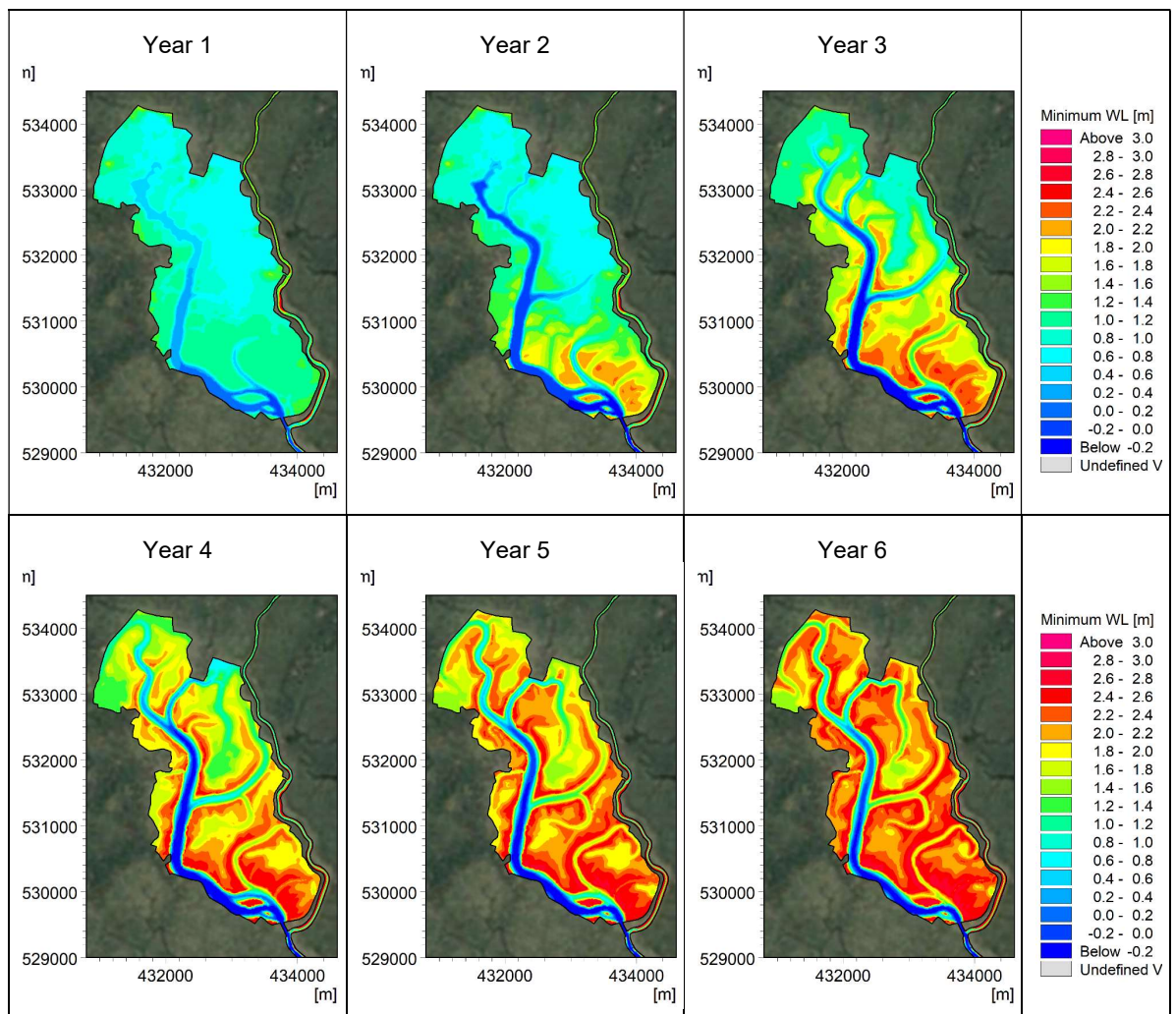


Figure 4-32 Minimum water level after activation of TRM at the southern end of the polder in the consecutive period of 6 years.

The maximum water level plots show mainly that the entire polder is being flooded at some point in time during each cycle. Furthermore, it is seen that the tidal maximum inside the beel is reached in Year 3.

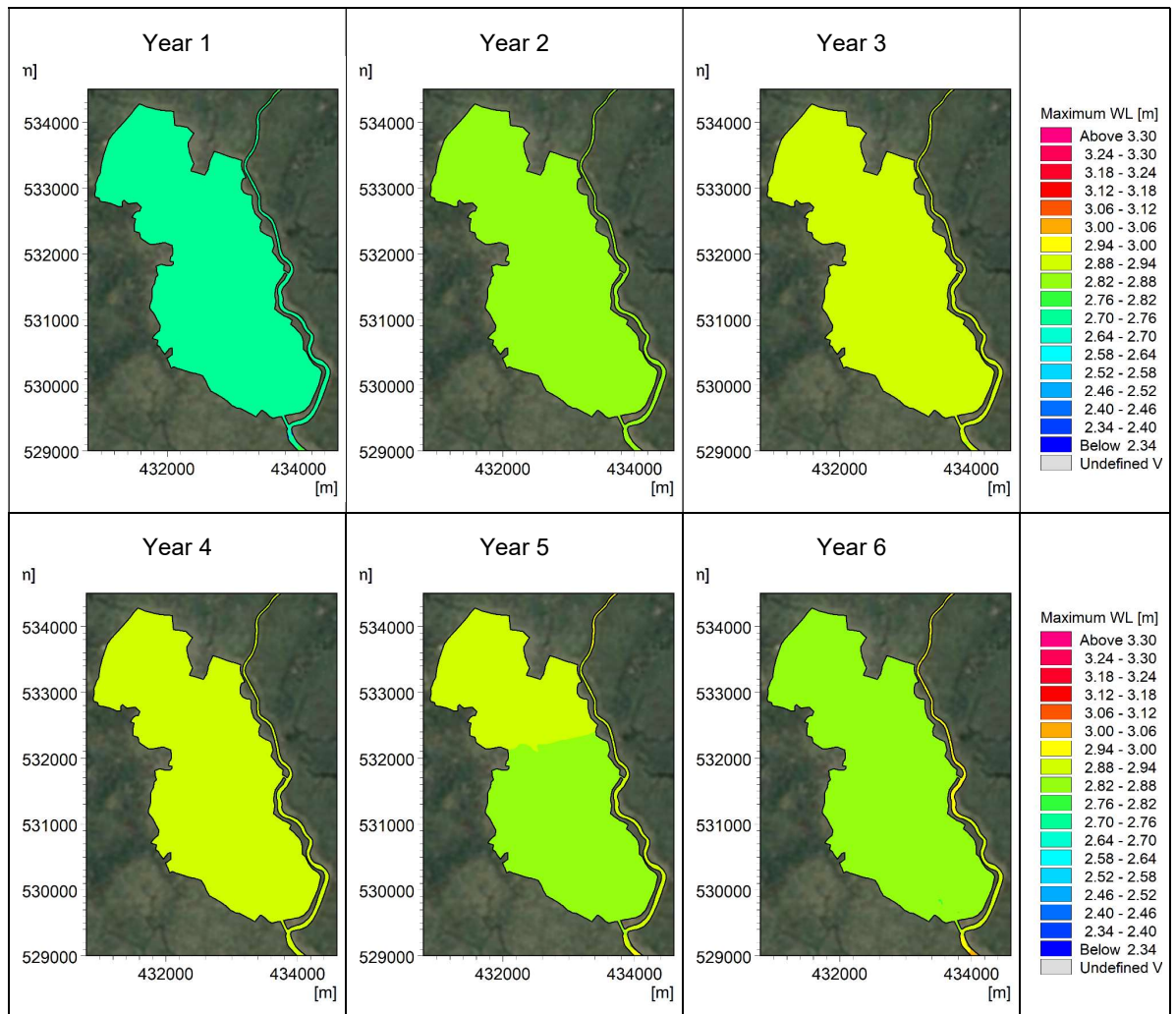


Figure 4-33 Maximum water level after activation of TRM at the southern end of the polder in the consecutive period of 6 years.

The temporal development of the tidal envelope is illustrated in Figure 4-34. A large tidal envelope inside the polder is important to maintain and ensure a significant sediment inflow to the entire polder. The images show how the tidal envelope is amplified in the side channels further to the north when the deposition in the southern part no longer can be flooded. The tidal envelope charts do also provide information on the drainage ability of the beel after closing the polder and stopping the TRM operation.

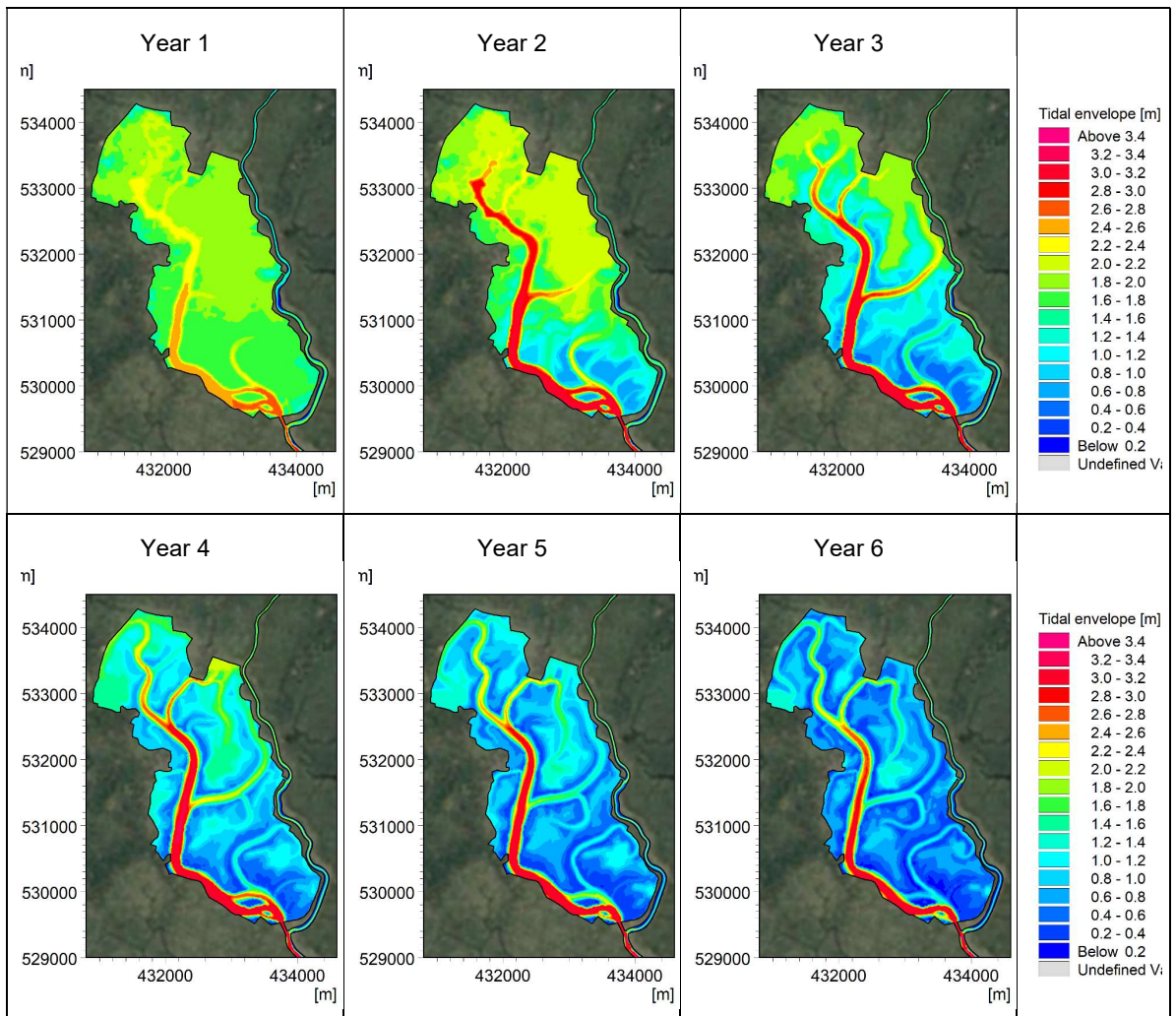


Figure 4-34 Tidal envelope after activation of TRM at the southern end of the polder in the consecutive period of 6 years.

One of the main purposes of TRM is to prevent drainage congestion. It is therefore of relevance to look at the temporal development of the tidal range at a location in Hari River just downstream the opening into the polder. Figure 4-35 shows how the tidal range is increased over time due the activation of TRM. It is the level of the ebb tide that controls the drainage ability of the beel/polder. From the plot it is seen that this improvement is achieved already in the second year of operation.

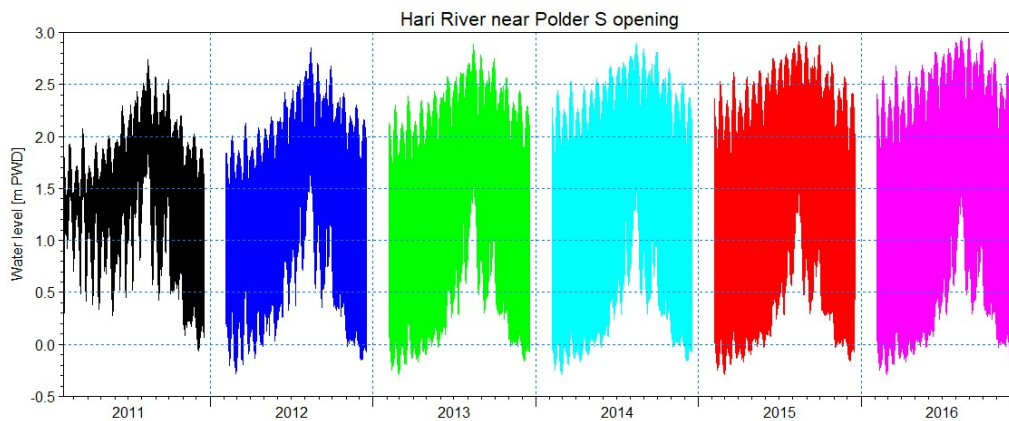


Figure 4-35 Tidal variation in Hari River near the polder opening after activation of TRM.

Figure 4-36 shows the initial bathymetry of the polder and the Hari River branch and the morphological development of bed levels the following six years after the opening into the southern part of the polder. The gradual build-up of the bed to levels above 2 m PWD and migration towards north and east is clearly seen from the images.

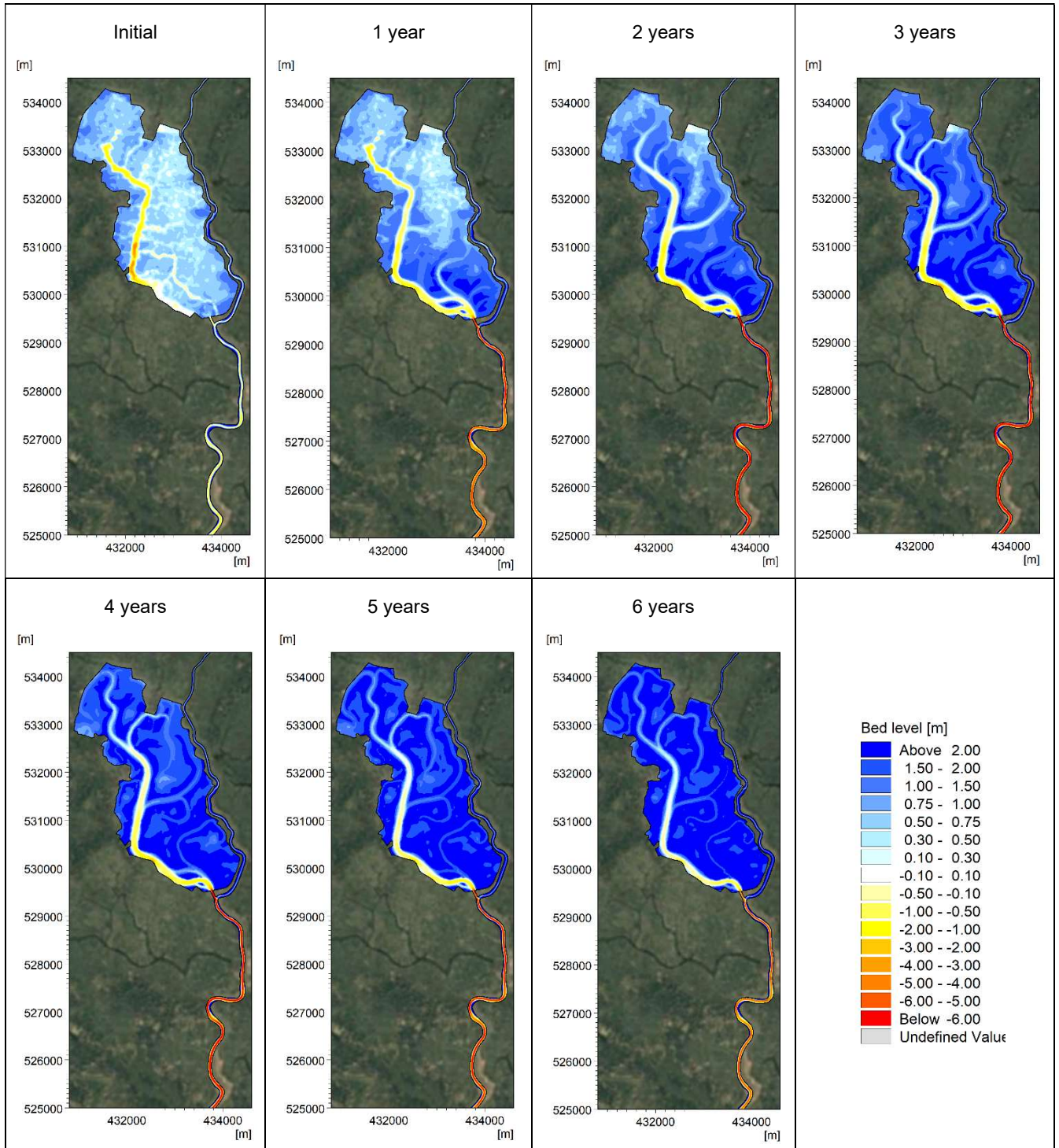


Figure 4-36 Bed level development after activation of TRM at the southern end of the polder in the consecutive period of 6 years.

The corresponding plots showing the accumulated bed level changes are shown in Figure 4-37. From the plots, it is seen how the siltation pattern gradually migrate into the polder during the first 3 years. The presence of an old channel network makes it possible for the sediment being flushed to penetrate

far inside the polder and distributed into the floodplains, where calm flow conditions allow sediment to settle. The plots also show a significant erosion taking place inside the Hari River branch downstream the opening into the polder. Erosion is also taking place in parts of the channel network inside the polder. This erosion is important to maintain the flushing ability of the polder and capability to penetrate water and sediment into the entire polder. It is also important to prevent water logging in the future system when TRM is abandoned.

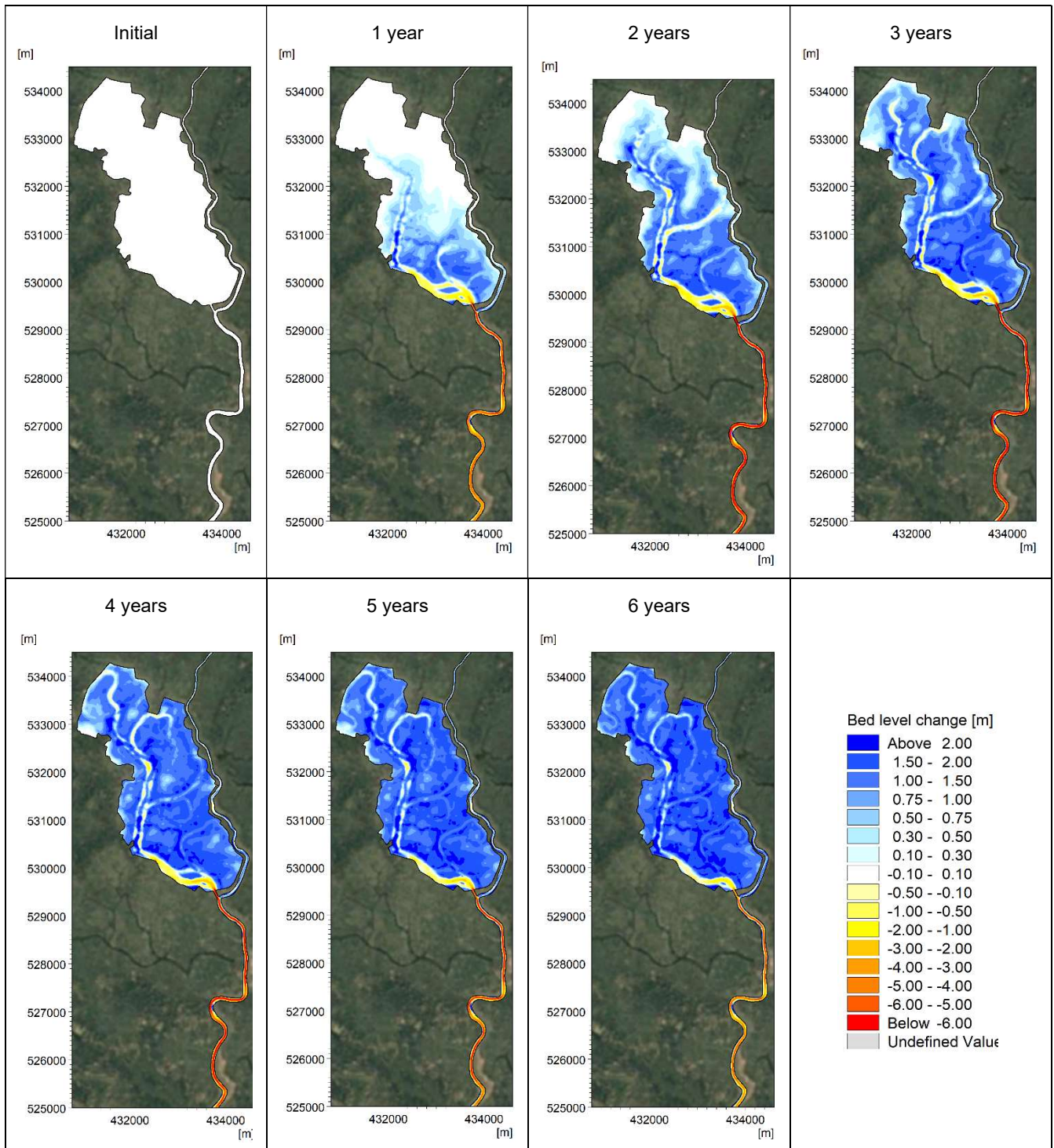


Figure 4-37 Bed level changes after activation of TRM at the southern end of the polder in the consecutive period of 6 years.

Figure 4-38 shows the annual sedimentation and erosion (i.e. for each cycle) inside the polder and the Hari River branch. It is seen that sediment is mainly settling in the southern part during Year 1. In Year 2 deposition is migrating to the middle part, while at the same time the channel network is eroding. In Year 3 settling are mainly taking place in the northern part of the polder. In this year the Hari River branch reaches an equilibrium, i.e. erosion has stopped. In year 4-6 the tidal volume of the polder is decreasing leading to siltation in the Hari River branch and the channel network inside the polder. The TRM has therefore lost its eligibility after 4 years.

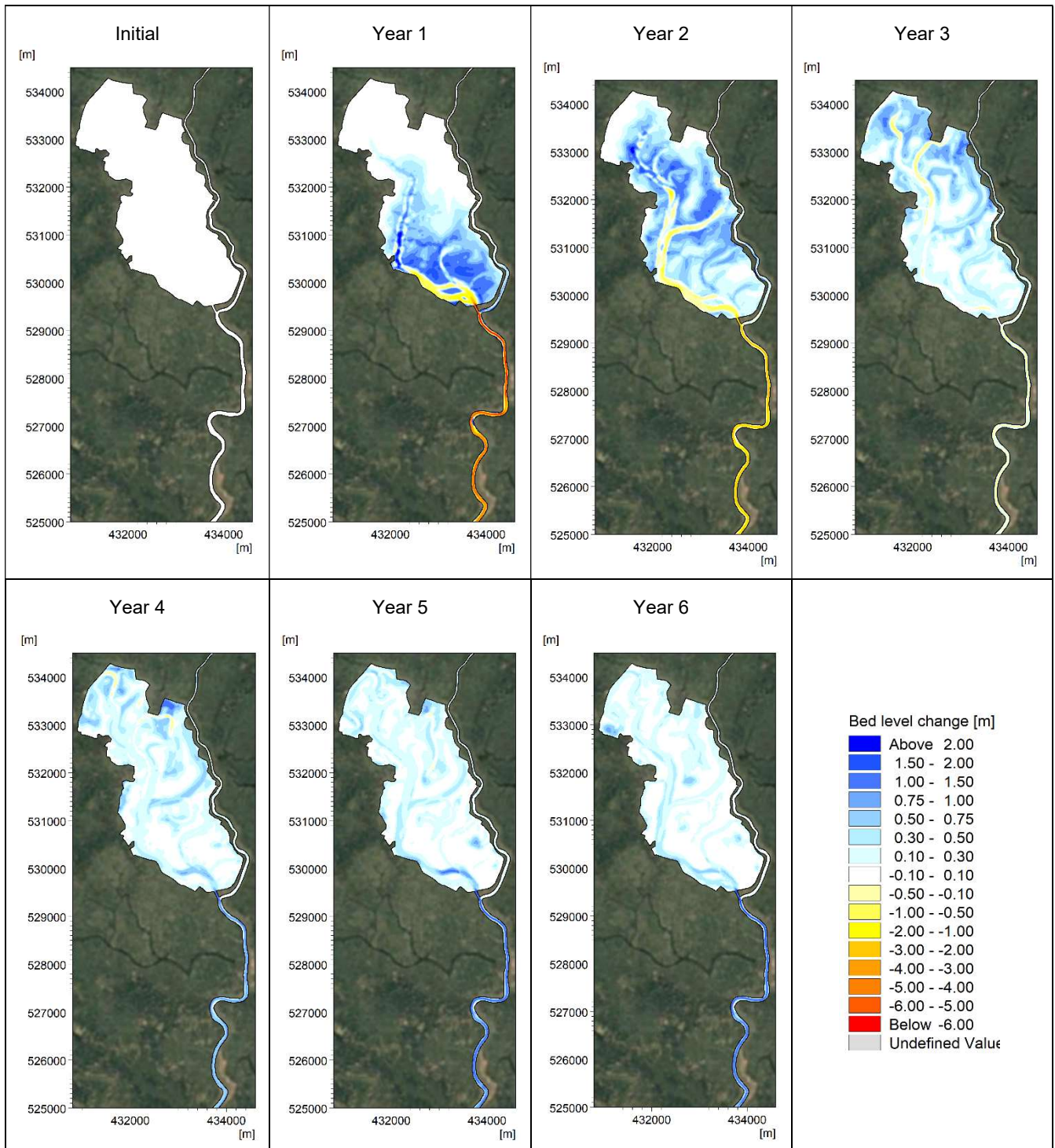


Figure 4-38 Annual bed level changes after activation of TRM at the southern end of the polder in the consecutive 6 years.

The temporal development of the upstream directed annual net sediment transport is shown in Figure 4-39 to Figure 4-42 for the cross sections at Ranai, Katakhal, Kanaishisa, and Polder S. It is seen that the largest net sediment transport is obtained for Year 2 at Ranai, Katakhal, and Polder S. Kanaishisa is located further upstream than the Polder S opening and thereby only weakly affected by the TRM.

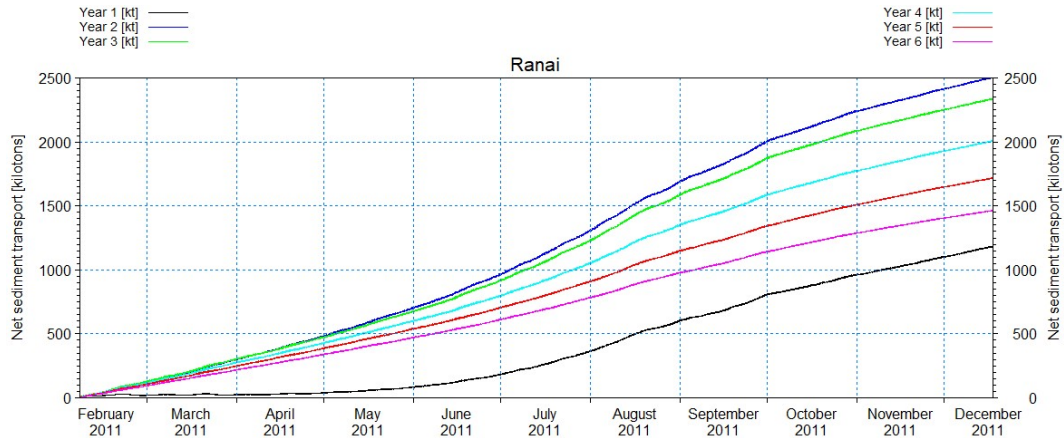


Figure 4-39 Net sediment transport at Ranai for each of the 6 consecutive years.

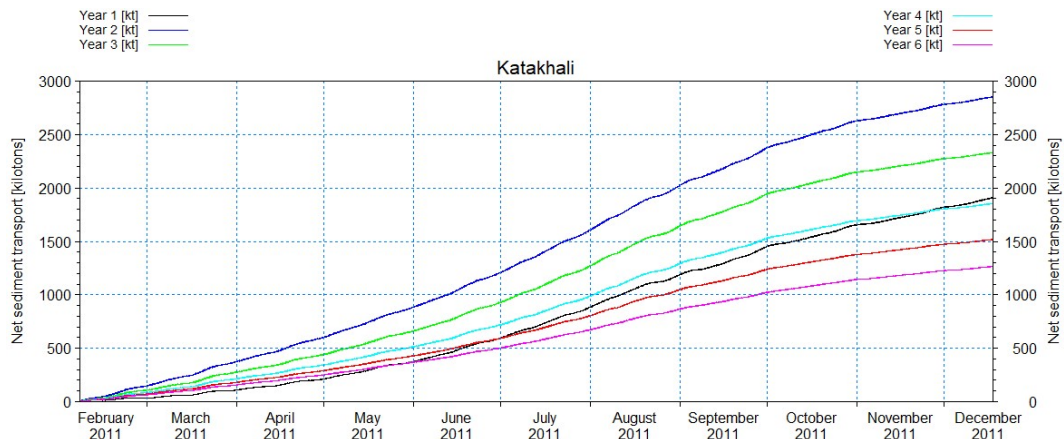


Figure 4-40 Net sediment transport at Katakhal for each of the 6 consecutive years.

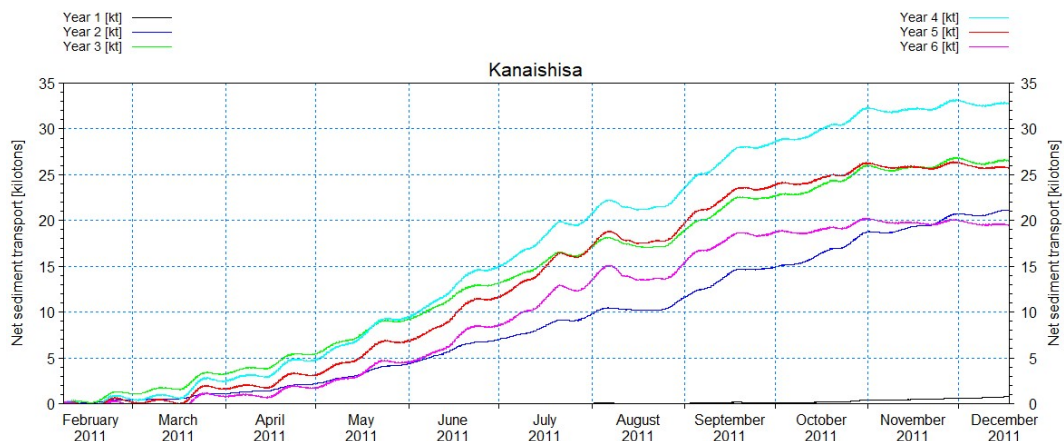


Figure 4-41 Net sediment transport at Kanaishisa for each of the 6 consecutive years.

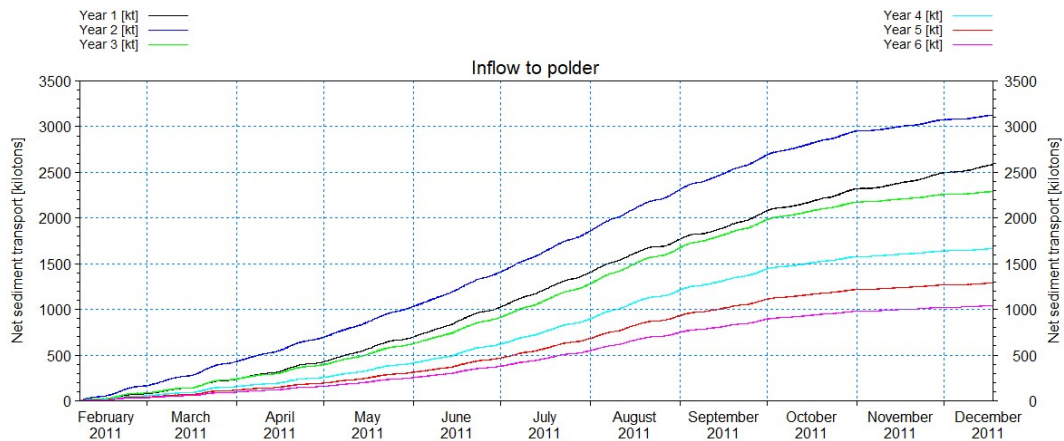


Figure 4-42 Net sediment transport at Polder S for each of the 6 consecutive years.

The calculated net sediment transport for each of the six cycles is listed in Table 4-5 for the cross sections at Ranai, Katakhal, Kanaishisa and Polder S. The net sediment transport at Katakhal is greater than the transport at Ranai in Year 1 and 2 due to the downstream migrating river erosion initiated by the opening to the polder and increased tidal prism. The beginning siltation of the river branch in Year 4 to 6 can also be revealed from the numbers in the table.

Table 4-5 Net sediment transport per cyclic period at Ranai, Katakhal, Kanaishisa, and Polder S.

Cyclic period	Ranai [kilotons]	Katakhal [kilotons]	Kanaishisa [kilotons]	Polder S [kilotons]
Year 1	1183	1909	0.7	2585
Year 2	2503	2852	21.1	3124
Year 3	2335	2330	26.5	2288
Year 4	2006	1853	32.8	1664
Year 5	1716	1517	25.7	1288
Year 6	1463	1264	19.5	1041

The achieved impact obtained by use of TRM is illustrated in Figure 4-43. The diagram shows the area inside the polder, which is located above a given bed level value for initial bathymetry and the consecutive 6 years. It is seen that it is primarily the first 3 years the TRM is well-functioning. Siltation is also taking place inside the polder in Year 4-6, but this is mainly in the drainage network, which is of severe importance for the operation of the polder after TRM operation has stopped. The diagram shows that it is almost the entire area of the beel which is elevated due to TRM. The TRM potential at a location like this is therefore very high and better than what has been achieved elsewhere.

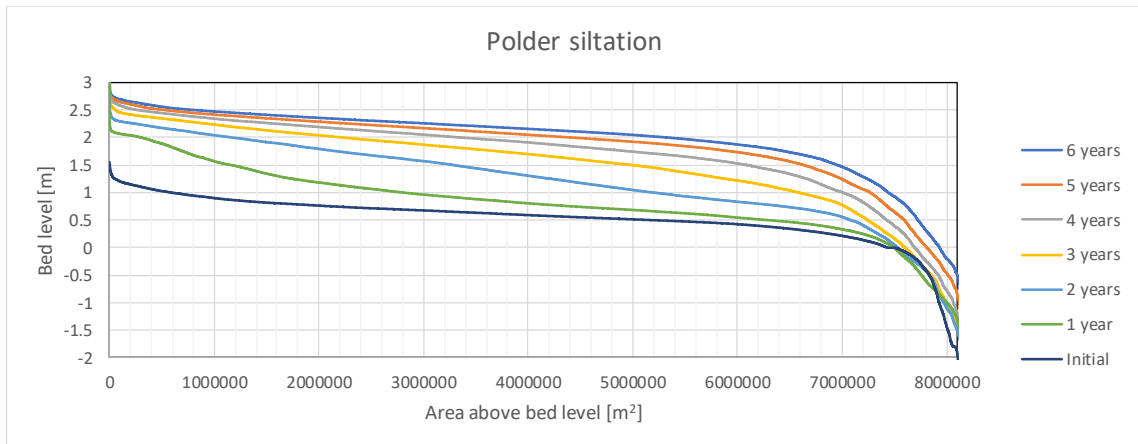


Figure 4-43 Area inside polder above a certain bed level during TRM operation.

A similar diagram (hypsothetic curve) is made for the Hari River branch and shown in Figure 4-44, however in this case with focus on the deepest parts. It is seen that significant (but favourable) erosion takes place during the first year. The erosion continues in the two following years, but with less pace. In Year 4 sediment starts to settle in the river branch and the siltation continues in Year 5 and 6 as the tidal prism of the polder decreases.

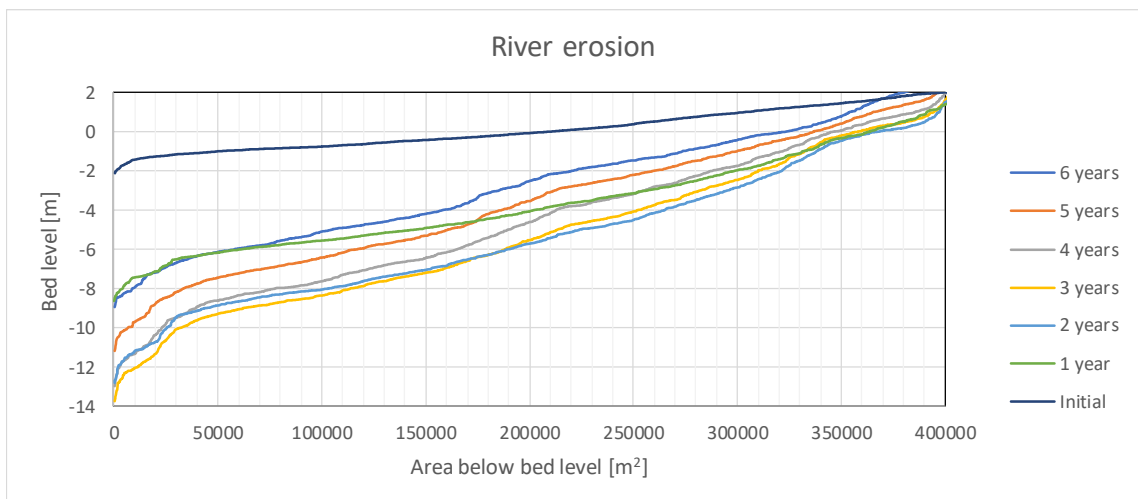


Figure 4-44 Area inside Hari River branch (downstream polder opening) below a certain bed level during TRM operation.

4.5.3 TRM with an Opening in the Eastern Side of the Beel

The opening at the eastern side of the beel is located further upstream than the opening in the south. The tidal generated discharges are therefore smaller at this location due to a smaller tidal prism (in the system without an opening). The bed levels inside the polder are relatively high in the area of the entrance channel and there is no nearby channels to help stimulating the tidal exchange. The location is not optimal compared to the southern opening, but it is examined since there historically also has been an opening at this location.

The tidal generated flow discharge at Ranai, Katakhal, Kanaishisa and at the Polder E entrance is shown in Figure 4-45 to Figure 4-48. It is seen how the largest amplification of the flow discharge takes place in the first two years due to the erosion of the peripheral Hari River. The tidal generated discharge peaks in Year 4 and 5, whereafter it decreases due the initiation of siltation in the peripheral river.

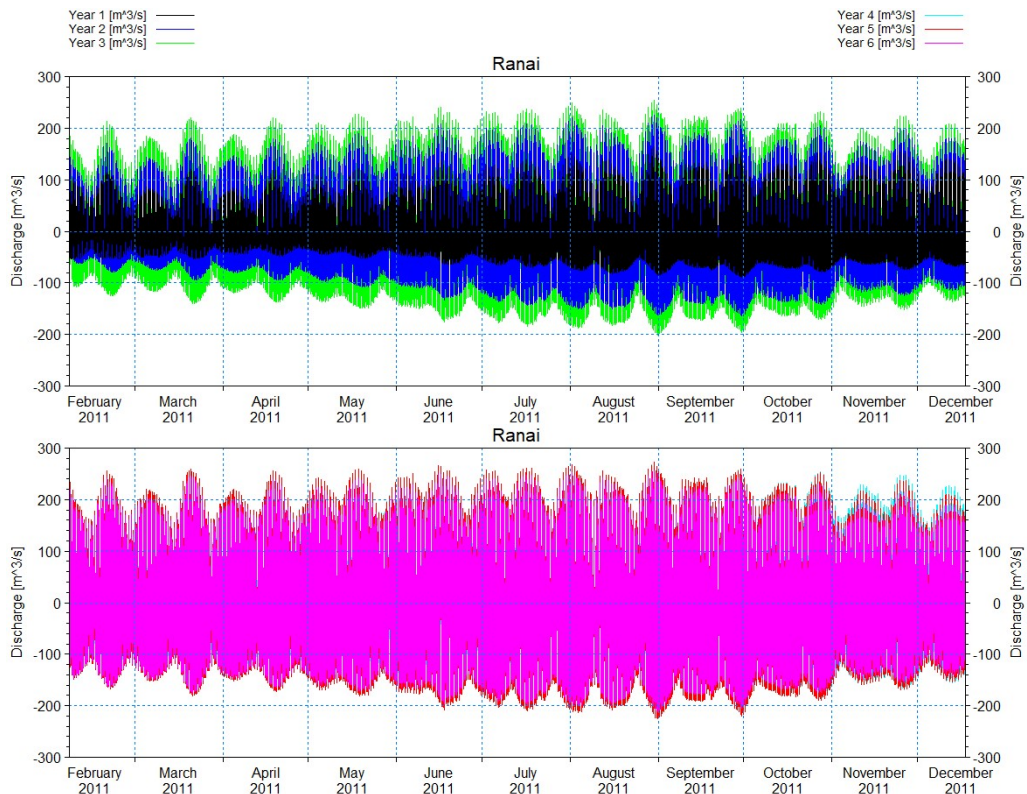


Figure 4-45 Modelled tidal generated flow discharge at Ranai for Year 1-3 (top) and Year 4-6 (bottom) with TRM and opening at the southern end. Discharge is defined positive for inflow to polder.

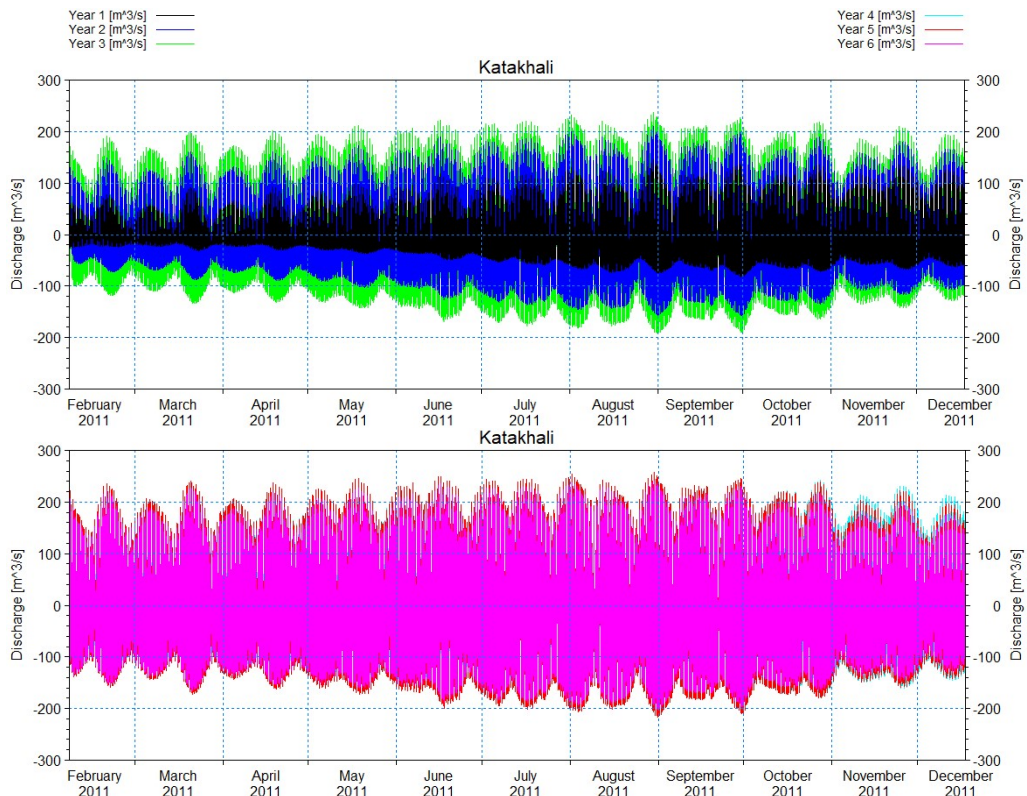


Figure 4-46 Modelled tidal generated flow discharge at Katakali for Year 1-3 (top) and Year 4-6 (bottom) with TRM and opening at the southern end. Discharge is defined positive for inflow to polder.

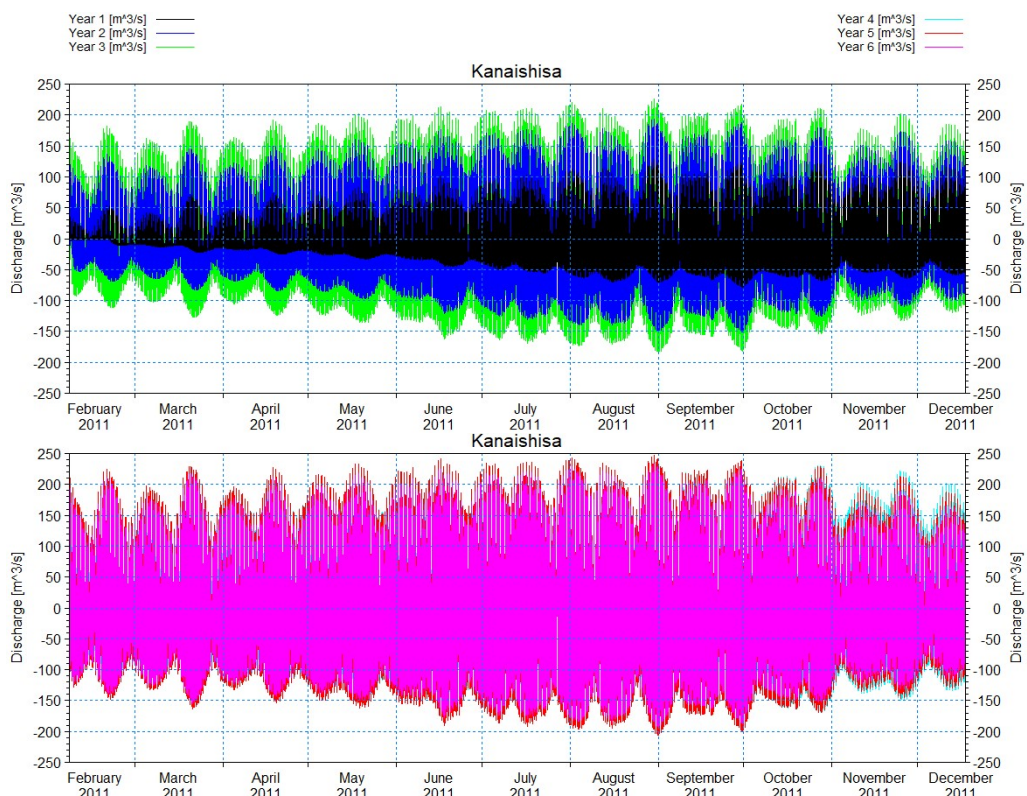


Figure 4-47 Modelled tidal generated flow discharge at Kanaishisa for Year 1-3 (top) and Year 4-6 (bottom) with TRM and opening at the southern end. Discharge is defined positive for inflow to polder.

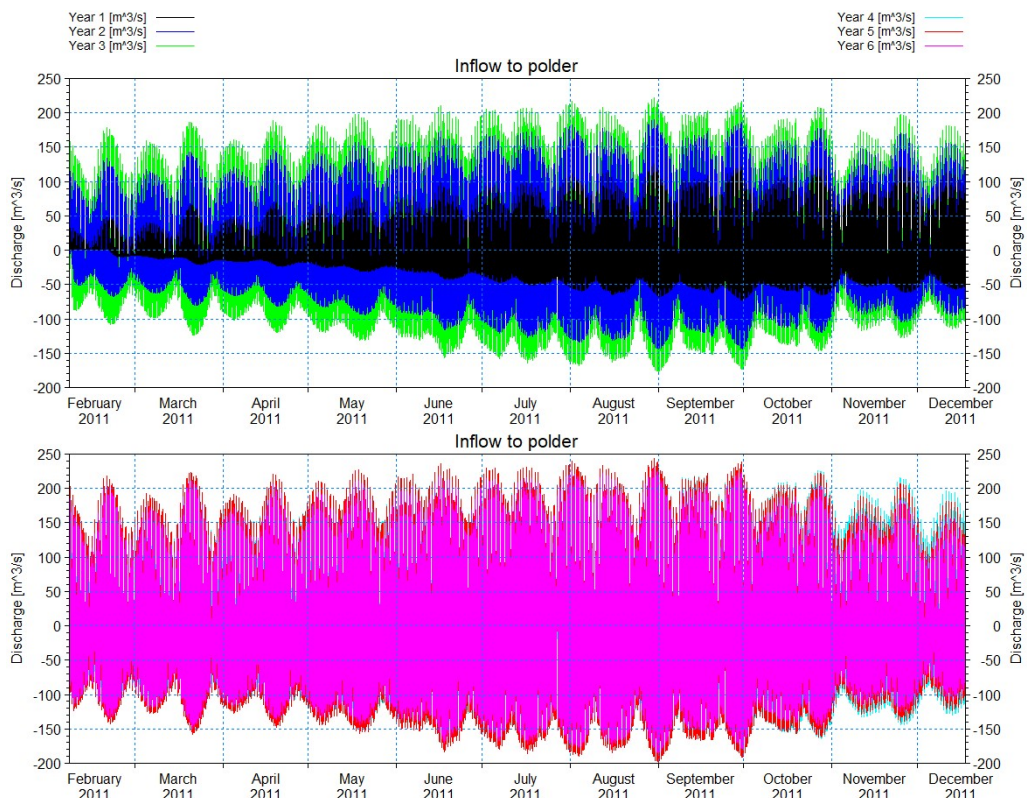


Figure 4-48 Modelled tidal generated flow discharge at Polder E for Year 1-3 (top) and Year 4-6 (bottom) with TRM and opening at the southern end. Discharge is defined positive for inflow to polder.

The significant amplification of the tidal generated discharge due to the increase of the tidal prism is quantified and illustrated in Table 4-6 by calculating the annual time-averaged gross discharge. To clarify the amplification of the annual time-averaged gross discharge the numbers for the first year without TRM is inserted in the end row. In the morphological simulations the entrance channel is defined alluvial and able to erode and thereby increase the initial cross section area. The gross discharge is therefore found to develop relatively slow and first peak in Year 4 or 5 (depending on the cross section) and thereafter slightly decrease due to the siltation of the area.

Table 4-6 Development of annual time-averaged gross discharge at Ranai, Katakhal, and Kanaishisa with TRM and opening at the eastern side.

Cyclic period	Ranai [m ³ /s]	Katakhal [m ³ /s]	Kanaishisa [m ³ /s]	Polder E [m ³ /s]
Year 1	47.9	40.4	37.4	36.5
Year 2	85.5	81.0	77.4	75.5
Year 3	108.7	104.0	100.0	97.6
Year 4	123.6	119.1	115.3	112.8
Year 5	127.3	121.3	115.6	112.4
Year 6	119.9	112.7	105.3	101.6
Year 1 without TRM	51.1	32.1	12.3	

When selecting a beel and a location for TRM, it can be a great advantage that it contains old branches from the time before the polders was established. The connection to old branches will ensure a high tidal envelope inside the polder and long reaches with floodplains, where flood tide can enter with sediment laden flow. While the opening in the southern end of the beel is located near an old main channel this is not really the case for the opening in the eastern side.

The tidal envelope, i.e. maximum water level minus minimum water level is illustrated in the following three figures. Figure 4-49 shows the minimum water level inside the polder and the peripheral river and Figure 4-50 the maximum water level for each of the six morphological cycles. The minimum water level plots show how the main channel and formation of side channels helps to penetrate the different areas of the polder and gradually moves the deposition areas towards north and east. However, the plots show that there are no channels inside the polder that could stimulate the tidal exchange except from the channel being eroded at the opening entrance and inwards.

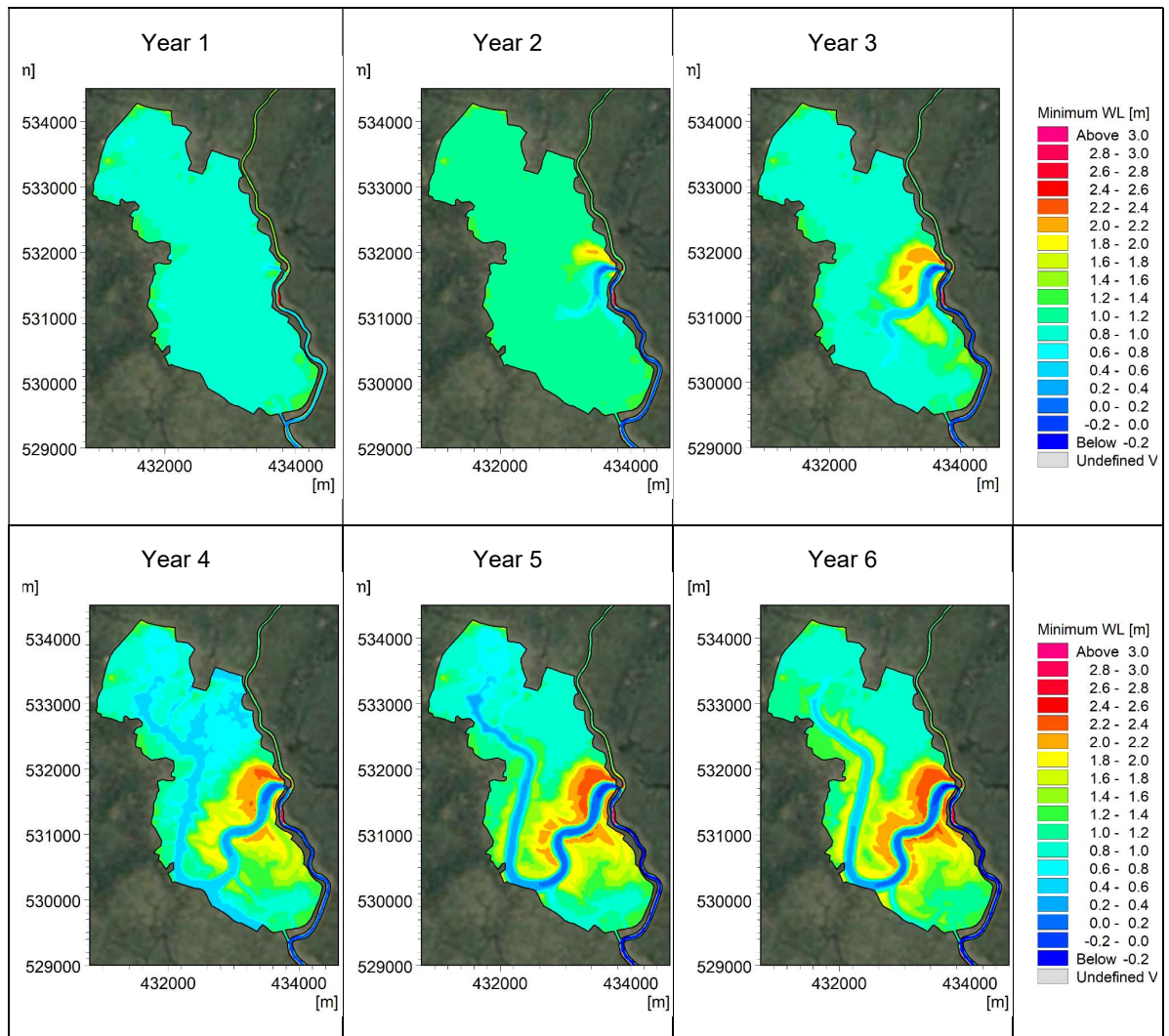


Figure 4-49 Minimum water level after activation of TRM at the eastern side of the polder in the consecutive period of 6 years.

The maximum water level plots show mainly that the entire polder is being flooded at some point in time during each cycle. Furthermore, it is seen that the tidal maximum inside the beel is reached in Year 3. It is also seen that the maximum water levels are smaller than what is achieved with an opening in the southern end. The efficiency of the TRM could have been improved if a channel connecting to the old channel network from before the polders were established had been pre-dredged.

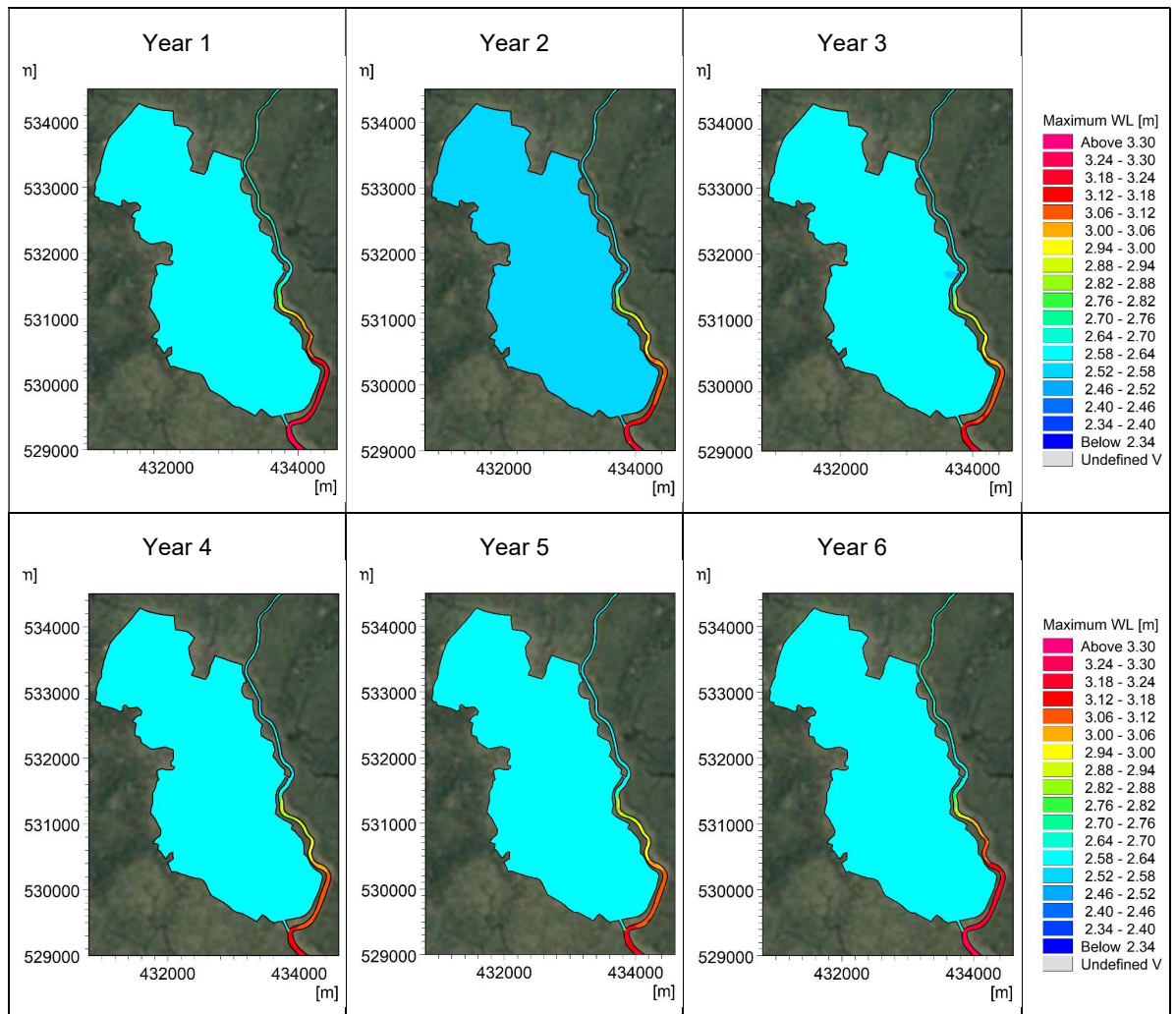


Figure 4-50 Maximum water level after activation of TRM at the eastern side of the polder in the consecutive period of 6 years.

The temporal development of the tidal envelope is illustrated in Figure 4-51. A large tidal envelope able to penetrate far inside the polder is important to maintain and ensure a significant sediment inflow to the entire polder and obtain a high TRM efficiency. The images show that the areas with a high tidal envelope only are related to the main channel. The lack of side channels limits the deposition to the nearby floodplain areas along with the main channel. The efficiency of the TRM is therefore not very good as compared to the scenario with an opening in the southern end. Pre-dredging or dredging inside the beel during the TRM operation to stimulate the generation of side channels seems to be a way forward to obtain and increased TRM efficiency.

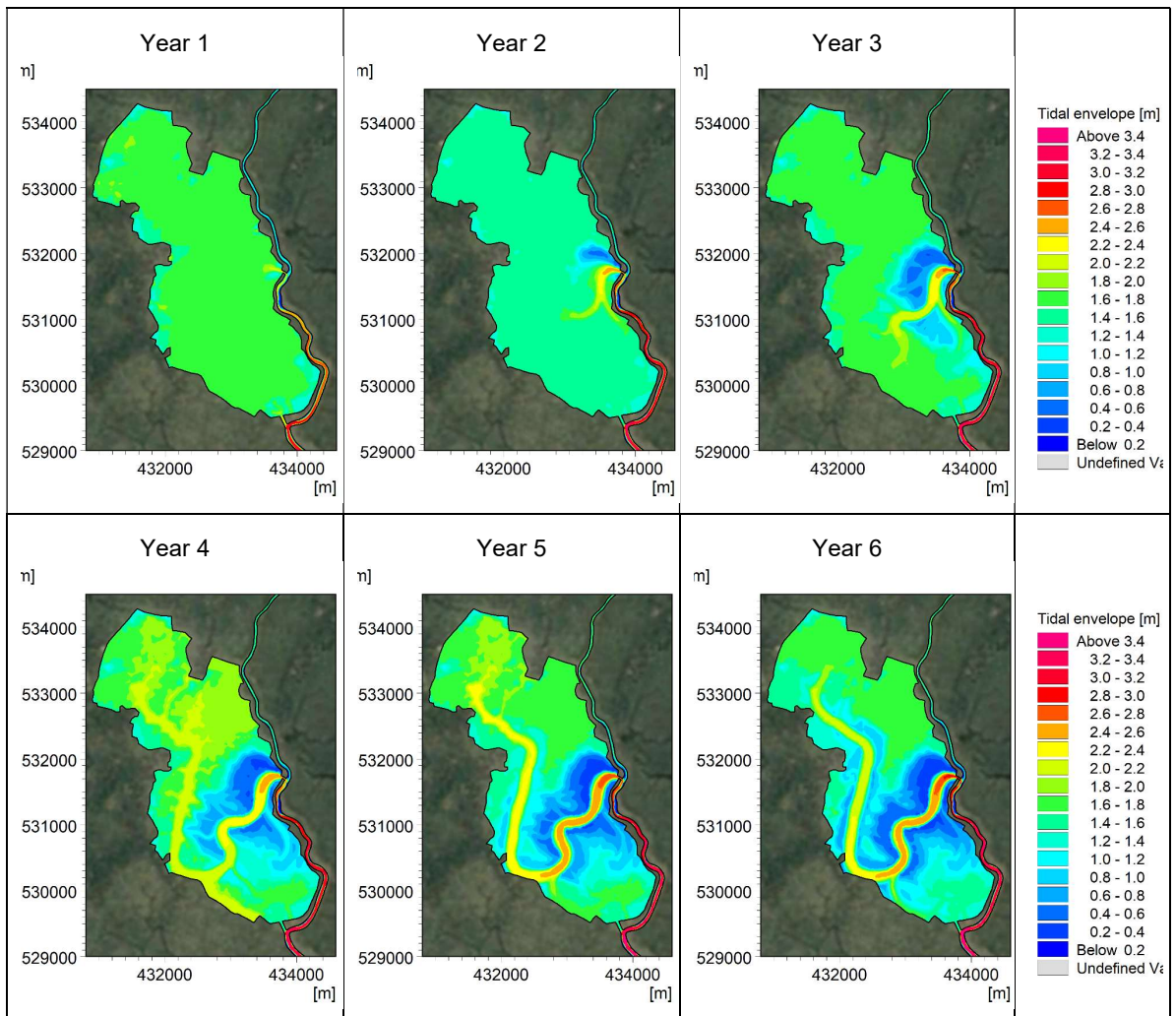


Figure 4-51 Tidal envelope after activation of TRM at the eastern side of the polder in the consecutive period of 6 years.

One of the main purposes of TRM is to prevent drainage congestion. It is therefore of relevance to look at the temporal development of the tidal range at a location in Hari River just downstream the opening into the polder. Figure 4-52 shows how the tidal range is increased over time due the activation of TRM. It is the level of the ebb tide that controls the drainage ability of the beel/polder. From the plot it is seen that this improvement is achieved already in the second year of operation.

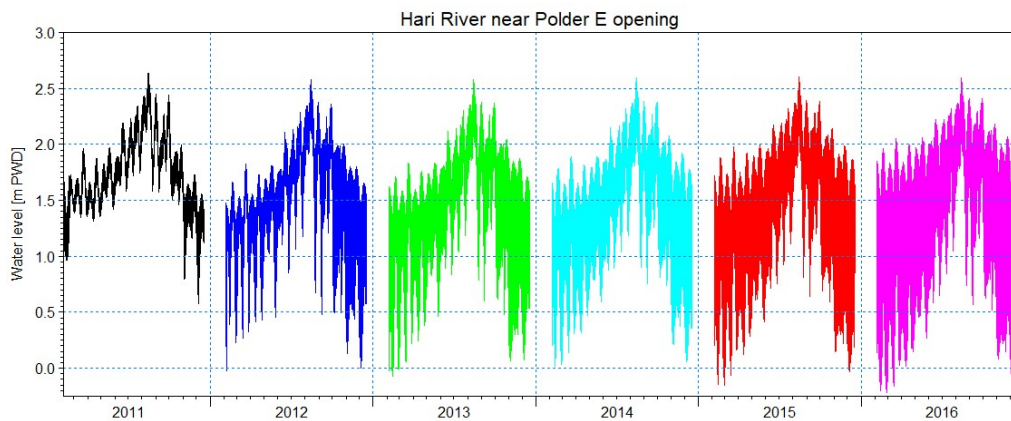


Figure 4-52 Tidal variation in Hari River near the polder opening after activation of TRM.

Figure 4-53 shows the initial bathymetry of the polder and the Hari River branch and the morphological development of bed levels the following six years after the opening into the eastern side of the polder. It is seen that the lack of side channels limits the deposition to areas along with the main channel being formed inside the polder and from Year 4 to 6 along with and inside the old main branch.

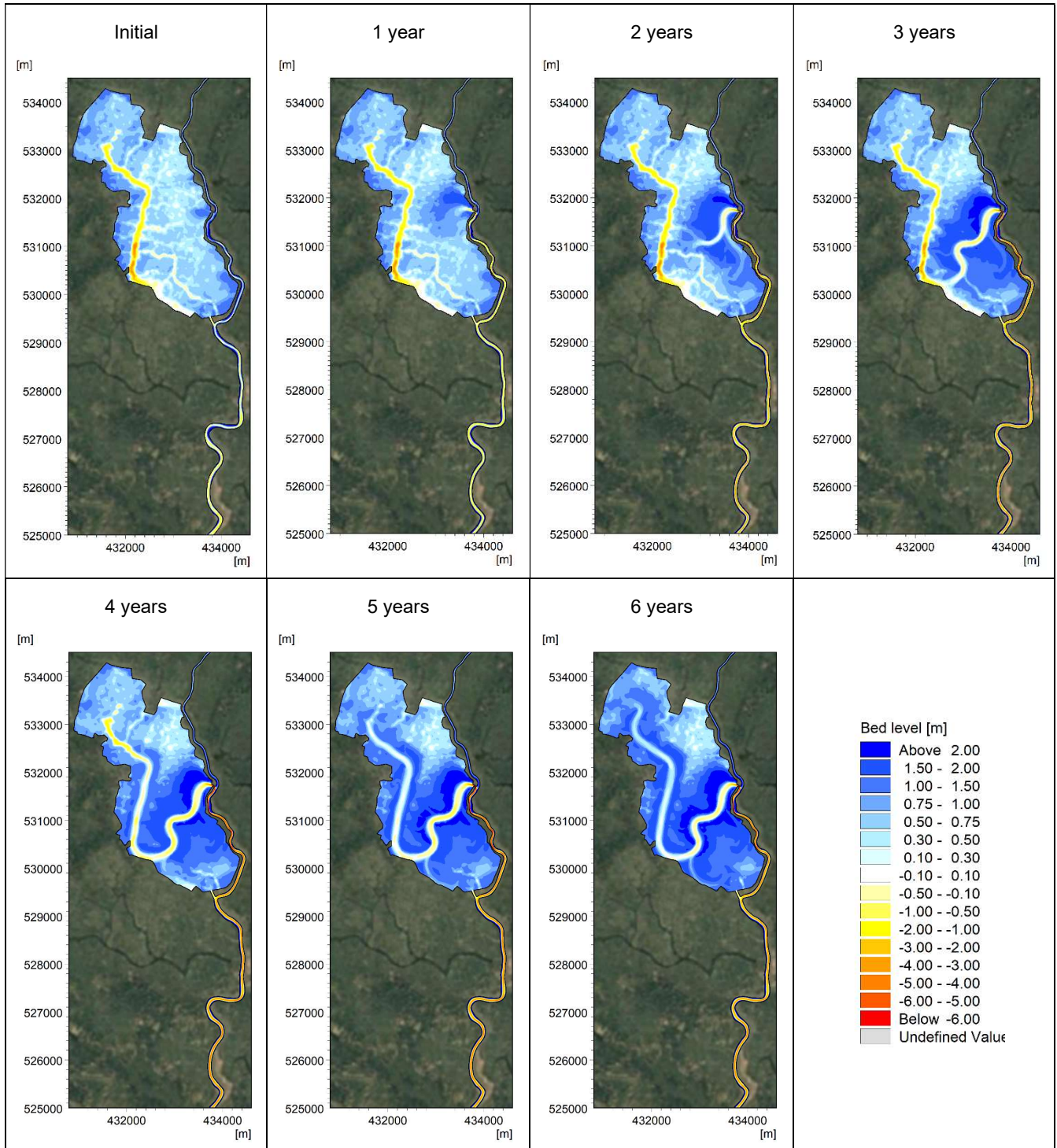


Figure 4-53 Bed level development after activation of TRM at the eastern side of the polder in the consecutive period of 6 years.

The corresponding plots showing the accumulated bed level changes are shown in Figure 4-54. From the plots, it is seen how the siltation pattern gradually migrate into the polder on the part of the low-lying floodplain next to the generated main channel inside the polder. When the generated main

channel reaches the major channel in the old channel network from before the polders were established (Year 3 and 4) siltation is mainly taking place in the drainage network. The plots also show a gradual erosion taking place inside the Hari River branch downstream the opening into the polder. Erosion is also taking place in parts of the channel network inside the polder. This erosion is important to maintain the flushing ability of the polder and capability to penetrate water and sediment into the entire polder. However, the results show that the TRM is less feasible than the opening in the southern end.

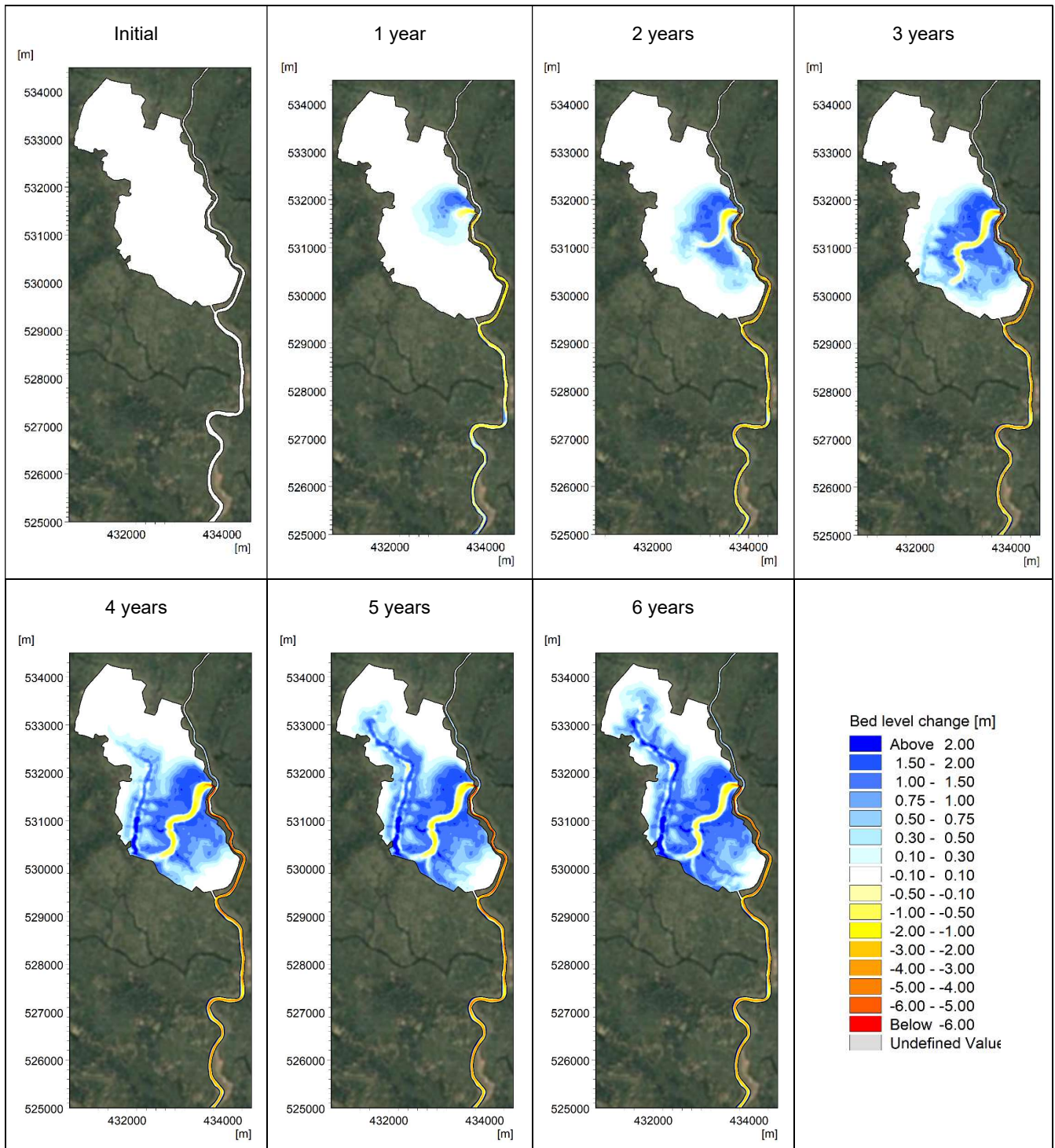


Figure 4-54 Bed level changes after activation of TRM at the eastern side of the polder in the consecutive period of 6 years.

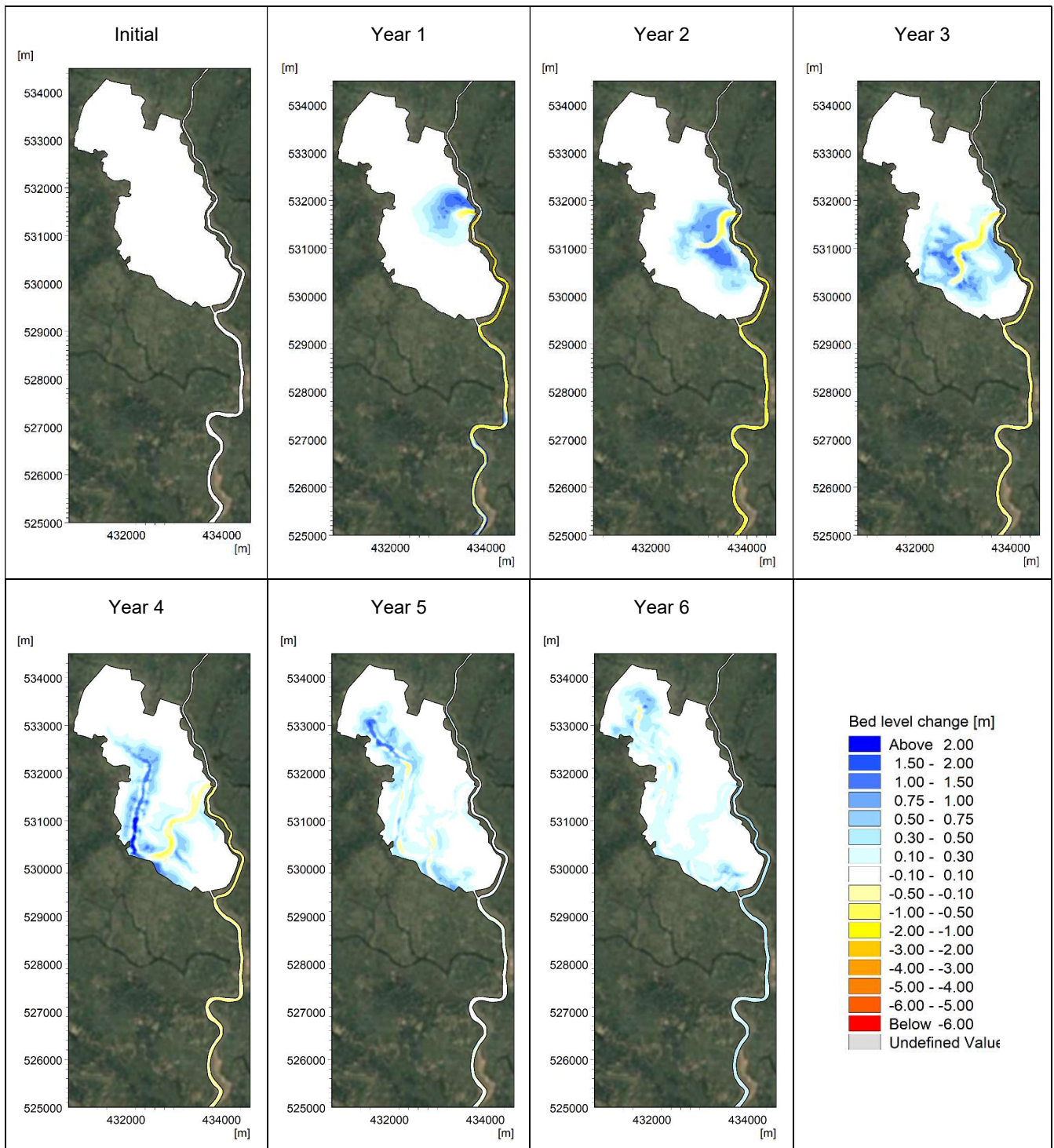


Figure 4-55 Annual bed level changes after activation of TRM at the eastern end of the polder in the consecutive 6 years.

Figure 4-55 shows the annual sedimentation and erosion inside the polder and the Hari River branch. It is seen that sediment is mainly settling in the area north of the eastern entrance channel during Year 1. In Year 2 deposition is migrating further inside and to the area south of the entrance channel, while at the same time the channel is eroding. In Year 3 the channel continues to erode and migrate towards south-southwest. Settling is mainly taking place in the southern part of the polder. In Year 4 the main channel continues to erode and migrate but reaches the old main channel. Deposition is mainly taking place in the old main channel and on the very nearby part of the floodplain. In Year 5 deposition is focused to the drainage network. In this year the Hari River branch reaches an

equilibrium, i.e. erosion has stopped. Year 6 tendencies are similar with Year 5. The tidal volume of the polder is decreasing leading to siltation in the Hari River branch and the channel network inside the polder. The TRM has therefore lost its eligibility after 5 years.

TRM is seen to be an effective way to erode the part of the peripheral river located downstream the opening and thereby prevent water logging and drainage congestion inside the polders. The tricky part is related to optimising the deposition pattern inside the polder.

The temporal development of the upstream directed annual net sediment transport is shown in Figure 4-56 to Figure 4-59 for the cross sections at Ranai, Katakhal, Kanaishisa, and Polder E. It is seen that the largest net sediment transport is obtained for Year 5 at Ranai and Katakhal, and Year 4 at Kanaishisa and Polder E.

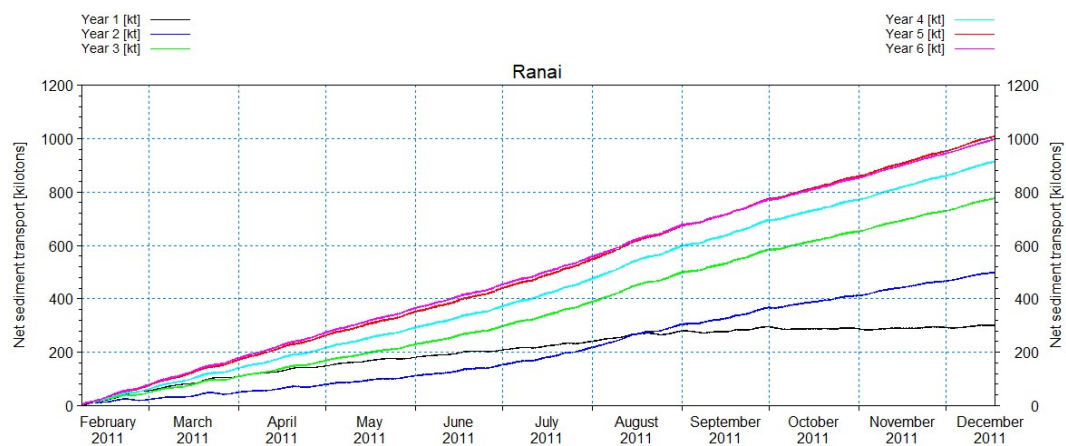


Figure 4-56 Net sediment transport at Ranai for each of the 6 consecutive years.

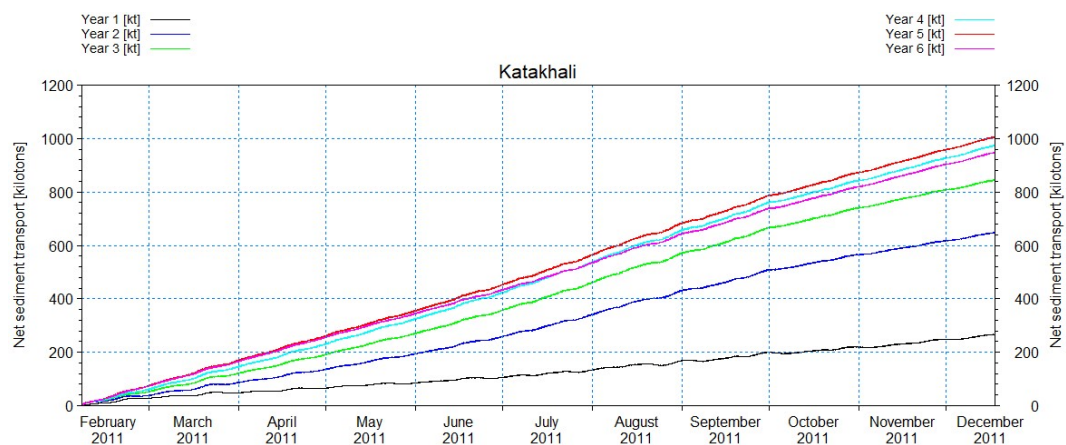


Figure 4-57 Net sediment transport at Katakhal for each of the 6 consecutive years.

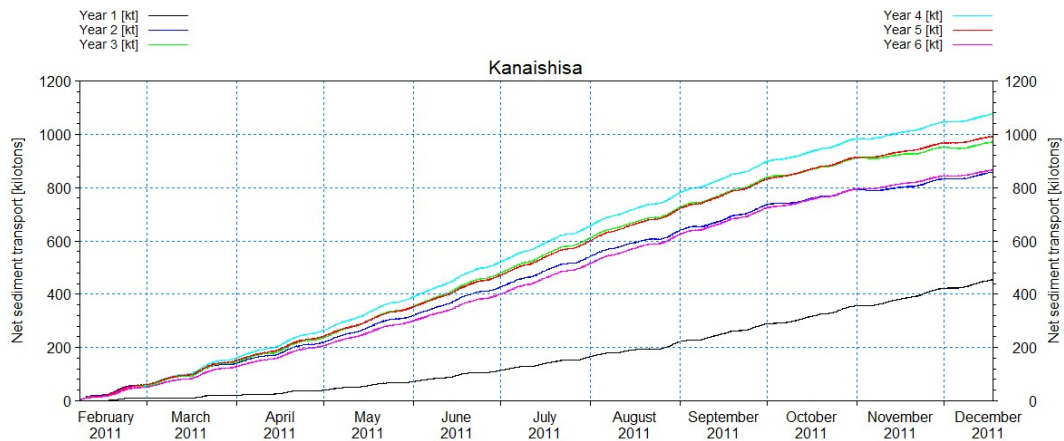


Figure 4-58 Net sediment transport at Kanaishisa for each of the 6 consecutive years.

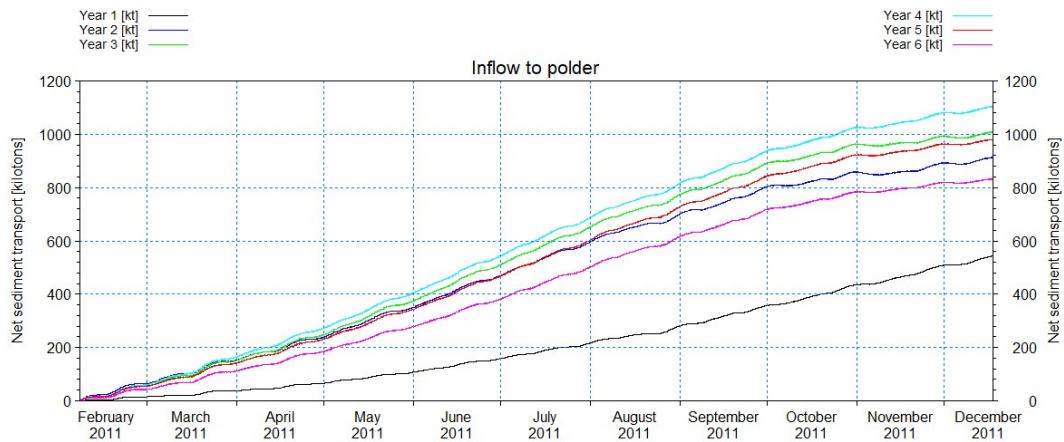


Figure 4-59 Net sediment transport at Polder E for each of the 6 consecutive years.

The calculated net sediment transport for each of the six cycles is listed in Table 4-7 for the cross sections at Ranai, Katakhal, Kanaishisa and Polder E. The net sediment transport at Kanaishisa is larger than the transport at Ranai and Katakhal in Year 1 to 4 due to the downstream migrating river erosion initiated by the opening to the polder and increased tidal prism. The beginning siltation of the river branch in Year 5 and 6 can also be revealed from the numbers in the table.

Table 4-7 Net sediment transport per cyclic period at Ranai, Katakhal, Kanaishisa, and Polder E.

Cyclic period	Ranai [kilotons]	Katakhal [kilotons]	Kanaishisa [kilotons]	Polder E [kilotons]
Year 1	301.4	266.7	454.3	543.2
Year 2	499.5	648.4	857.9	913.6
Year 3	776.6	844.6	971.1	1009.1
Year 4	915.0	974.5	1075.8	1104.7
Year 5	1009.3	1006.8	992.2	980.5
Year 6	997.1	948.3	865.2	832.1

The achieved impact obtained by use of TRM is illustrated in Figure 4-60. The diagram shows the area inside the polder, which is located above a given bed level value for initial bathymetry and the consecutive 6 years. It is seen that it is primarily the first 3 years the TRM is well-functioning. Siltation is also taking place inside the polder in Year 4-6, but this is mainly in the drainage network, which is of severe importance for the drainage ability of the polder after TRM operation has stopped. When comparing the diagram with the one shown in Figure 4-43, it is seen that the TRM efficiency is much less than what was obtained with the southern opening.

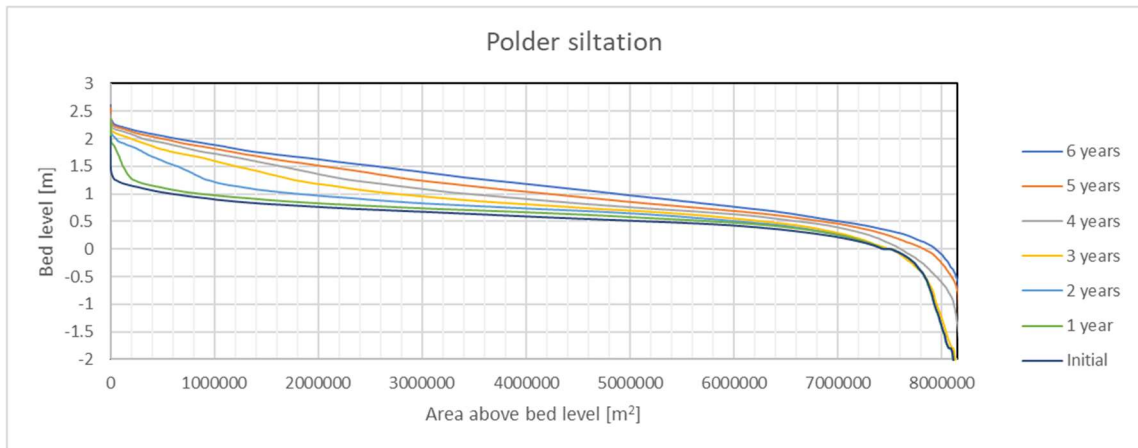


Figure 4-60 Area inside polder above a certain bed level during TRM operation.

A similar diagram (hypsothetic curve) is made for the Hari River branch and shown in Figure 4-61, however in this case with focus on the deepest parts. It is seen that significant (but favourable) erosion takes place during the first three years. The erosion continues in the two following years, but with less pace. In year 6 sediment starts to settle in the river branch as the tidal prism of the polder decreases.

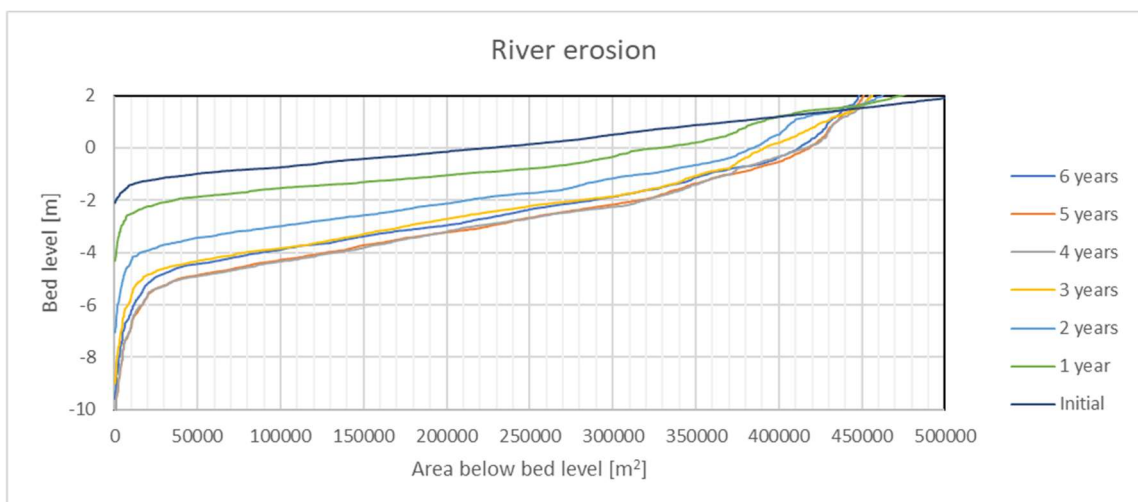


Figure 4-61 Area inside Hari River branch (downstream polder opening) below a certain bed level during TRM operation.

5 Model Development (MIKE 21) future conditions

5.1 Introduction

The impact of climate change and subsidence will affect the river and estuary branches in the delta and the polders. Sea level rise and subsidence will in combination tend to aggravate water logging and drainage congestion issues. Changes in the net precipitation related to the global warming will also have an impact. The overall impact on polder exchange dynamics is thus more complex than just being related to sea level rise and subsidence since the future precipitation trends are less clear. If the net precipitation increases, it will tend to amplify water logging further. However, it may be a bit more complex, since it is the duration time and rainfall intensity of the most severe events that causes the largest risk for water logging and inundation of the polders.

5.2 Future conditions

Sea level rise and subsidence are continuous processes gradually taking place over the next 50-100 years and will thereby allow the delta to gradually adapt. However, the morphological development of the entire delta on a micro-scale level (polder level and adjacent peripheral rivers) is impossible to predict in detail due to the too many unknowns. Considering this, it has been chosen only to include the impacts of subsidence and sea-level rise in the analysis of future conditions and issues related to water logging and drainage congestion. Issues which are difficult to mitigate and thereby must be foreseen as an increasing severe challenge in many of the low-lying polders.

5.2.1 Subsidence rates

Information of land subsidence is obtained from the “Interim Subsidence Report (2021)”, which is published under the “Long Term Monitoring, Research and Analysis of Bangladesh Coastal Zone (Sustainable Polders Adapted to Coastal Dynamics)” project. Subsidence rates at Polder 24 are found to vary between 3.72 – 5.17 mm/year. The closest value representing the subsidence of the Hari River is according to the subsidence plot shown in Figure 5-1 about 4.7 mm/year. The impact of subsidence on the present (2019) bed levels of Hari River in 2050 and 2100 is hereby expected to be as indicated in Table 5-1.

Table 5-1 Impact of subsidence on the present bed levels of Hari River in 2050 and 2100.

Configuration	Bed level change due to subsidence [m]
Present Hari River bathymetry	0
Hari River bathymetry in 2050	-0.15
Hari River bathymetry in 2100	-0.39



Figure 5-1 Subsidence rates at Polder 24.

5.2.2 Sea level rise

The development in sea level rise will depend on the future carbon emission. Different RCP-scenarios (Representative Concentration Pathways) have been developed to describe the potential development. Table 5-2 shows the most common applied scenarios and their meaning in relation to radiation, greenhouse gas concentration, and temperature increase. The present greenhouse gas concentration (March 2022) is approximately 419 ppm CO₂ equivalents¹. The RCP8.5 is known as the “do nothing” scenario and is therefore often chosen for design purposes. The RCP8.5 scenario is a rather pessimistic scenario in the sense that global warming will continue after 2100. This contrasts with the other scenarios, which stabilises or even decrease after having reach a peak. Climate change has become a matter on the political agenda and measures are taken to reduce CO₂ emissions. However, it is still unclear which of the four scenarios that is the most “realistic scenario”. In the end it will be a matter of belief. When it comes to engineering designs there is a tendency to use a conservative approach and worst-case scenarios. However, taking the great uncertainties into account, it makes most sense to think in adaptive solutions, which can be gradually updated over time.

¹ co2.earth

Table 5-2 RCP-scenarios and their meaning.

ID	Radiation	Greenhouse gas concentration	Temperature increase
RCP8.5	>8.5 W/m ² in 2100	>1370 ppm CO ₂ equivalents in 2100	4,5 °C
RCP6.0	Stabilises at 6 W/m ² after 2100	~850 ppm CO ₂ equivalents when stabilising after 2100	2,6 °C
RCP4.5	Stabilises at 4.5 W/m ² after 2100	~650 ppm CO ₂ equivalents when stabilising after 2100	1,7 °C
RCP2.6	Peaks at 3 W/m ² before 2100 and decreases afterwards	Peaks at ~490 ppm CO ₂ equivalents before 2100 and decreases afterwards	0,8 °C

The impact on sea level rise increases with the radiation impact, but even for each scenario there is an uncertainty on the year 2100 estimate. The sea level rise is therefore given by a central estimate and an upper and lower estimate reflecting the uncertainty. For the future conditions analysis, it has been decided to use the RCP8.5 scenario based on the 95th percentile sea level rise graph since it is the scenario with the most severe impact on sea level rise. The hereby chosen sea level rise estimate is therefore to be considered as a worst-case scenario, which may never happen. The applied sea level rise for 2050 and 2100 is estimated relative to present conditions (2019). Figure 5-2 shows the applied expected sea level rise development over time at the Bay of Bengal region.

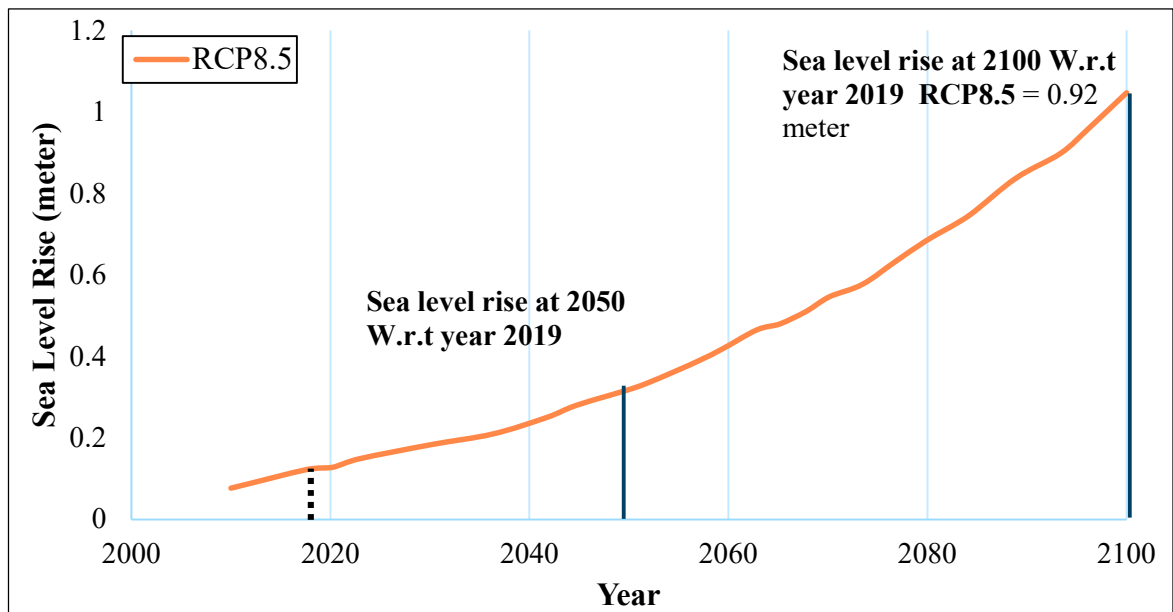


Figure 5-2 Sea level rise graph of the 95th percentile related to the RCP8.5 scenario. (Source: Climate Change Scenarios, 2021).

Based on the curve shown in Figure 5-2 estimates for sea level rise in 2050 and 2100 relative to present conditions (2019) are calculated and listed in Table 5-3. It is seen that there is a significant difference in the estimate for 2050 and 2100, which to some degree is related to the increased uncertainty as we look forward in time and uses the 95th percentile. Having this in mind, it once again illustrates that it mainly makes sense to focus on adaptive design solutions, which if required can be updated over time to deal with the worst-case scenario.

Table 5-3 Sea level rise estimates for the Bay of Bengal.

Year	Sea level rise relative to 2019 [m]
2050	0.20
2100	0.92

The impact of the sea level rise in the Bay of Bengal will be felt differently inside the delta. The mean water level increase at the Hari River in 2050 and 2100 have been estimated using the Southwest regional model for 2019, 2050 and 2100 conditions including the impact of sea-level rise and subsidence. Impact of the morphological adaptation is not included. It is seen that the impact of sea-level rise is slightly lower in the Hari River than in the Bay of Bengal.

Table 5-4 Mean water level increase at Ranai (Hari River) relative to 2019.

Year	Mean water level increase at Ranai relative to 2019 [m]
2050	0.196
2100	0.844

5.3 Hari River bathymetry present and future

The model bathymetry of Hari River representing 2050 and 2100 is generated based on the 2019 bathymetry (2015) and the level changes related to subsidence listed in Table 5-1. Figure 5-3 shows the initial model bathymetries applied to represent conditions in 2019, 2050, and 2100.

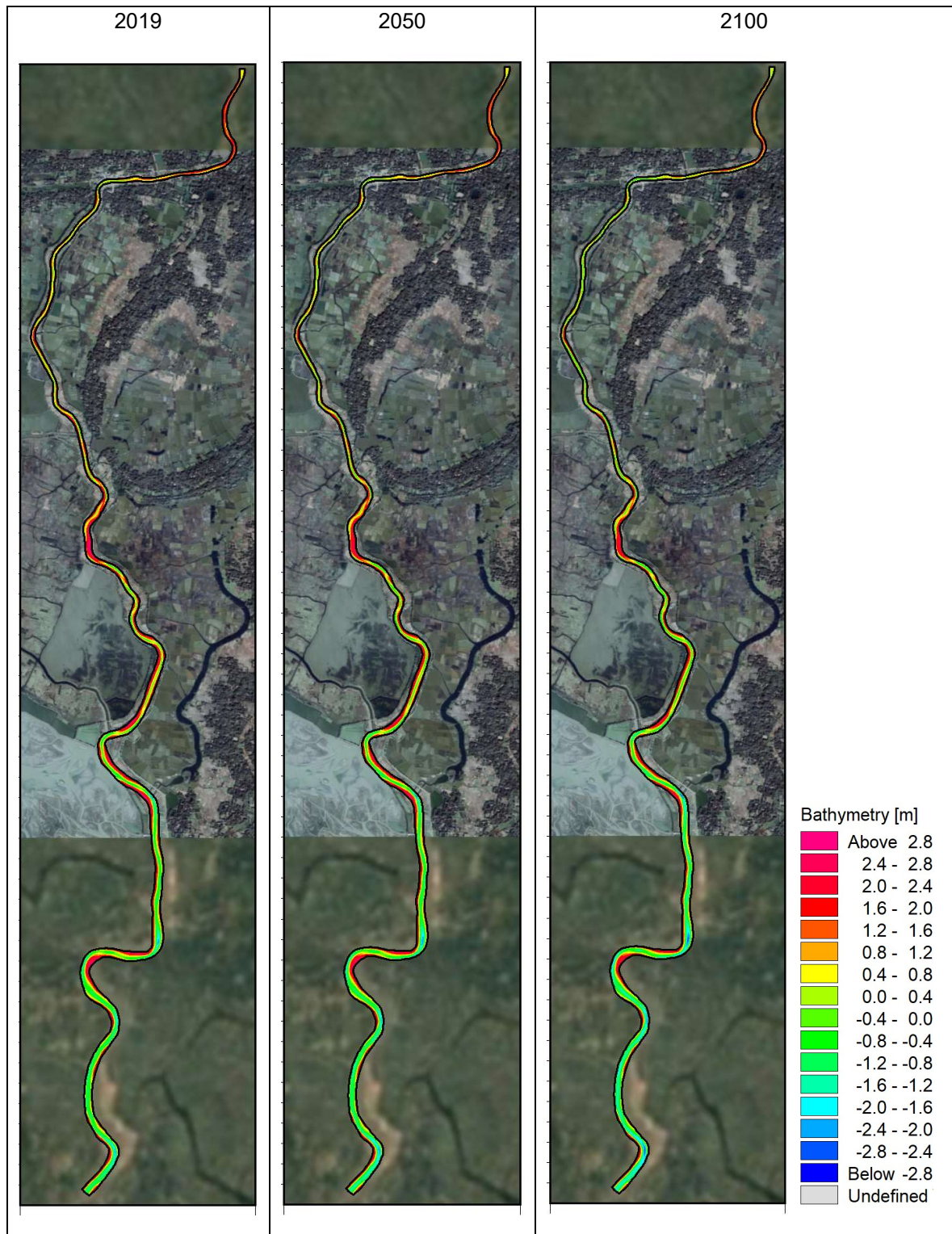


Figure 5-3 Hari River model bathymetry for present conditions (2019), and future conditions (2050 and 2100).

5.4 Model results and scenarios for Hari River year 2050 and 2100

The Hari River model without TRM is applied to investigate the impact of sea level rise and subsidence on tidal envelopes, morphological development, and time scales for siltation. The scenarios are as follows:

- Scenario 1: Hari River year 2050
- Scenario 2: Hari River year 2100
- Scenario 3: Hari River year 2100 with a 50% increase of upstream discharges
- Scenario 4: Hari River year 2100 with a 100% increase of upstream discharges

The last two scenarios are representing the situation with rather extreme increased net precipitation over the basin and are included to illustrate the sensitivity. Figure 5-4 shows the upstream discharges with a 50% increase (blue curve) and 100% increase (green curve) assuming an unchanged distribution over time.

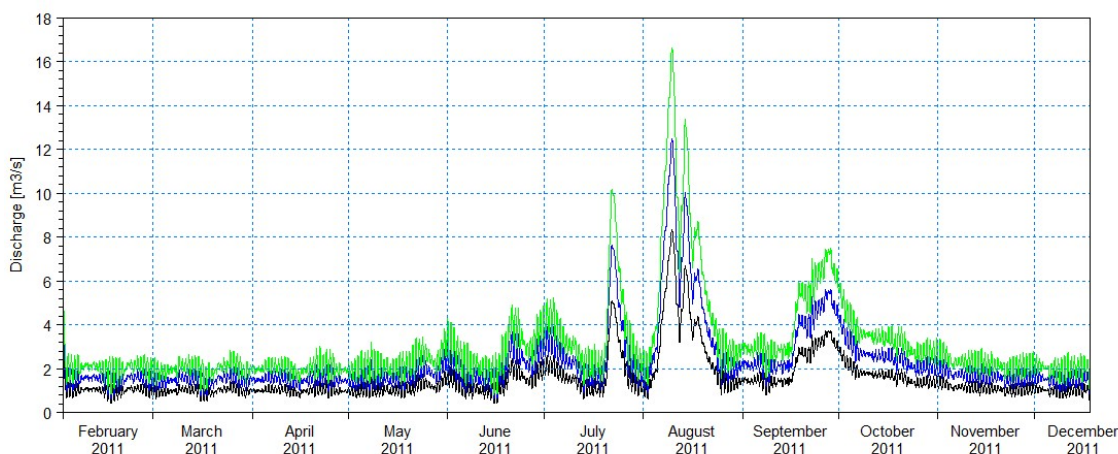


Figure 5-4 Discharge time series applied for the upstream boundary condition.

5.4.1 Hari River discharges

The conceptual model developed for the Hari River without TRM is applied to investigate the future conditions. The Hari River has a tendency to siltation caused by the tidal asymmetry, which creates an upstream directed net sediment transport that decreases with the tidal prism. Maintenance dredging or TRM is therefore required to maintain the system in a quasi-steady equilibrium. The conceptual Hari River model developed to represent present conditions is slightly modified to investigate the impact of climate changes looking ahead to year 2050 and 2100. The main changes of the conceptual model is the lowering of the bathymetry taking subsidence into consideration and elevating the mean water level at the downstream boundary in order to account for the expected sea level rise. This approach is a crude first order approximation since the tide in reality will be changed in a more complex manner due to changes in the celerity inside the channel system of the delta. As in the simulation of present condition a constant value of 0.4 g/l for the suspended sediment concentration is applied at the downstream boundary

For the first three scenarios (1-3) the morphological model is run cyclic six times, i.e. the modelling period covering almost a year is modelled repeatedly using the end bathymetry of the previous cycle. The modelling is thereby representing a period of almost six years. The fourth scenario (4) is run for 9 morphological cycles in an attempt to reach a new quasi-steady equilibrium.

For a siltating branch as the Hari River the tidal generated discharge will slightly decrease over time as a consequence of an increased flow resistance and the reduction of the tidal prism unless regular maintenance dredging is carried out.

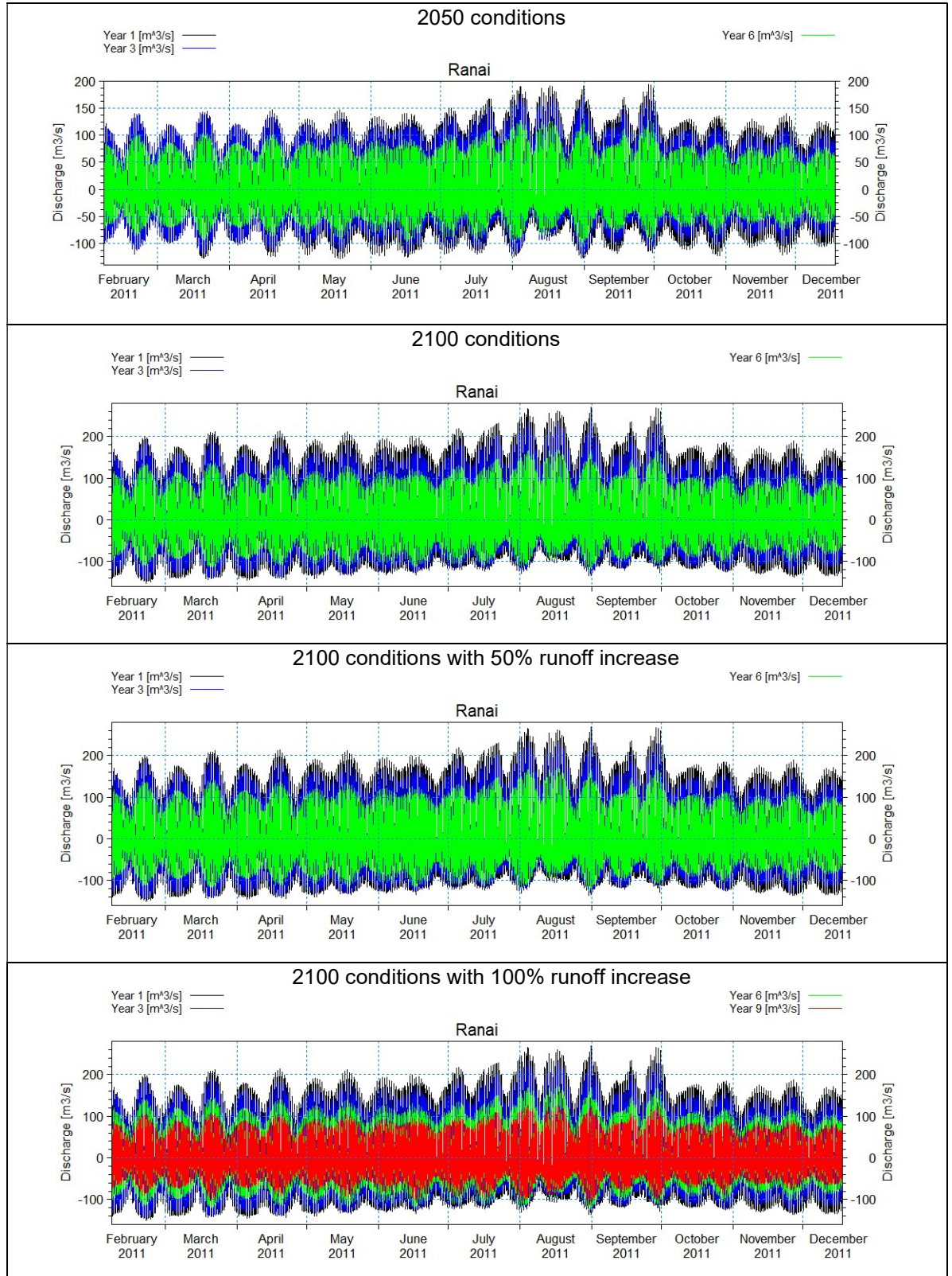


Figure 5-5 Development of tidal generated discharges at Ranai.

The modelled flow discharges at Ranai, Katakali and Kanaishisa are plotted in Figure 5-5 to Figure 5-7 for selected cycles. The plots show how the tidal discharge decreases when moving upstream due to the smaller tidal prism and how siltation of the Hari branch over the morphological cycles gradually reduces the tidal generated discharge amplitudes.

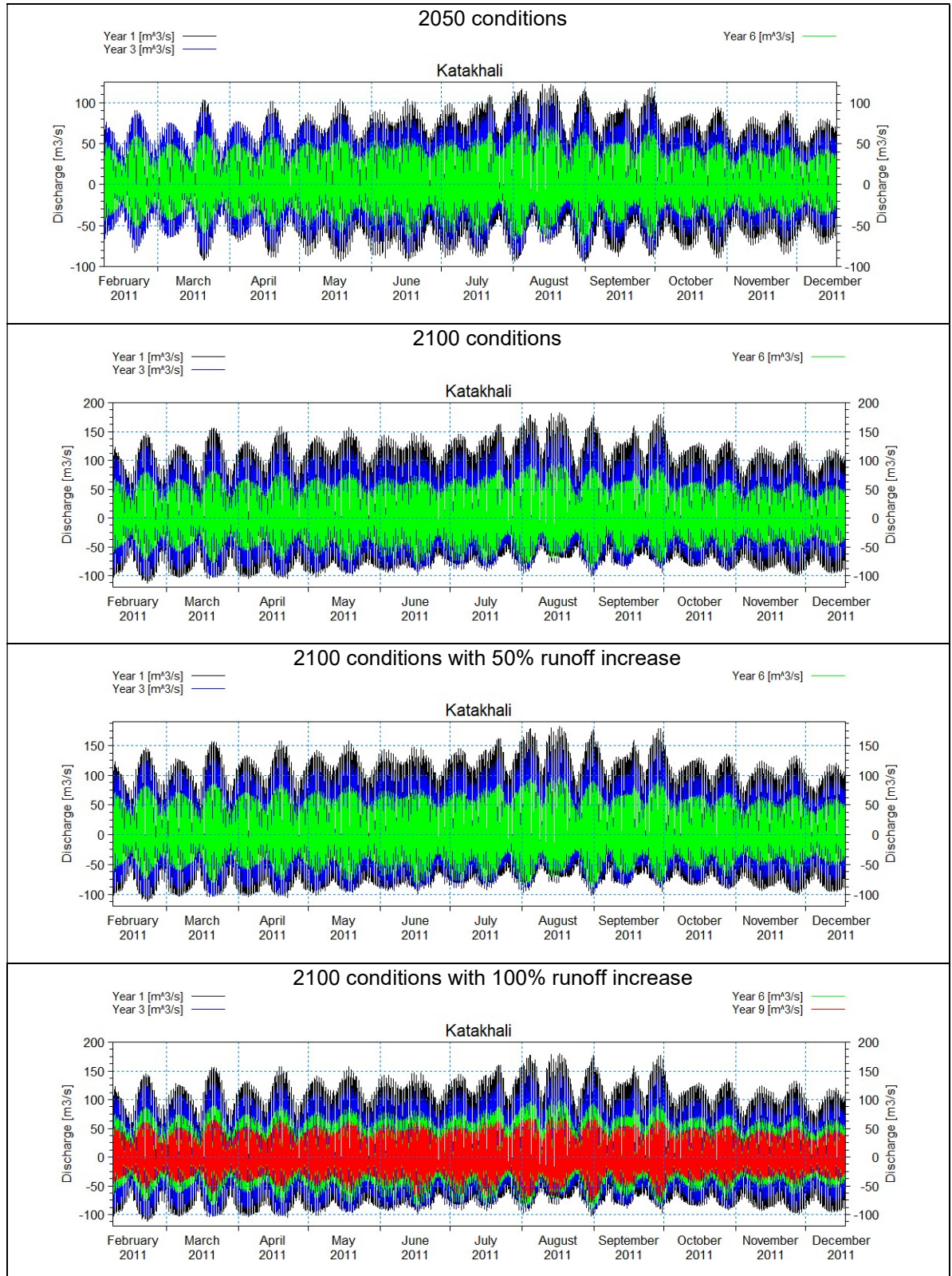


Figure 5-6 Development of tidal generated discharges at Katakali.

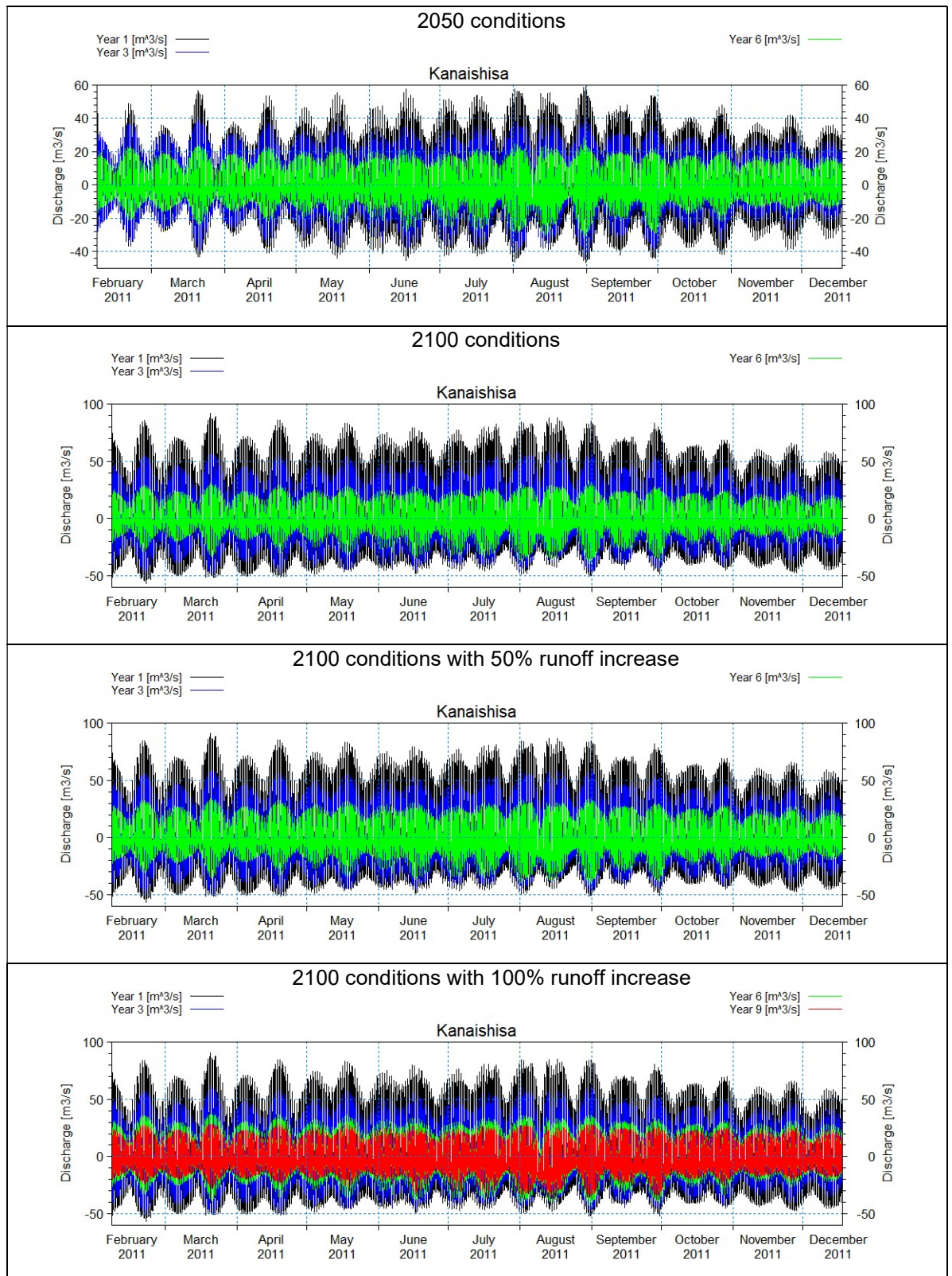


Figure 5-7 Development of tidal generated discharges at Kanaishisa.

The initial bathymetry and water level variation are shifted abruptly to year 2050 and 2100 conditions, even though the changes will take place slowly over a timescale of decades. By running the model with morphological update and as a cyclic event the system will tend to move against a quasi-steady equilibrium. This can be seen from Figure 5-8 to Figure 5-10, which compare the 2019, 2050, and

2100 discharges at Ranai, Katakali, and Kanaishisa in the first and sixth morphological cycle. It is seen that the discharge amplitudes decrease quite fast over time and approaches the present discharges. This indicates that the timescale for adaption is much shorter than the timescales for the climate changes.

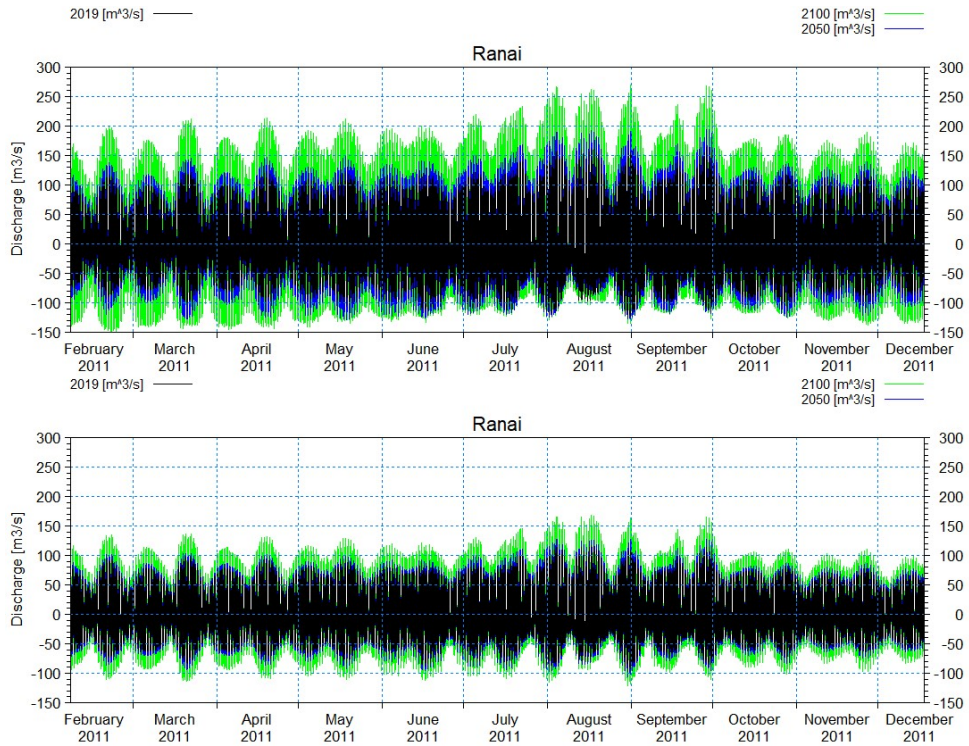


Figure 5-8 Tidal generated discharges in 2019, 2050 and 2100 at Ranai. Top: First morphological cycle. Bottom: Sixth morphological cycle.

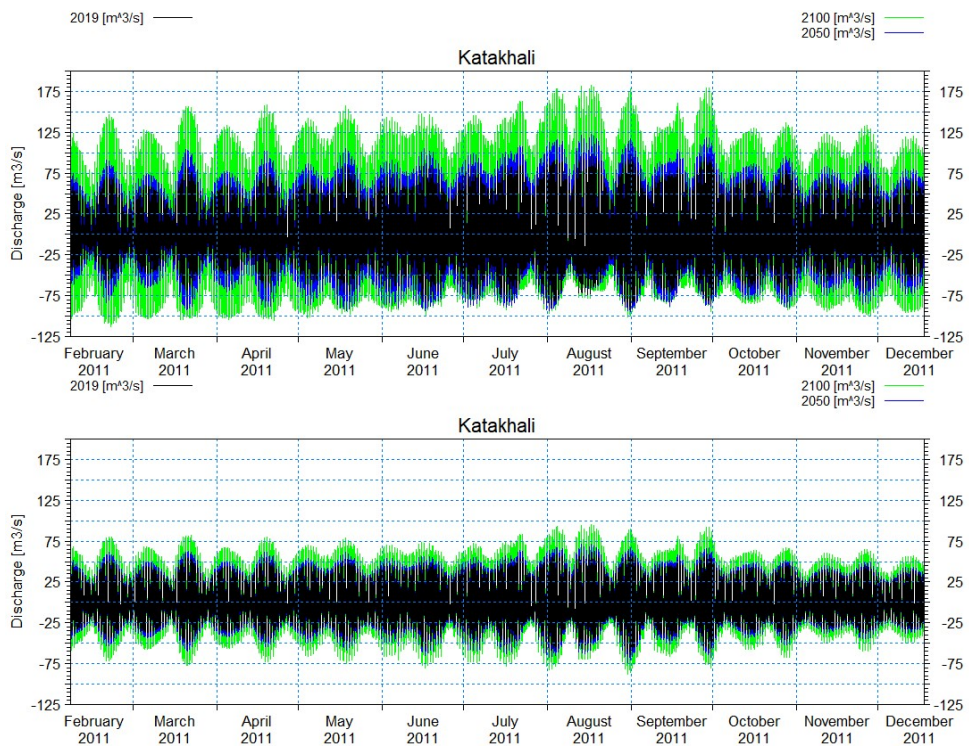


Figure 5-9 Tidal generated discharges in 2019, 2050 and 2100 at Katakali Top: First morphological cycle. Bottom: Sixth morphological cycle.

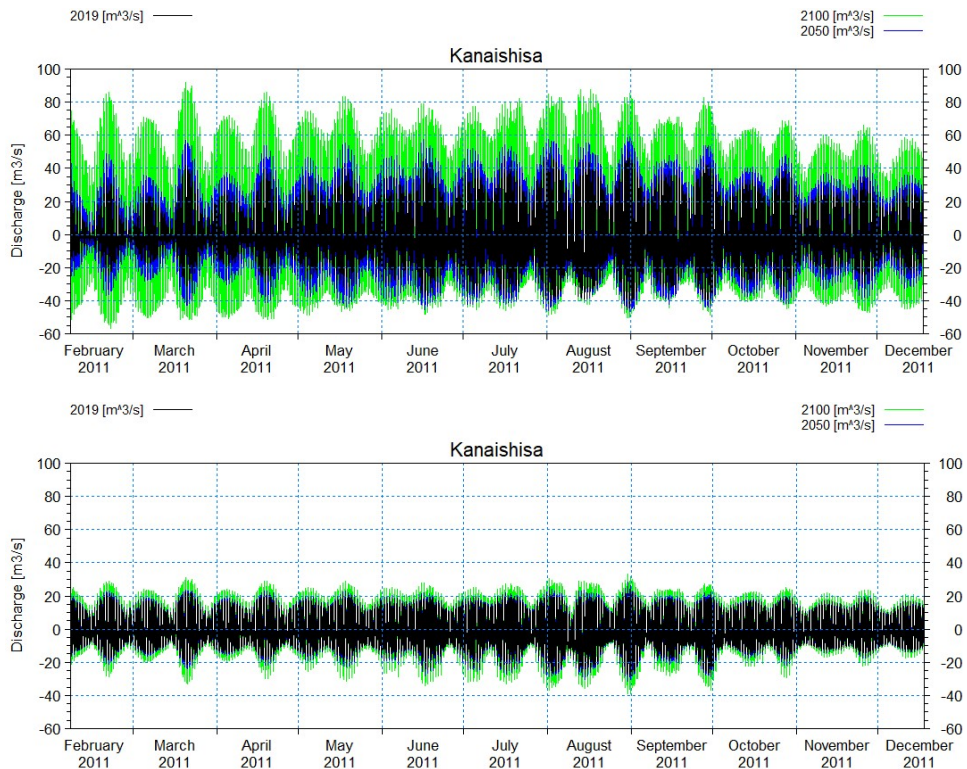


Figure 5-10 Tidal generated discharges in 2019, 2050 and 2100 at Kanaishisa Top: First morphological cycle. Bottom: Sixth morphological cycle.

5.4.2 Hari River mean gross discharges

The gradual damping of the tidal generated discharge and volume of the tidal prism can also be illustrated and quantified by calculating the annual time-averaged gross discharge, i.e. averaging the absolute value of the flow discharge. Table 5-5 shows how the time-averaged gross discharge decreases over time for the 2050 conditions due to gradual siltation of the branch and increased flow resistance. There is only a minor difference between the numbers for Year 1 and 2. This can be explained by the morphological adjustment of the initial bathymetry, which improves the conveyance of the system and thereby counteracts the impact of siltation. In the following years, the decrease in gross discharge is only (mainly) related to the impact of siltation and thereby larger. It is seen that the gross discharge is approximately halved in year 6 compared to year 1.

Table 5-5 Development of annual time-averaged gross discharge at Ranai, Katakhal, and Kanaishisa with year 2050 conditions.

Cyclic period	Ranai [m ³ /s]	Katakhal [m ³ /s]	Kanaishisa [m ³ /s]
Year 1	60.9	39.9	16.3
Year 2	58.3	37.2	14.7
Year 3	52.8	32.6	12.2
Year 4	47.3	28.5	10.3
Year 5	42.4	24.8	8.9
Year 6	38.1	21.8	8.0

Table 5-6 shows the similar number for year 2100 conditions, while Table 5-7 and Table 5-8 shows the numbers with a 50% and 100% increase of runoff. The latter is run for 9 morphological cycles.

Table 5-6 Development of annual time-averaged gross discharge at Ranai, Katakhal, and Kanaishisa with year 2100 conditions.

Cyclic period	Ranai [m ³ /s]	Katakhal [m ³ /s]	Kanaishisa [m ³ /s]
Year 1	81.4	56.8	25.4
Year 2	75.6	50.8	21.0
Year 3	68.4	44.3	13.4
Year 4	61.4	38.2	13.6
Year 5	54.7	32.9	11.1
Year 6	48.5	28.3	9.3

Table 5-7 Development of annual time-averaged gross discharge at Ranai, Katakhal, and Kanaishisa with year 2100 conditions and 50% increase of upstream discharges.

Cyclic period	Ranai [m ³ /s]	Katakhal [m ³ /s]	Kanaishisa [m ³ /s]
Year 1	81.6	57.0	25.7
Year 2	76.1	51.4	21.7
Year 3	69.3	45.2	17.9
Year 4	62.5	39.4	14.9
Year 5	56.1	34.3	12.6
Year 6	50.2	29.9	11.0

Table 5-8 Development of annual time-averaged gross discharge at Ranai, Katakhal, and Kanaishisa with year 2100 conditions and 100% increase of upstream discharges.

Cyclic period	Ranai [m ³ /s]	Katakhal [m ³ /s]	Kanaishisa [m ³ /s]
Year 1	81.7	57.1	26.0
Year 2	76.6	51.9	22.3
Year 3	70.1	46.0	18.9
Year 4	63.6	40.5	16.2
Year 5	57.5	35.8	14.3
Year 6	52.1	31.8	12.8
Year 7	47.3	28.5	11.8

Cyclic period	Ranai [m ³ /s]	Katakali [m ³ /s]	Kanaishisa [m ³ /s]
Year 8	43.3	26.0	11.1
Year 9	40.1	24.0	10.6

From the tables above, it is seen that the increased runoff only has a very weak impact on the gross discharges. The main reason for this is that the upstream runoff discharge in all cases is small compared to the downstream tidal generated discharges.

The tabled information is plotted in Figure 5-11 to Figure 5-13. The curves illustrate the impact of the siltation on the mean gross discharge and that it tends to converge against the present conditions when the runoff is unaffected. In the two scenarios with an increased runoff the mean gross discharge is found to converge at slightly greater mean gross discharge as one would expect.

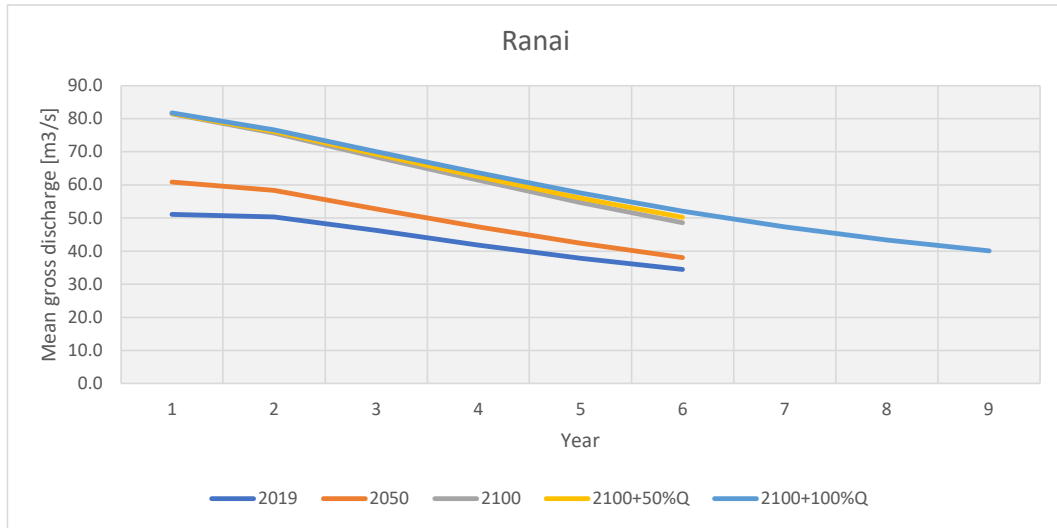


Figure 5-11 The impact of siltation on the mean gross discharge at Ranai.

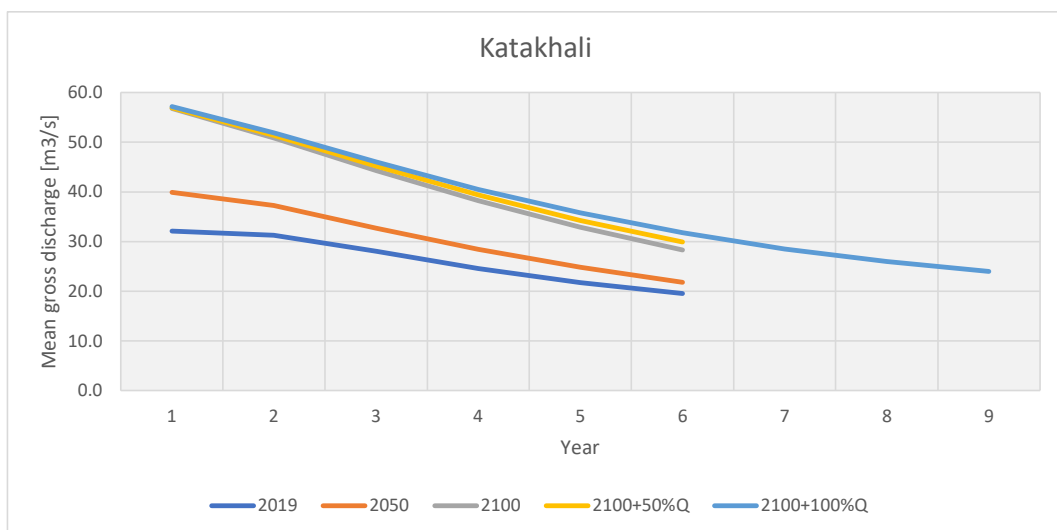


Figure 5-12 The impact of siltation on the mean gross discharge at Katakali.

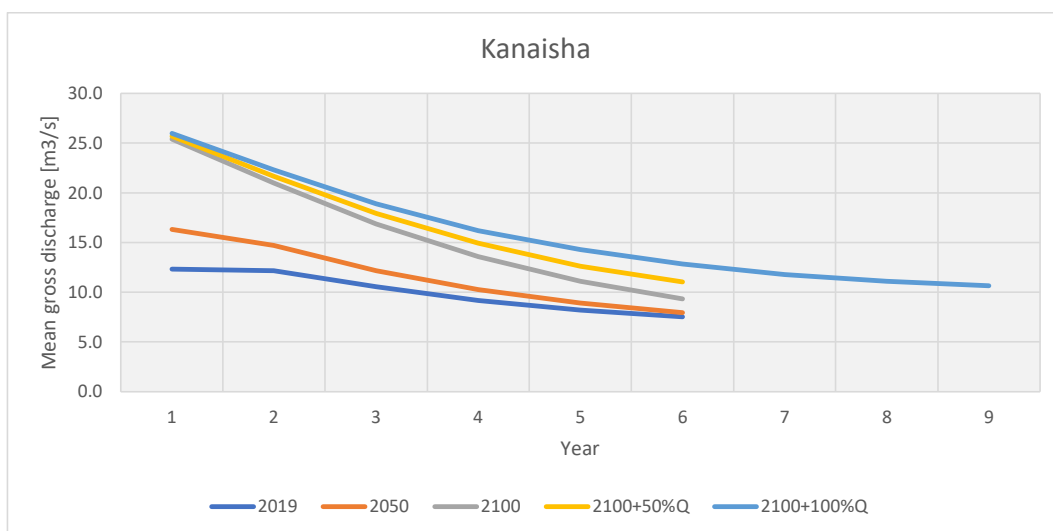


Figure 5-13 The impact of siltation on the mean gross discharge at Kanaishisa.

5.4.3 Hari River net sediment transport

The temporal development of the upstream directed annual net sediment transport at Ranai near the downstream boundary is shown in Figure 5-14 for all four scenarios. The net upstream directed sediment transport in the 2050 scenario is significantly smaller in the first morphological cycle than the following five cycles and the largest net sediment transport is obtained for year 3. This indicates that the internal adjustment of the initial bathymetry plays a role for a longer period than revealed from the development of the gross discharges.

For the three 2100 scenarios where the initial flow depths are increased by about 1.23 m the internal adjustment of the initial bathymetry is less pronounced. The largest net sediment transport is obtained for year 2 and the upstream directed annual net sediment transport in the first year is larger than what is obtained for year 4 and beyond.

Similar plots are shown for Katakhal and Kanaishisa further upstream in Figure 5-15 and Figure 5-16. The time scales for the initial adjustment of the bathymetry are seen to be lower at both Katakhal and Kanaishisa. At Katakhal the upstream directed annual net sediment transport in the first year is only slightly lower than the transport in the second year in the 2050 scenario. For the three 2100 scenarios the largest upstream directed annual net sediment transport is obtained for the first year. At Kanaishisa this is the case for all four scenarios. The plots show how the net upstream transport gradually decreases over time due to the siltation on banks and river channel.

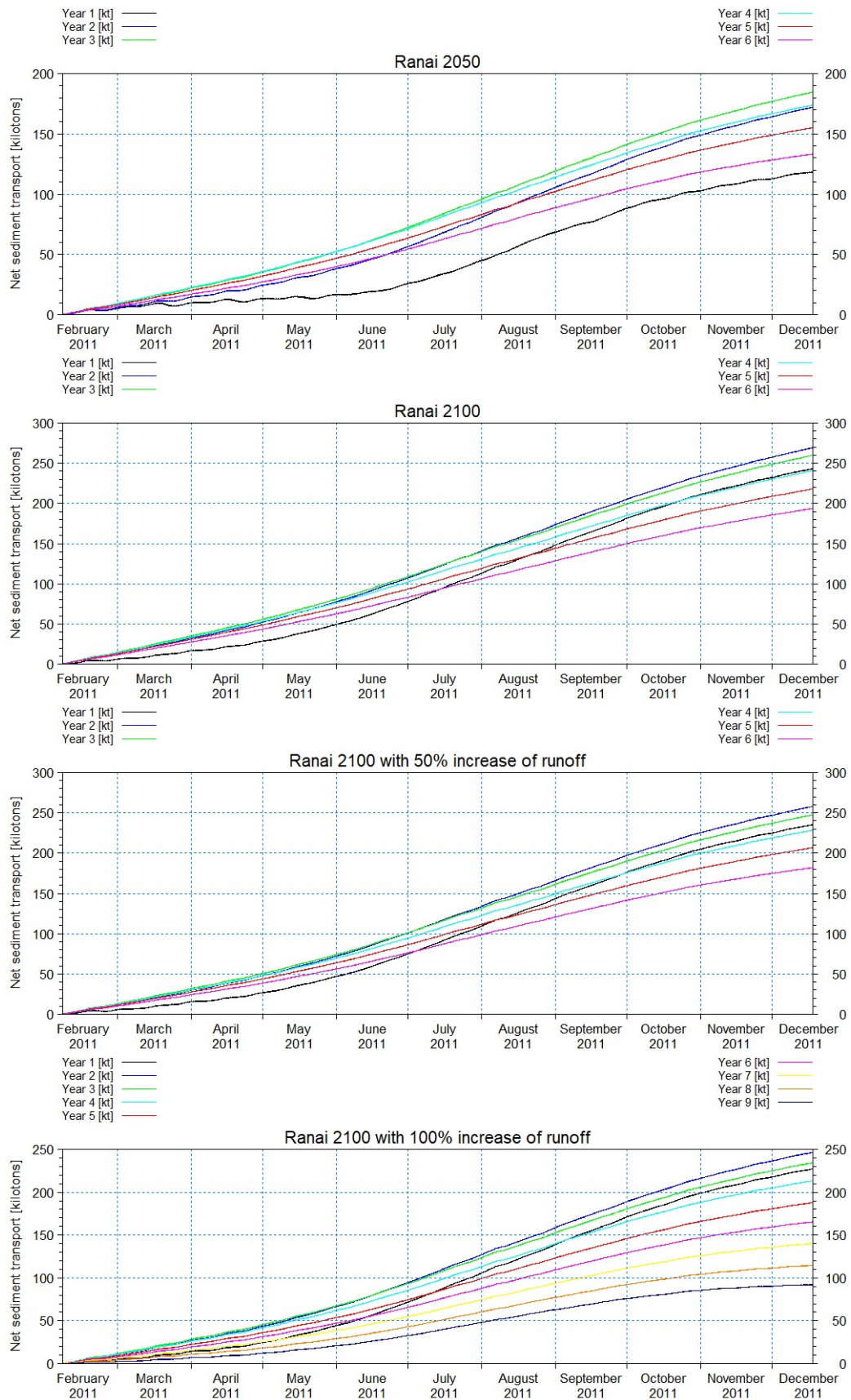


Figure 5-14 Net sediment transport (upstream directed) at Ranai for each of the 6 (9) consecutive years.

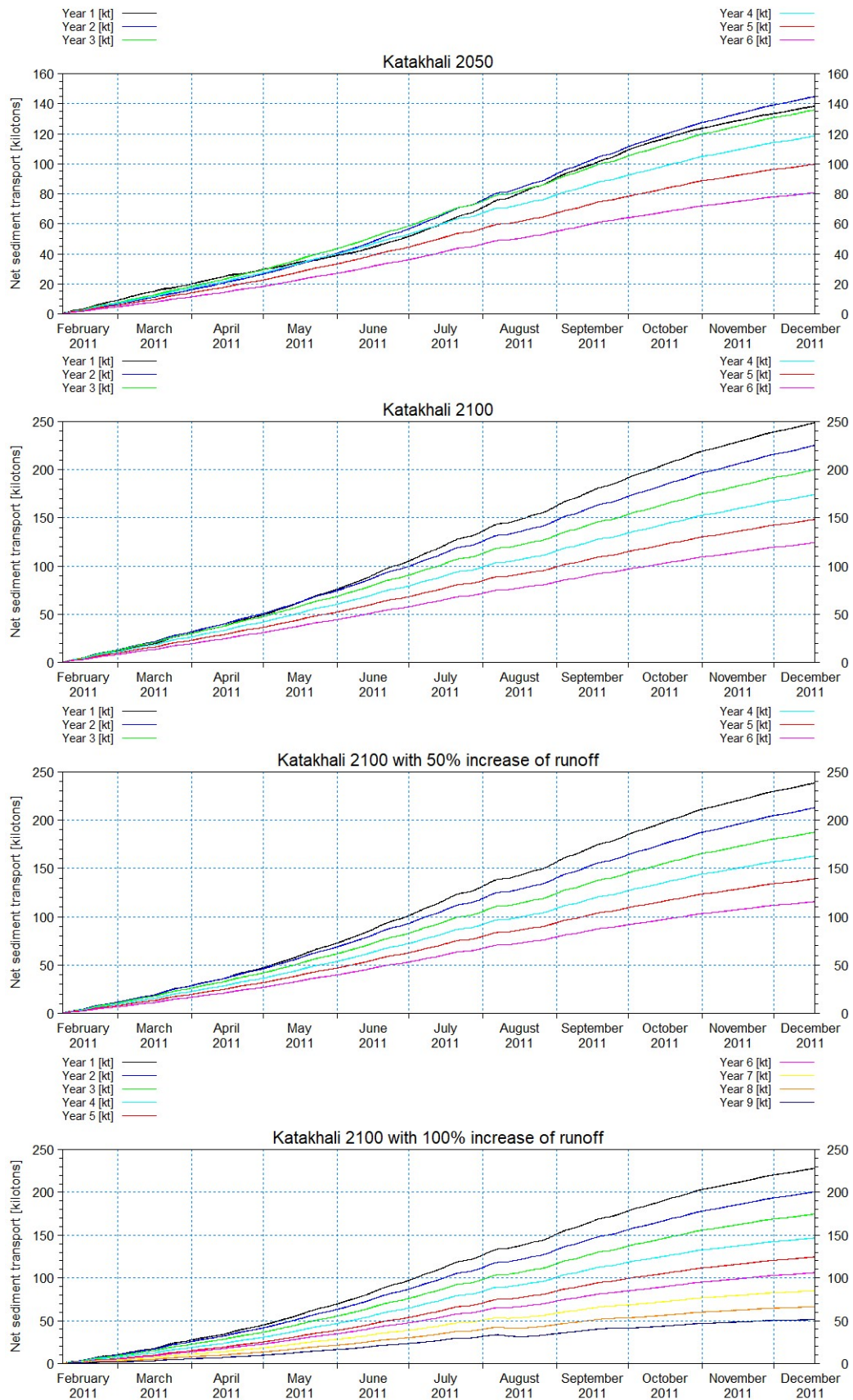


Figure 5-15 Net sediment transport (upstream directed) at Katakali for each of the 6 (9) consecutive years.

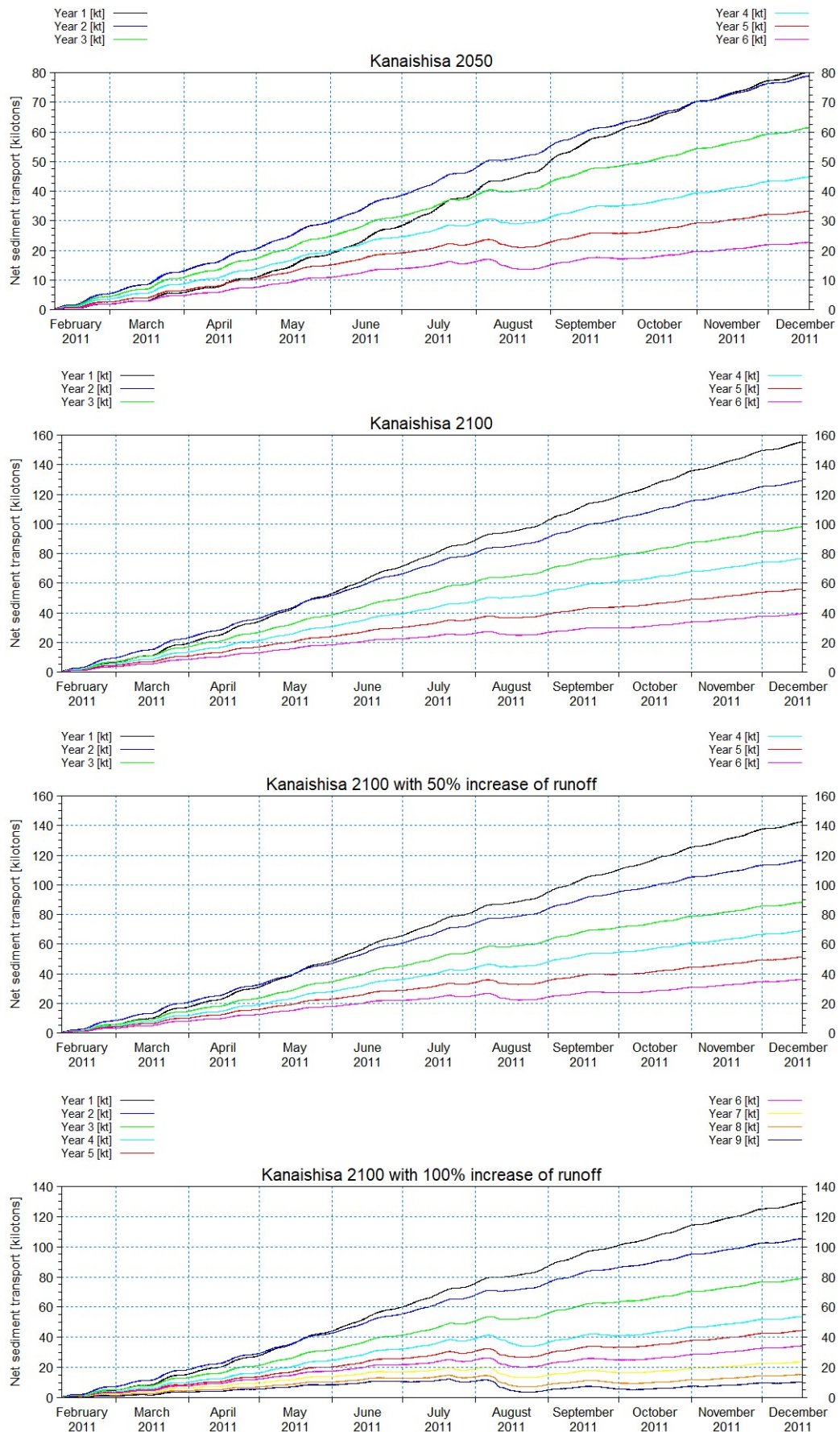


Figure 5-16 Net sediment transport (upstream directed) at Kanaishisa for each of the 6 (9) consecutive years.

The calculated net sediment transport for each of the six cycles is listed in Table 5-9, Table 5-10 and Table 5-11 for the cross sections at Ranai, Katakhal, Kanaishisa S. The net sediment transport at Katakhal is greater than the transport at Ranai in Year 1 due to the impact of the internal bathymetry adjustment. The bold numbers indicate the cyclic period (year), where the largest net upstream sediment transport takes place at the specific location. From the tables, it is seen that the increased runoff acts as a damping mechanism on the upstream directed net sediment transport.

Table 5-9 Net sediment transport in kilotons per cyclic period at Ranai.

Cyclic period	2050	2100	2100 + 50%Q	2100 + 100%Q
Year 1	118.4	243.0	235.1	227.0
Year 2	172.0	269.2	257.9	246.4
Year 3	184.7	259.9	247.5	234.3
Year 4	173.9	240.6	228.4	213.2
Year 5	155.1	218.0	206.7	187.8
Year 6	133.2	193.6	181.9	165.3

Table 5-10 Net sediment transport in kilotons per cyclic period at Katakhal.

Cyclic period	2050	2100	2100 + 50%Q	2100 + 100%Q
Year 1	138.3	248.7	238.5	227.9
Year 2	144.7	225.2	212.8	200.4
Year 3	135.9	154.0	187.5	174.5
Year 4	118.4	174.2	162.9	146.6
Year 5	99.7	148.4	139.2	124.5
Year 6	80.6	124.3	115.6	106.1

Table 5-11 Net sediment transport in kilotons per cyclic period at Kanaishisa.

Cyclic period	2050	2100	2100 + 50%Q	2100 + 100%Q
Year 1	80.3	155.4	142.6	129.5
Year 2	78.9	129.3	116.5	105.4
Year 3	61.4	98.1	88.2	78.8
Year 4	44.8	76.6	68.9	53.7
Year 5	33.2	56.1	51.2	44.4
Year 6	22.7	39.2	36.0	34.2

5.4.4 Siltation of the Hari River

The scenario models are introducing the years 2050 and 2100 conditions as a sudden discontinuous abrupt change that moves the system further away from a quasi-steady equilibrium. To compensate for this and bring the system closer to a quasi-steady equilibrium the models are run as cyclic morphological events representing a period of almost 6 years. The modelling of the present conditions indicates that the system in general is transient rather than in a quasi-steady equilibrium due to the siltation tendency caused by the tidal asymmetry. The gradual and accelerated siltation of the river branch caused by the tidal asymmetry and the transfer to 2050 and 2100 conditions can be illustrated by hypsometric curves as presented in the diagrams shown in Figure 5-17 to Figure 5-19. The diagrams show the area inside the Hari River branch below a certain bed level for the initial bathymetry in 2019, 2050, and 2100, and after each of the six following morphological cycles. The diagrams clearly show the gradual buildup of the bed caused by the upstream directed net sediment transport induced by tidal asymmetry and modest runoff. For the 2050 and 2100 conditions, it is seen that the bed levels at the riverbanks are elevated compared to the 2019 conditions. Furthermore, it is seen that the area under the hypsometric curves increases for the 2050 scenario and even more for the 2100 scenario due to the increased net sediment transport.

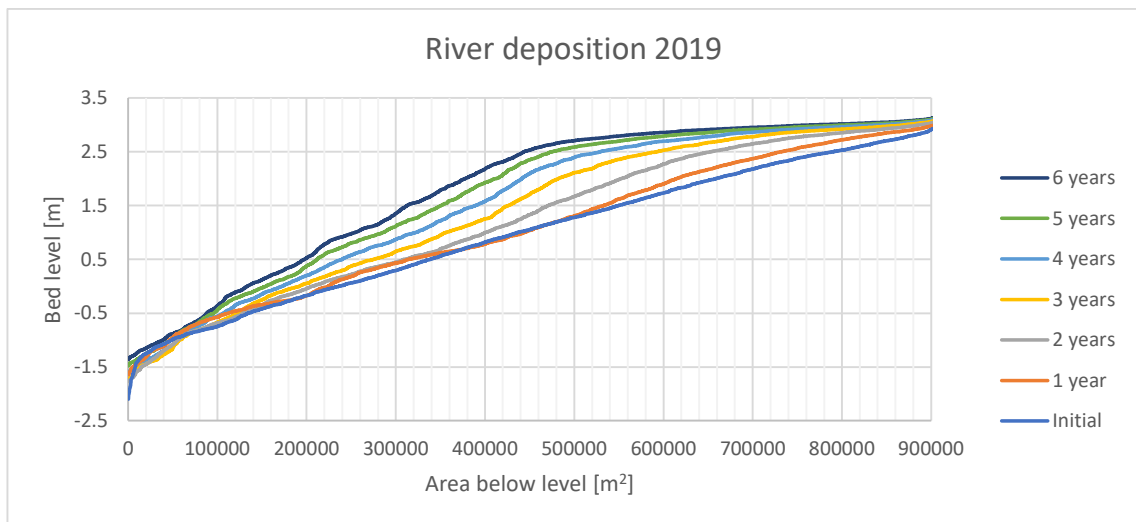


Figure 5-17 Area inside Hari River branch below a certain bed level without TRM operation over a period of 6 years for present conditions (2019).

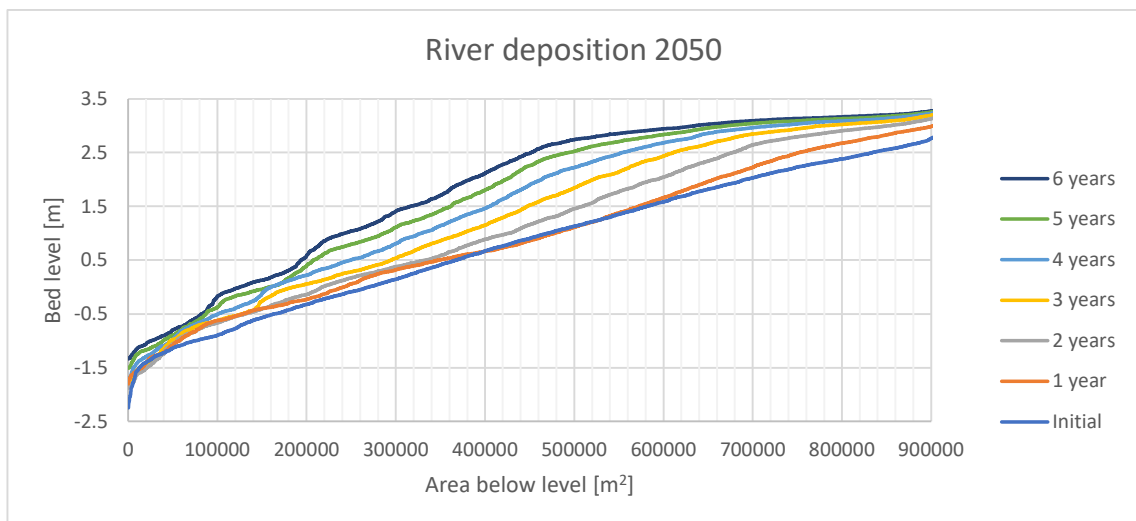


Figure 5-18 Area inside Hari River branch below a certain bed level without TRM operation over a period of 6 years for future conditions (2050).

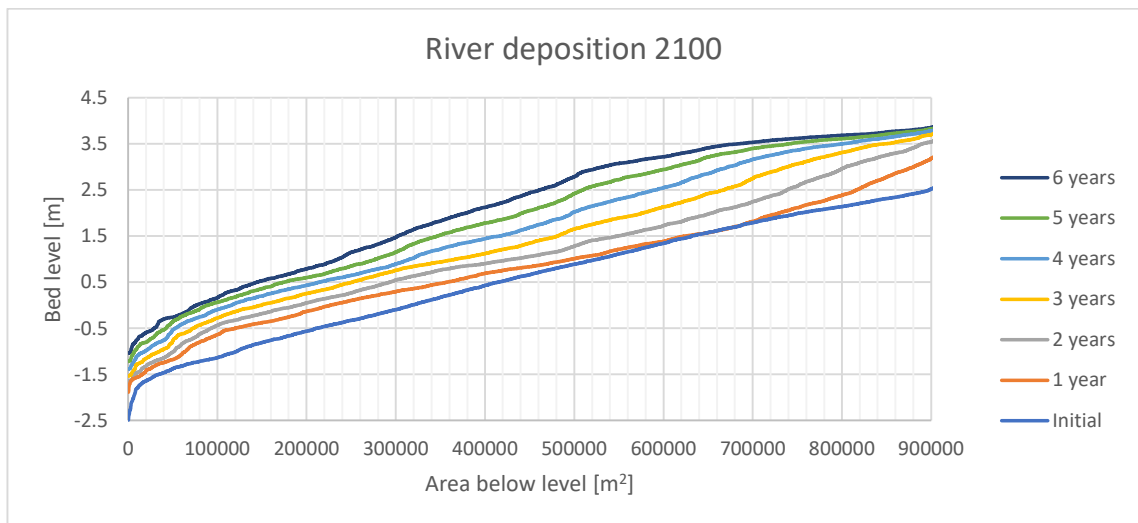


Figure 5-19 Area inside Hari River branch below a certain bed level without TRM operation over a period of 6 years for future conditions (2100).

Figure 5-20 and Figure 5-21 shows the hypsometric curves for Scenario 3 and 4 where the runoff from upstream is increased by 50% and 100%. The increased runoff has a dampening effect on the upstream directed net sediment transport. The area under the hypsometric curves is therefore less than what is obtained for Scenario 2, which is run assuming an unaffected runoff compared to present conditions.

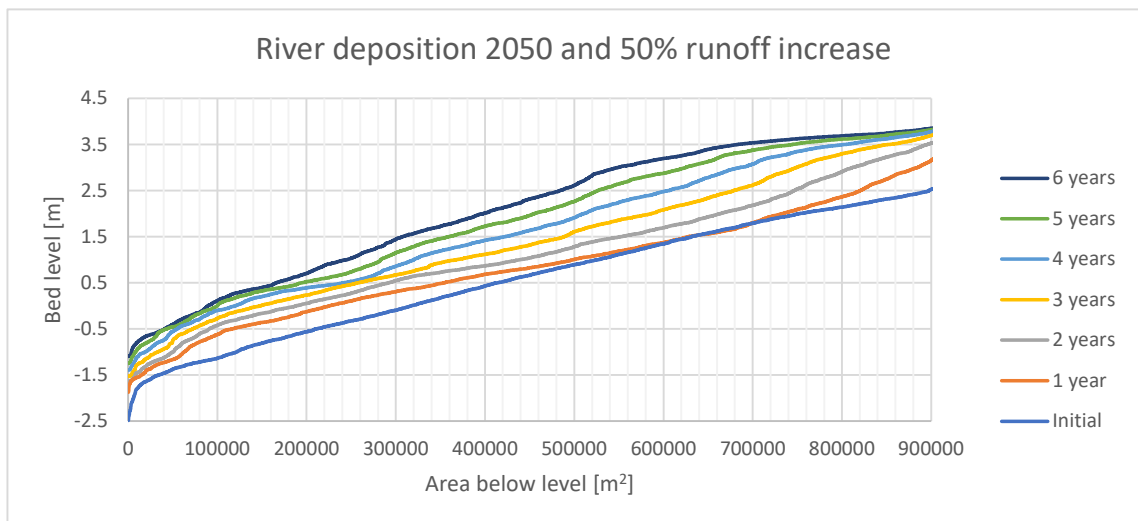


Figure 5-20 Area inside Hari River branch below a certain bed level without TRM operation over a period of 6 years for future conditions in 2100 with 50% increase of runoff.

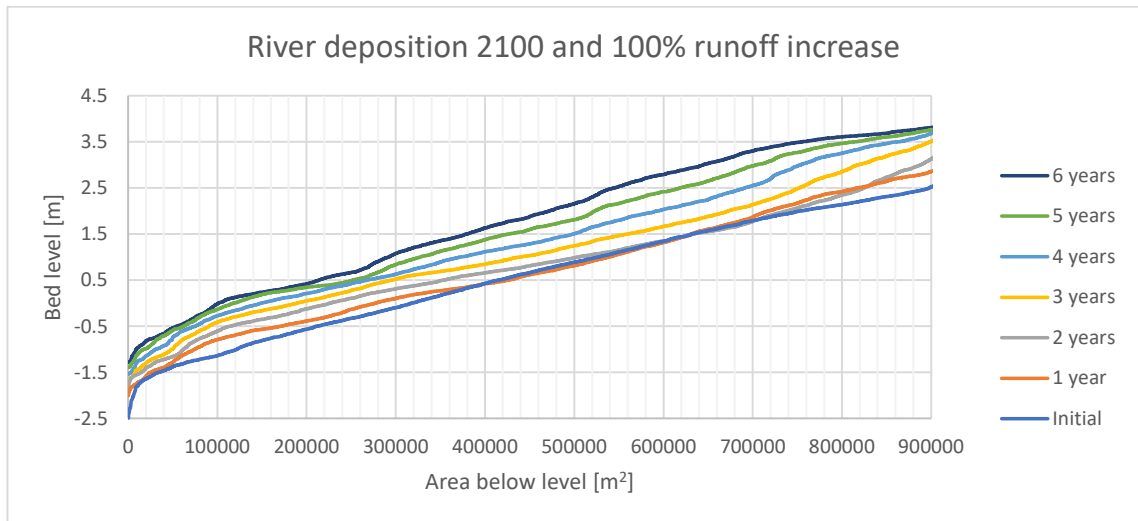


Figure 5-21 Area inside Hari River branch below a certain bed level without TRM operation over a period of 6 years for future conditions in 2100 with 100% increase of runoff.

Figure 5-22 shows the initial bathymetry of the Hari River branch in 2019, 2050 and 2050, and the morphological development of bed levels after six years (cycles) for each of the four modelled scenarios. The siltation of the river branch can be seen from the gradual downstream migration of the blue colour representing the highest bed levels. The presented bed levels are referring to m PWD.

Figure 5-23 shows the bed level changes after the six morphological cycles for each of the four modelled scenarios. The blue colours represent areas with deposition, while the red and yellow areas represent erosion. The plots show the general tendency of siltation in the entire system. Only in the riverbend south of Polder 24 is indicating erosion. The reason for this is most likely that the surveyed cross sections applied for the generation of the initial bathymetry are distributed with a too far distance to resolve the riverbend properly.

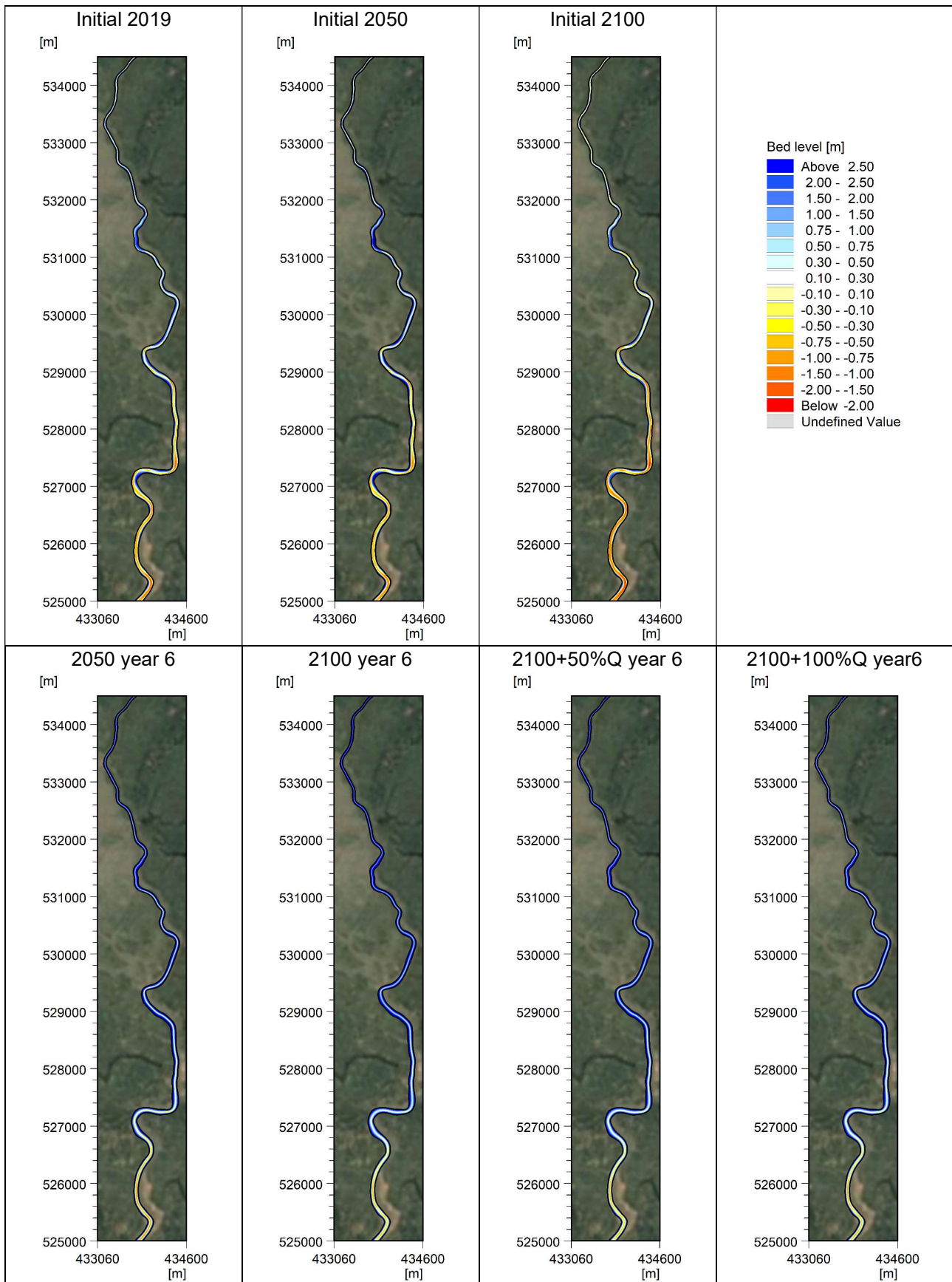


Figure 5-22 Future bed level development of Hari River.

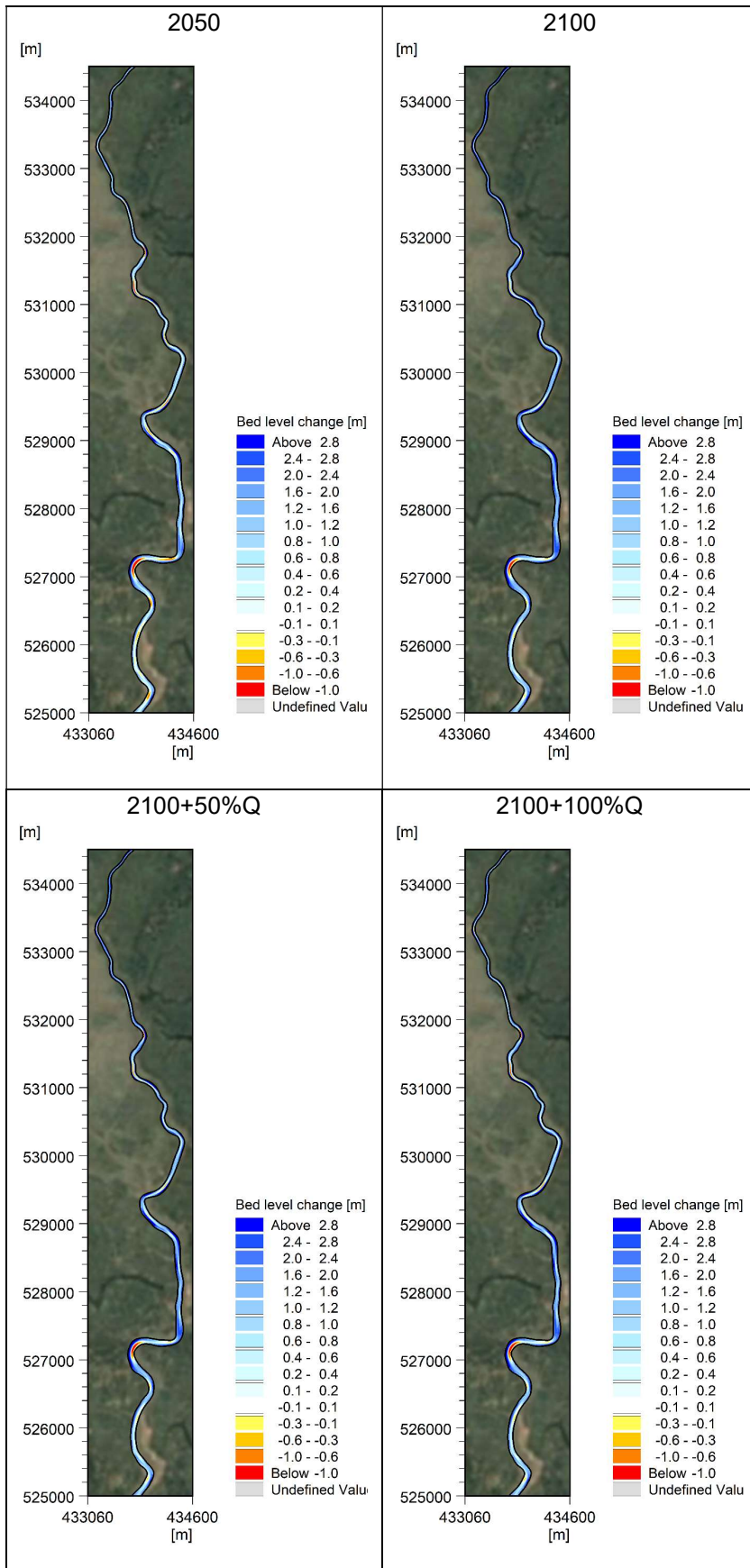


Figure 5-23 Future bed level development of Hari River. Predicted bed level changes after 6 years.

5.4.5 Drainage congestion and water logging

The combination of subsidence and sea level rise affects the ability to drain the polders and increases the risk for drainage congestion and water logging. Figure 5-24 shows the temporal development of the polder bathymetry in 2050 and 2100 due to subsidence and assuming no sediment exchange with Hari River and the polder.

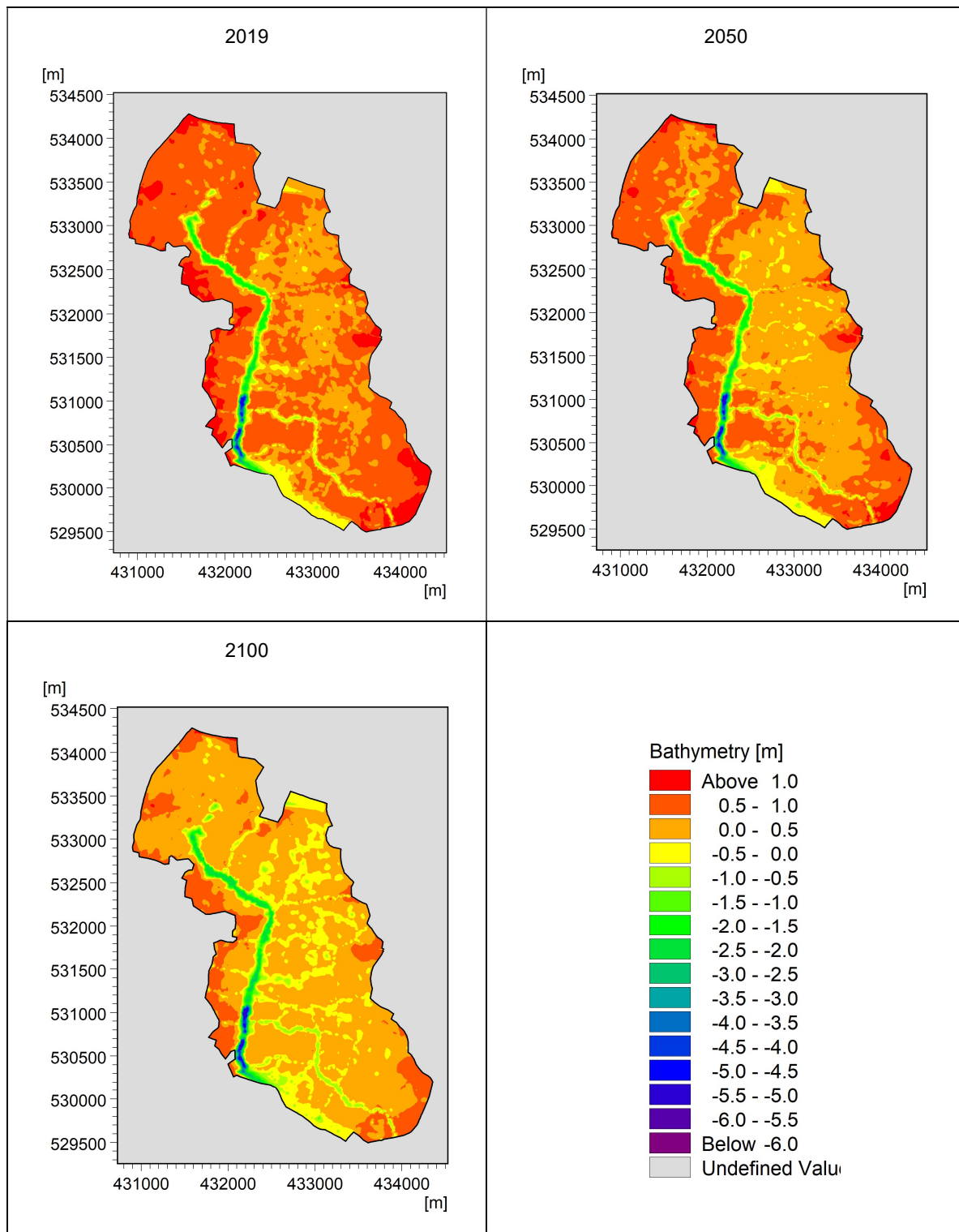


Figure 5-24 2019, 2050 and 2100 polder bathymetry.

The gradual lowering of the topography and increase of water level in the Hari River implies that the contained water volume inside the polder increases with time unless 1) drainage improvement measures are implemented, 2) the topography inside the polder is elevated using TRM, 3) dredged material from the Hari River is distributed to selected areas inside the polder or 4) to lower the polder water levels using pumping. The polder drainage of precipitation can be optimized and controlled using different kind of regulators. This is treated separately and in more detail in the polder drainage models. However, the critical drainage of precipitation is taking place in the monsoon period, where the mean water level in general is increased and drainage efficiency is reduced. On top of this is the risk that climate change will increase precipitation and intensity.

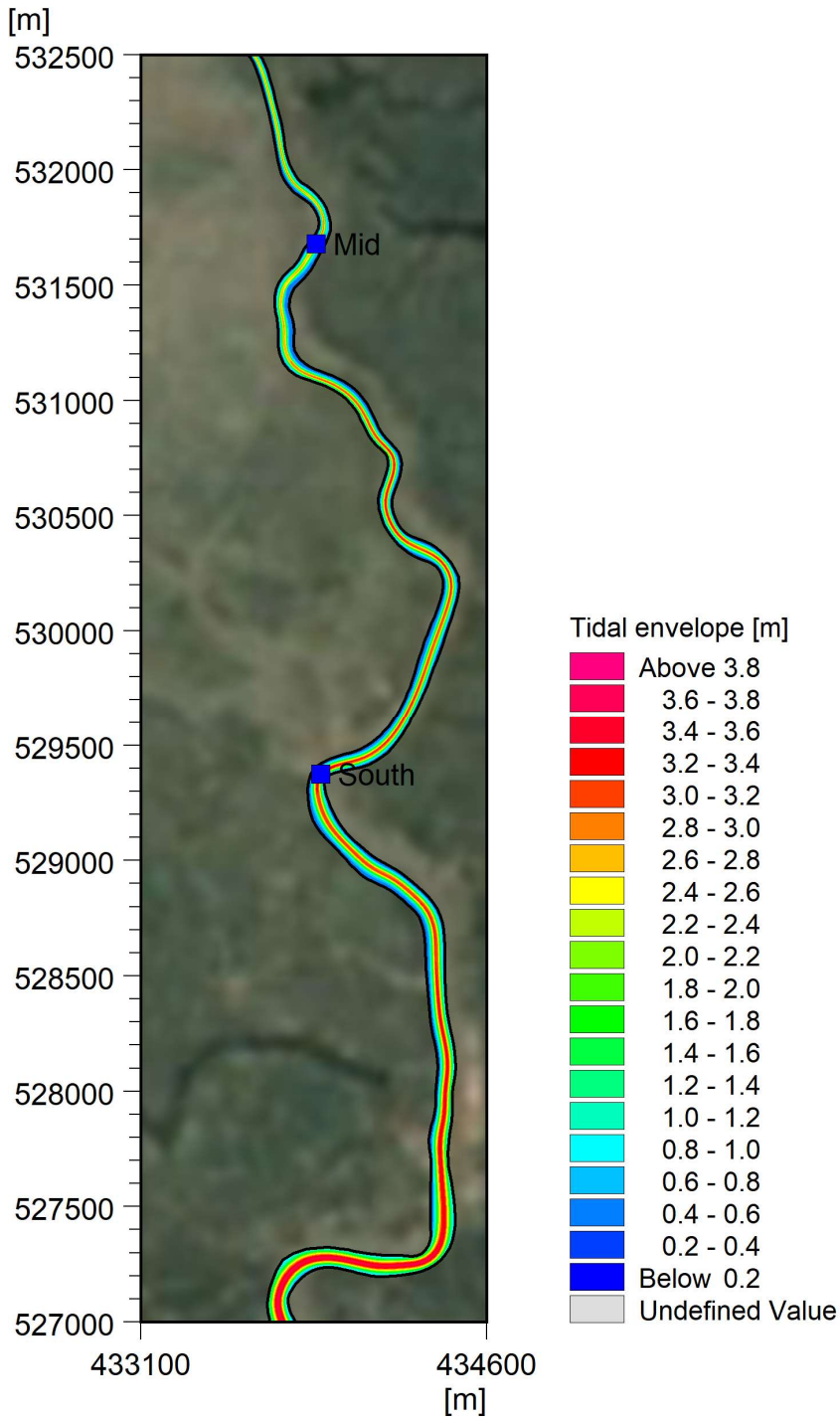


Figure 5-25 Water level extraction points used for calculation of drainage potential.

The drainage efficiency will depend on the drainage network inside the polder, the topography of the polder, the precipitation event, the design of the regulators and how they are operated, and the tidal water elevation in the peripheral river. Siltation in front of the regulators (riverside) may also affect the drainage efficiency. Inspection and maintenance dredging (if required) ahead of the monsoon is thereby important to ensure an optimal polder drainage efficiency.

The analyses applied here to investigate the increased risk for drainage congestion and water logging are built on some simplified assumptions only looking at the trends and changes in water levels in the Hari River and the topography of Polder 24. The ebb levels increase as one moves upstream implying that the drainage potential will be less in the northern part of the polder compared to the southern part. The tidal driven water level elevation at the two stations indicated on Figure 5-25 is shown in Figure 5-26 for the six morphological cycles and 2050 conditions. A similar plot is shown in Figure 5-27 for the 2100 conditions. It is clear from the time series at the Hari River mid extraction point that the 2050 bathymetry contain some artificially obstacles, which is being eroded in the first cycles and thereby results in a lowering of the modelled ebb tides in the following cycles.

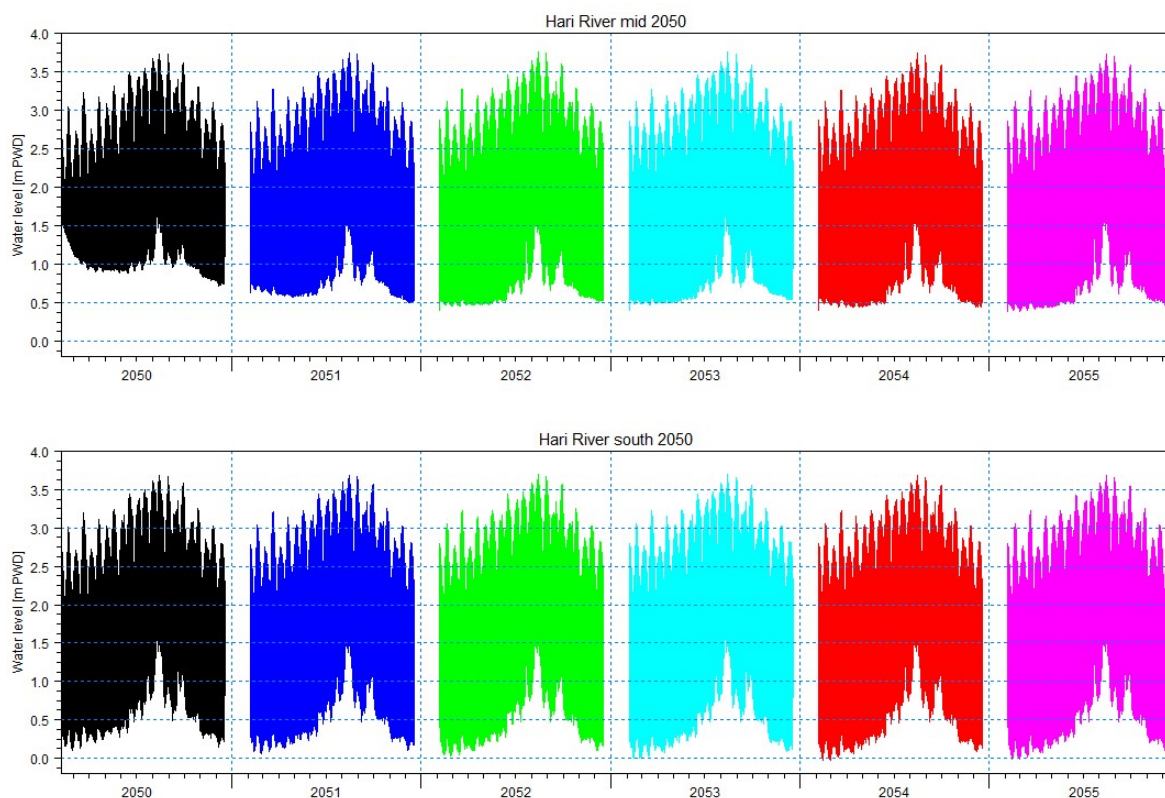


Figure 5-26 Tidal variation in Hari River 2050 at extraction point mid and south.

Statistical parameters (mean value and standard deviation) are calculated for the tide elevation for each morphological cycle representing a year. The numbers are presented in Table 5-12 for extraction point south and in Table 5-13 for extraction point mid. A similar analysis is carried out for the monsoon period (August). The findings of this analysis are shown in Table 5-14 and Table 5-15. It is seen that the mean level during the monsoon period is increased by more than 0.5m compared to the annual mean. Likewise, the standard deviation is lowered by approximately 0.1 m indicating that the tidal dynamics are weakened during the monsoon period with increased runoff.

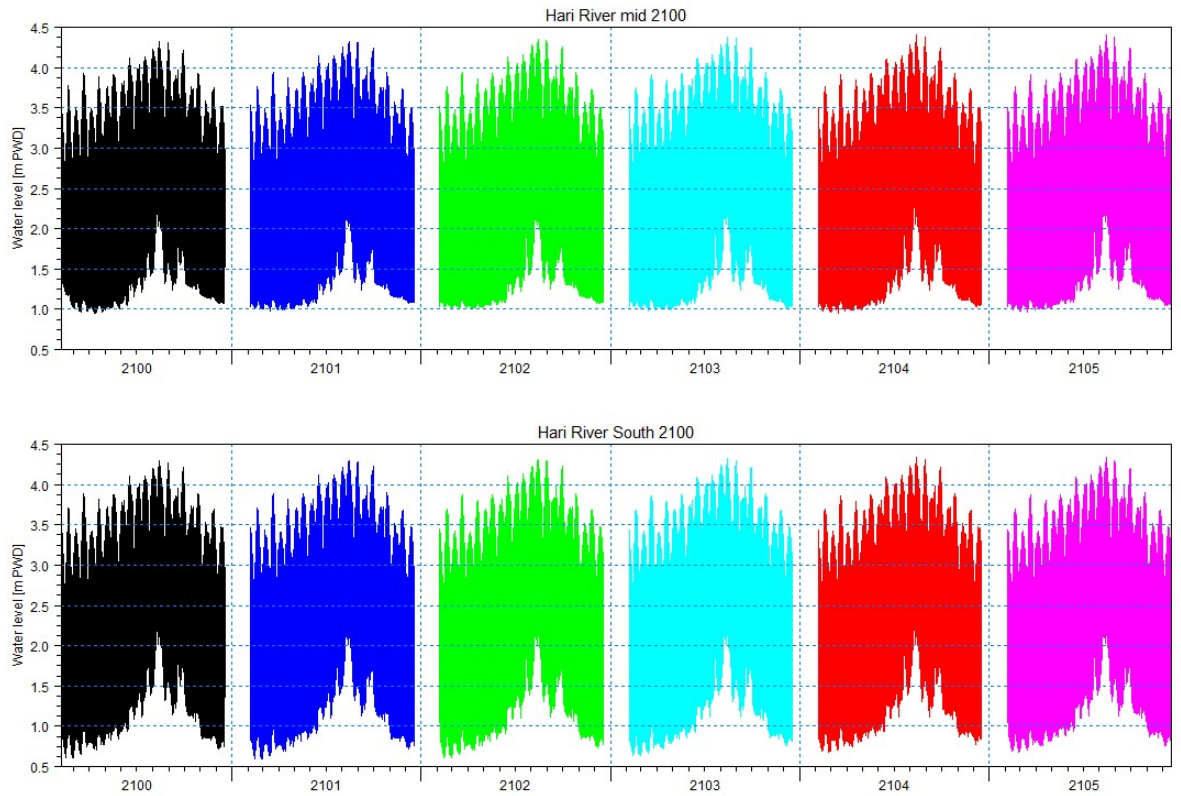


Figure 5-27 Tidal variation in Hari River 2100 at extraction point mid and south.

Table 5-12 Statistical parameters for the annual tide at extraction point south.

Morphological cycle	Annual mean 2019	Annual mean 2050	Annual mean 2100	Standard deviation 2019	Standard deviation 2050	Standard deviation 2100
1	1.49	1.65	2.27	0.80	0.84	0.87
2	1.45	1.63	2.26	0.84	0.86	0.88
3	1.44	1.63	2.26	0.86	0.87	0.88
4	1.44	1.63	2.30	0.87	0.87	0.88
5	1.44	1.63	2.30	0.87	0.87	0.87
6	1.44	1.63	2.31	0.86	0.87	0.87

Table 5-13 Statistical parameters for the annual tide at extraction point mid.

Morphological cycle	Annual mean 2019	Annual mean 2050	Annual mean 2100	Standard deviation 2019	Standard deviation 2050	Standard deviation 2100
1	1.73	1.80	2.31	0.59	0.69	0.83
2	1.58	1.71	2.31	0.73	0.79	0.84
3	1.52	1.68	2.32	0.79	0.81	0.84
4	1.51	1.69	2.27	0.80	0.81	0.84
5	1.49	1.68	2.27	0.82	0.82	0.84
6	1.50	1.69	2.28	0.81	0.82	0.83

Table 5-14 Statistical parameters for the monsoon tide (August) at extraction point south.

Morphological cycle	Annual mean 2019	Annual mean 2050	Annual mean 2100	Standard deviation 2019	Standard deviation 2050	Standard deviation 2100
1	2.02	2.20	2.84	0.75	0.76	0.77
2	2.01	2.20	2.84	0.77	0.77	0.78
3	2.01	2.20	2.84	0.77	0.77	0.78
4	2.01	2.20	2.84	0.77	0.77	0.78
5	2.01	2.20	2.85	0.77	0.77	0.78
6	2.02	2.21	2.85	0.77	0.77	0.77

Table 5-15 Statistical parameters for the monsoon tide (August) at extraction point mid.

Morphological cycle	Annual mean 2019	Annual mean 2050	Annual mean 2100	Standard deviation 2019	Standard deviation 2050	Standard deviation 2100
1	2.11	2.24	2.84	0.67	0.72	0.78
2	2.06	2.22	2.84	0.73	0.76	0.78
3	2.04	2.22	2.85	0.75	0.77	0.78
4	2.04	2.23	2.86	0.76	0.76	0.77
5	2.05	2.23	2.86	0.76	0.77	0.77
6	2.05	2.24	2.87	0.76	0.77	0.77

The drainage of the polder is controlled by the internal drainage network in polders, the regulators, and the tidal variation in the peripheral rivers. The (minimum) drainage level in the polders is controlled by the minimum water level in the peripheral river. Therefore, a simplified indicator for the drainage level of the polder suitable for relative comparison between scenarios can be obtained as:

$$WL_{\text{Drainage level}} = WL_{\text{Mean}} - \sigma$$

Where the water levels and standard deviation are obtained as the average of the statistical parameters at the two extraction points mid and south. The water logging volume V_{wlv} inside the polder can then be calculated as:

$$V_{wlv} = \sum D_i (WL_{\text{Drainage level}}) A_i$$

Where D_i refers to the local water depth in the element covering the area A_i inside the polder.

The polder storage volume V_{psv} is defined with reference to mean water level as:

$$V_{psv} = \sum D_i (WL_{\text{Mean}}) A_i$$

And the potential drainage volume V_{pdv} as:

$$V_{pdv} = \sum (D_i (WL_{\text{Mean}} - D_i (WL_{\text{Drainage level}}))) A_i$$

The polder drainage potential is then defined as:

$$\theta = \frac{V_{pdv}}{V_{psv}}$$

The indicators above are not intended to provide exact numbers but can be used to evaluate the impact of sea level rise and subsidence on the drainage potential looking ahead to year 2050 and 2100.

The annual mean and drainage water level as calculated by the formulas are shown in Table 5-16 for the 2019, 2050, and 2100 conditions. It is seen that the numbers become relatively stable after the first to morphological cycles. Table 5-17 shows the same numbers, but for the monsoon period (August). It is seen that the numbers are significantly larger in the period with the most urgent need for drainage.

Table 5-16 Annual mean and drainage water level of the polder

Morphological cycle	Annual mean level 2019	Annual mean level 2050	Annual mean level 2100	Annual drainage level 2019	Annual drainage level 2050	Annual drainage level 2100
1	1.61	1.73	2.28	0.91	0.97	1.43
2	1.51	1.67	2.28	0.73	0.84	1.42
3	1.48	1.65	2.28	0.65	0.81	1.43
4	1.47	1.66	2.29	0.64	0.82	1.43
5	1.47	1.66	2.29	0.62	0.81	1.44
6	1.47	1.66	2.30	0.63	0.81	1.45

The numbers for Scenarios 3 and 4 are not shown but are quite similar to numbers for the year 2100 conditions without increased runoff.

Table 5-17 Monsoon mean and drainage level of the polder.

Morphological cycle	Annual mean level 2019	Annual mean level 2050	Annual mean level 2100	Annual drainage level 2019	Annual drainage level 2050	Annual drainage level 2100
1	2.06	2.22	2.84	1.35	1.48	2.07
2	2.03	2.21	2.84	1.29	1.44	2.07
3	2.02	2.21	2.85	1.26	1.44	2.07
4	2.03	2.21	2.85	1.26	1.45	2.07
5	2.03	2.22	2.86	1.26	1.45	2.08
6	2.03	2.22	2.86	1.27	1.46	2.09

The expected development in the polder water logging volume expressed as the annual average is shown in Figure 5-28 for the present conditions and the four investigated scenarios. It is seen that the water logging volume increases by more than a factor of five in the year 2100 scenarios compared to present conditions. The only way to reduce the water logging is to introduce pumping of water from polder to the peripheral river or elevate the bed levels using TRM for a period or distribute dredged sediment inside the polder.

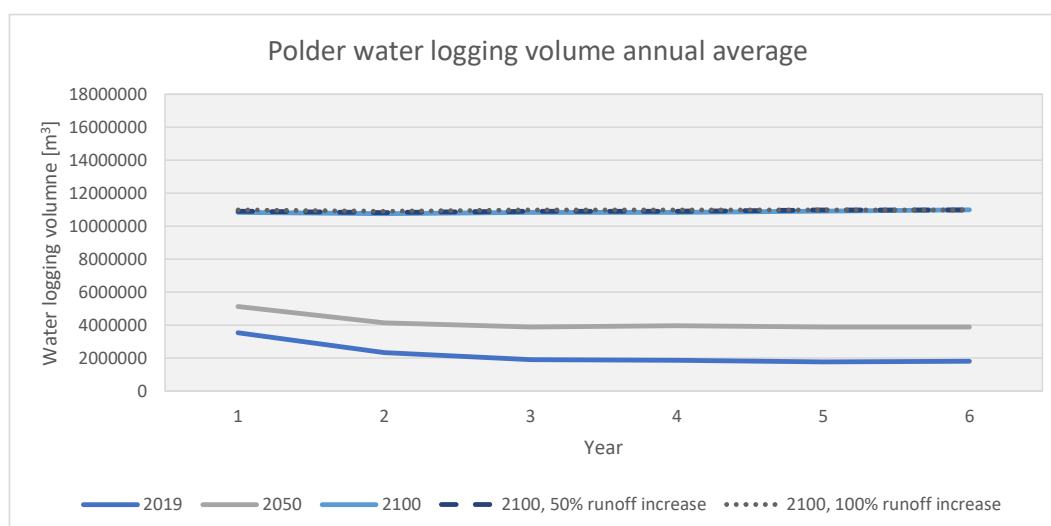


Figure 5-28 Polder water logging volume – annual average.

The polder drainage volume expressed as the annual average is shown in Figure 5-29 for the present conditions and each of the four investigated scenarios. The polder drainage volume is seen to slightly increase from nowadays conditions to the conditions in year 2050. The change from 2050 to 2100 is small indicating that the flooded area and standard deviation of the water level are almost the same.

Figure 5-30 shows the polder storage volume expressed as the annual average for the present conditions and scenarios. It is seen that the volume increases with the impact of subsidence and sea level rise.

The indicator, polder drainage potential, is defined as the ratio between the polder drainage volume and the polder storage volume. The polder drainage potential expressed as the annual average is

shown in Figure 5-31. It is seen that the drainage potential is significantly weakened due to the impact of polder subsidence and sea level rise affecting the mean water level in the peripheral rivers.

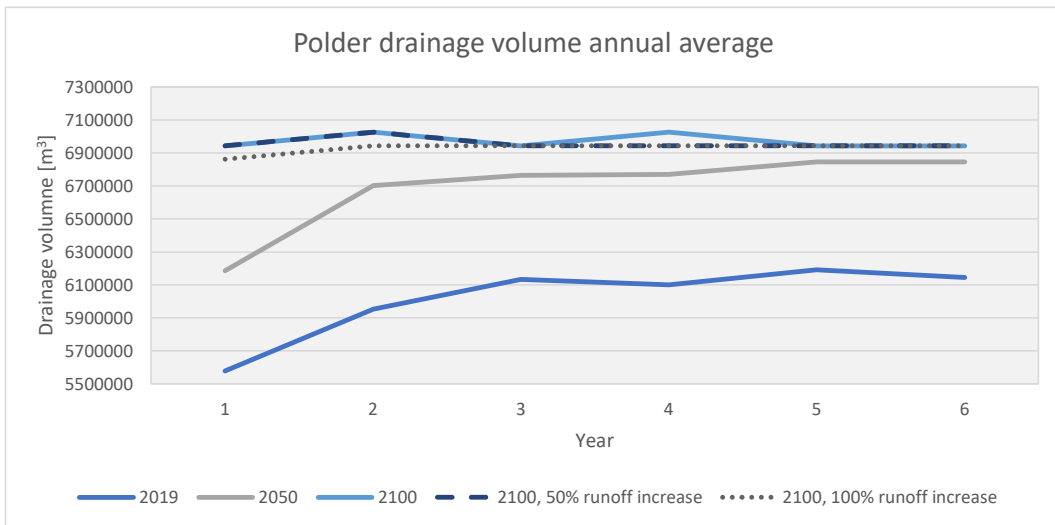


Figure 5-29 Potential polder drainage volume - annual average.

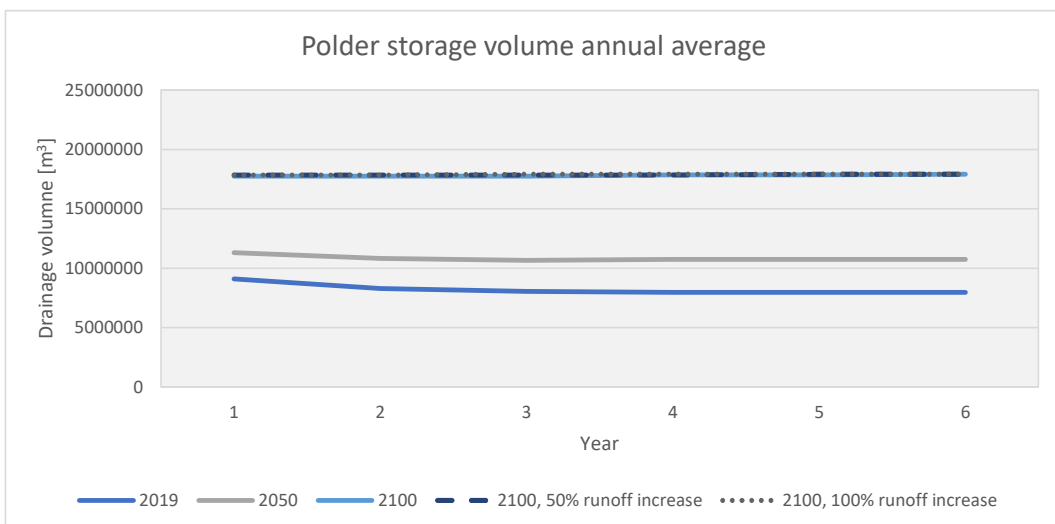


Figure 5-30 Potential polder storage volume – annual average.

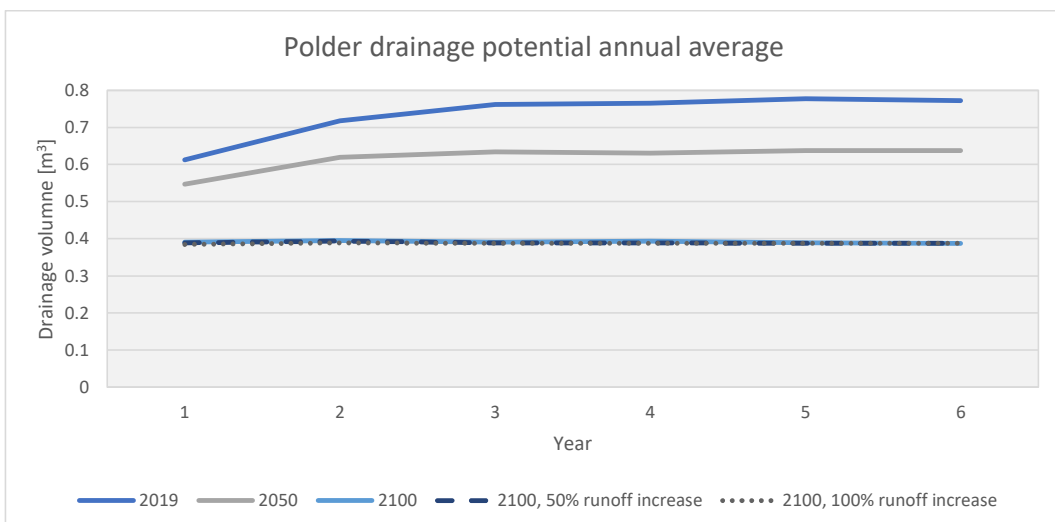


Figure 5-31 Polder drainage potential – annual average.

The critical conditions occur in the monsoon period and during severe rainfall events. The increased runoff increases the mean water level and dampens the tide in the peripheral river. Both phenomena that in combination with increased precipitation and rainfall intensity will make polder drainage more difficult.

The expected development in the polder water logging volume expressed as the monsoon average is presented in Figure 5-32 for the present conditions and the four investigated climate change scenarios. It is seen that the water logging volume increases by a factor slightly less than three in the year 2100 scenarios compared to present conditions. The only way to reduce the water logging is to introduce pumping of water from polder to the peripheral river or elevate the bed levels using TRM for a period or distribute dredged sediment inside the polder.

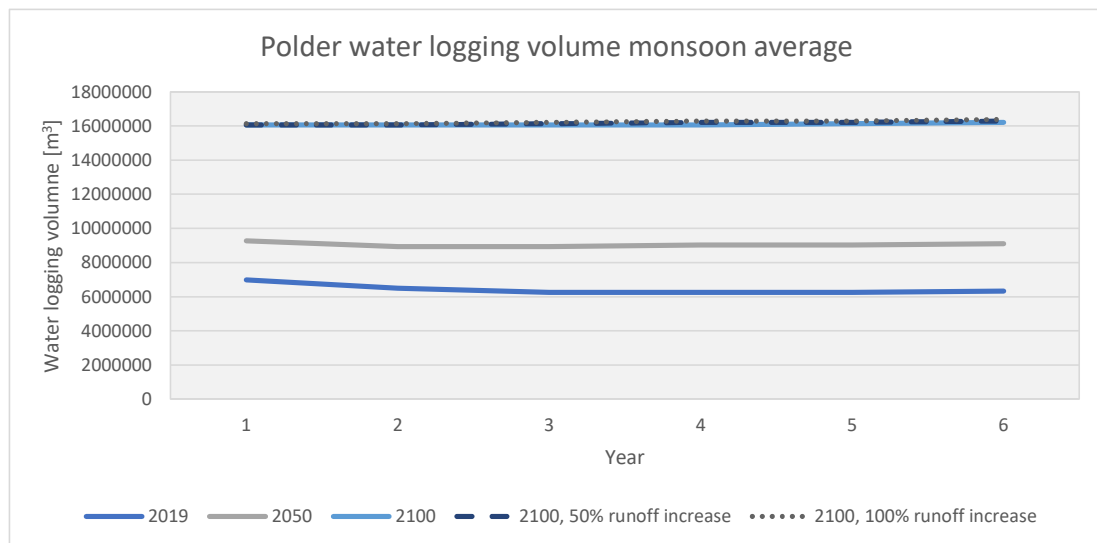


Figure 5-32 Polder water logging volume – monsoon average (August)

The polder drainage volume expressed as the monsoon average is shown in Figure 5-33 for the present conditions and each of the four investigated scenarios. The polder drainage volume is seen to slightly smaller than what is obtained for the annual average, due to the weakening of the tide.

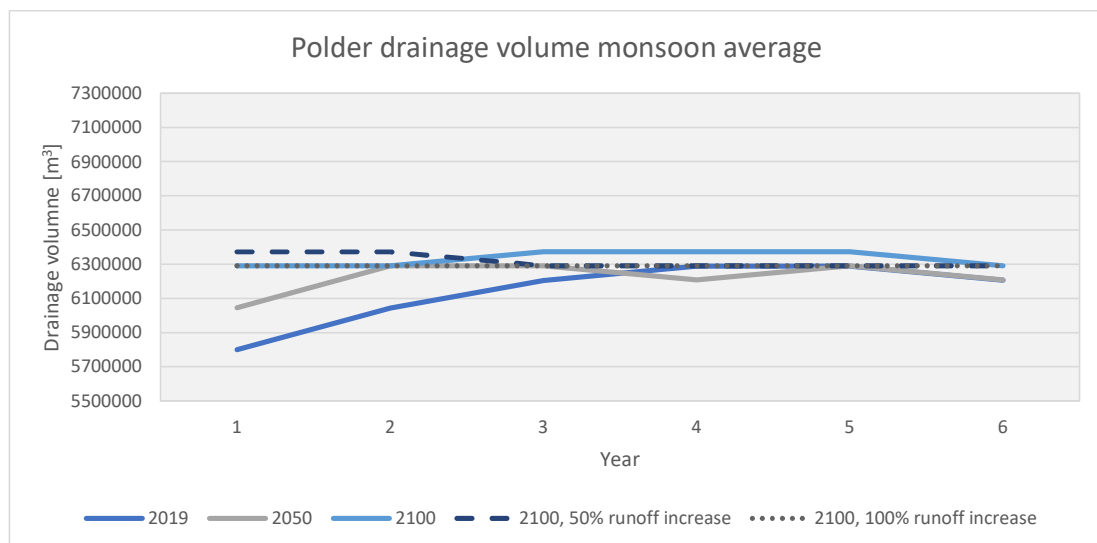


Figure 5-33 Potential polder drainage volume – monsoon average (August).

Figure 5-34 shows the polder storage volume expressed as the monsoon average for the present conditions and scenarios. It is seen that the volume is greater than the annual average and increases with the impact of subsidence and sea level rise.

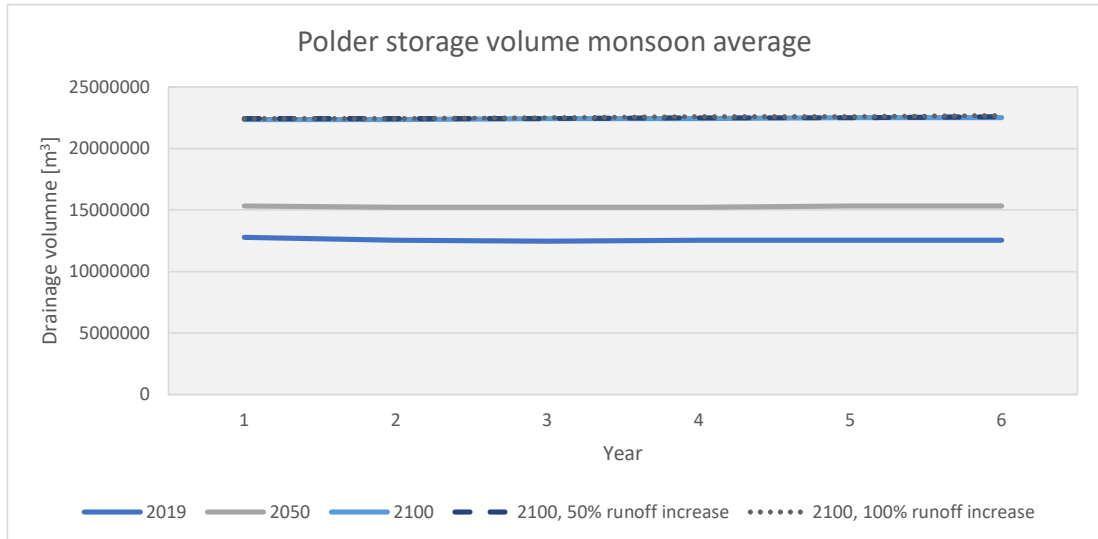


Figure 5-34 Potential polder storage volume – monsoon average (August).

The polder drainage potential expressed as the monsoon average is shown in Figure 5-35. It is seen that the drainage potential is significantly weakened due to the impact of polder subsidence and sea level rise affecting the mean water level in the peripheral rivers.

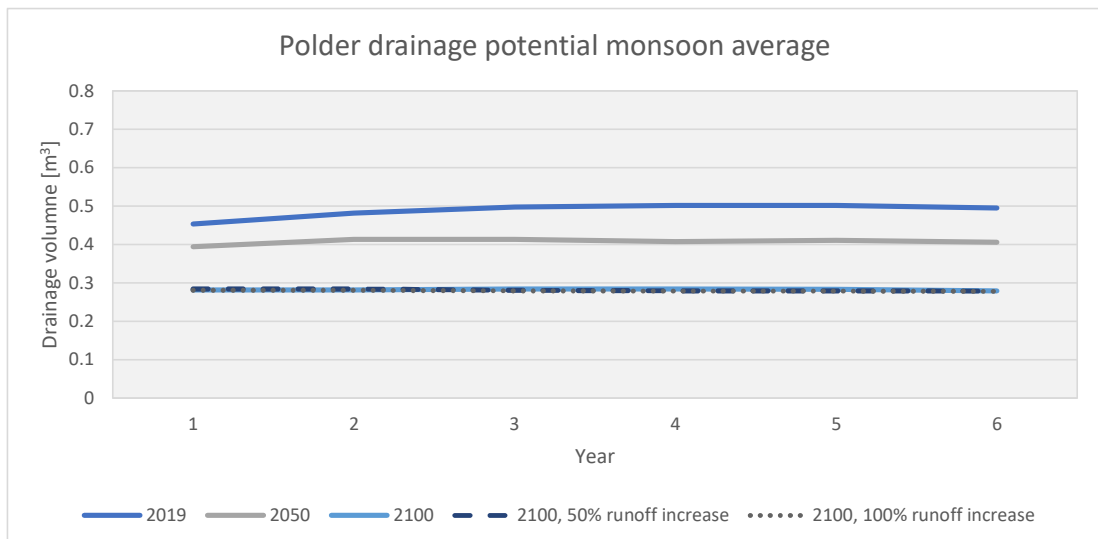


Figure 5-35 Polder drainage potential – monsoon average (August).

The above analyses show that Polder 24 will be severely threatened in the future due to polder subsidence and sea level rise. The polder area is lowlying and very exposed even with nowadays conditions.

6 Conclusions, discussions, and recommendations

6.1 Conclusions and discussions

TRM has for many years been considered a viable way to maintain the drainage capacity of the peripheral rivers and for compensating the impact of subsidence by increasing land level inside the polders through deposition of silt. The key problem with TRM is that the area inside the polders, which are subjected to tidal flooding cannot be used for the intended purpose of the polders (viz. agriculture) while TRM is ongoing hence the population of the polders must be paid compensation and alternative livelihood created. An issue with TRM operation is also that deposition inside the polders is highly non-uniform. There is thus much to win if TRM operation can be optimised, i.e. accelerate erosion in the peripheral rivers, accelerated deposition within the polders and by ensuring a more uniform deposition pattern. The objective of TRM modelling is to establish a modelling approach that can be used to test alternative TRM operations and help identifying the most effective operations.

The purpose of modelling presented in the first interim report was to explore what will be required in terms of modelling to optimise TRM operation and is based on the application of a very simple 1D modelling approach and a state-of-the art 2D modelling approach. The models simulate the hydrodynamics and advection-dispersion of suspended sediment represented by one (representative) size fraction only. Erosion and deposition are as sources and sinks in the advection-dispersion model and calculated as simple/standard functions of the cross-sectional average bed shear stress (1D) and spatially resolved in the 2D approach (thus a standard cohesive sediment modelling approach).

The TRM operation implemented for East Beel Khuksia has been used as pilot case because this is the best described and most successful TRM operation. Furthermore, it contains accessible information and data. The Beel and River system of the area is shown in Figure 1.4. Tidal River Management had been adopted since 1998 in the north-west part of the Khulna Jessore Drainage Rehabilitation Project to solve drainage congestion. Beel Bhaina and Beel Kedaria (see Figure 1.4 for location of these polders) were subjected to tidal flooding and created sufficient tidal volume to maintain the drainage capacity of Tekka and Hari Rivers. During the dry season of 2005 TRM operation of Beel Kedaria ceased and the Hari river was rapidly silting up. A rough estimate suggested that 800,000 tons of silt was deposited during a period of three months.

In response to the lost drainage capacity of the Hari River TRM operation was initiated at the East Beel Khuksia on 30 November 2006. Ahead of the opening of the TRM basin about $0.8 \times 10^6 \text{ m}^3$ was dredged from the peripheral Hari River along a reach of approximately 8 km to amplify the tide. Before the opening of the TRM basin the tidal volume of the Hari River was about $0.9 \times 10^6 \text{ m}^3$ but increased to $1.95 \times 10^6 \text{ m}^3$ after two months of operation and $5.3 \times 10^6 \text{ m}^3$ after 5.5 months. A major part of the tidal volume increase was caused by flushing of the peripheral rivers that at Rania was deepened by more than 2 meters. A minor part of the tidal volume increase is related to seasonal variations of the tide, which typical has the largest range in the months of March and April. Significant erosion took place in the peripheral rivers and an estimated 1.2 mill tons of silt was deposited within the polder.

1D model

A curtailed version of the SWRM was used in this study for the 1D modelling and to provide boundary conditions for the 2D model. The MIKE 11 model was used for simulation of the siltation after TRM operation of Beel Kedaria ceased and for the erosion of peripheral rivers and siltation within Beel Khuksia when TRM operation commenced. Both of these events took place during the dry season. No model boundary conditions were available for the period 2005 through 2007. Instead, a period from January to April 2011 was used. Despite of this, the agreement between model and observations were surprisingly good. Water level variations during spring tide compared well with the observed variation. During neap tide the simulated low waters became lower. This behaviour was not found in the observations, suggesting that bed elevations in the model was too low. The application of a morphological model (with update of bed elevations due to erosion and deposition) would probably improve this.

Simulated and observed sediment concentrations compared remarkably well in the Hari River when the tidal range is well predicted by the HD model (1D). The (calibrated) sediment parameter values used are all quite similar to those used in other model studies in Bangladesh and elsewhere. Inside the polder the agreement is less. Here it also seems that the measurements are less accurate. In the model the concentration during ebb flow is zero (suggesting that all sediment entering the East Beel Khuksia will deposit). Sediment and water will enter the polder via the drainage canals and deposition first take place when the water spills into the polder. This discrepancy thus suggests that a 2D description is required to correctly represent the conditions within the polders. Another contributing explanation could be that part of the finer sediment fractions will remain in suspension inside the polder because of the low settling velocity, whereas the observed concentration may be larger than zero. A multi-fraction approach may render better agreement with the observations. 2D modelling of the East Beel Khuksia would also improve the model performance.

The simulation shows a strong asymmetry (between flood and ebb flow) in sediment transport leading to a significant net transport of some 400,000 tons into the Hari River. This should be compared with the net accumulation of 800,000 tons estimated from observed cross-sections for a similar period.

Simulation of TRM operation of the East Beel Khuksia shows that about 200,000 tons of sediment erodes from the riverbed and some 400,000 tons of sediment enters the Hari River from downstream. The sediment eroded from the riverbed plus the net sediment transport into Hari River ends up in the East Beel Khuksia, where thus close to 600,000 tons deposit. For a period of four months, we have calculated the deposited volume to 1.2 mill tons (an uncertain estimate, see Section 2.3), thus the model predicts the right order of magnitude.

2D-model present conditions

A conceptual state-of-the-art 2D model was developed to simulate the gradual siltation of Hari River caused by the tidal asymmetry and modest runoff from the catchment, which thereby creates a net upstream directed sediment transport. Even though the applied HD boundary was based on a channel bathymetry from a different period (2015) the model was able to simulate a gradual siltation of the branch. The siltation time scales depend strongly on the sediment concentration specified as boundary condition on the downstream boundary, but that makes it on the other hand easy to adjust the siltation rates if/when calibration/validation data becomes available. For the modelling a constant sediment concentration was applied. In a detailed study it would be possible to refine the boundary condition introducing a neap-spring variation and/or a seasonal variation. However, this does not make much sense to do so with the present data basis.

The Hari River model was extended to include the East Beel Khuksia located inside Polder 24 and openings at the southern end and at the eastern side. Openings that have been used for the TRM operation of the beel. The Hari River bathymetry was established from measured cross sections in 2015 and do thereby not represent the branch at the time when TRM was initiated. The modelling carried out is thereby only conceptual but represents a morphological time scale of almost 6 years.

Two TRM scenarios were investigated. One with an opening in the southern end of the polder and one with an opening in the eastern end of the polder. The modelling with a southern opening revealed a strong potential for TRM, while the modelling with an eastern opening showed less potential. In both cases the TRM had a significant improving impact on flushing the part of the peripheral river located downstream the polder opening. The concept is thereby found feasible for this purpose.

With regard of the purpose of siltation and increase of bed levels inside the polder number of lessons was learned. Placing the polder opening as far as downstream as possible compared to the beel will ensure the largest tidal discharge and largest tidal envelope. This is important ensure a strong interaction with the beel. By placing the entrance channel, so that it becomes connected with the old channel network from before the polder was established, it can be better ensured that the siltation will takes in a larger part of the beel. The TRM system with an opening in the south contains a network with several side channels which stimulate a more evenly distribution of the imported sediment. This was not the case for the TRM system with an opening in the eastern side of the beel. This system had mainly a main channel along which the sediment deposited. The eastern opening was located in an

area of the polder with a relatively high bed level and no presence of an existing channel network, i.e. incoming water had to erode its own channel. This is not optimal with regard of getting a more uniform distribution of the imported sediment inside the polder and a large tidal prism. A better TRM efficiency can thereby be achieved by pre-dredging an internal channel inside the polder that ensures good connectivity with the existing channel network inside the polder.

2D-model future conditions

The Hari River model was updated to represent future conditions in 2050 and 2100 assuming the sea level rise to follow the trends of the RCP8.5 using the 95th percentile for the water level increase. Likewise, the subsidence rate for the area was applied to estimate the future lowering of the bathymetry. The abrupt jump forward in time implies that the initial system responds with increased sedimentation, due the increase in water depths and tidal discharge. To account for this and reach the new quasi-steady equilibrium the models is run for six morphological cycles corresponding to almost six years. The time scale for adaption of the future conditions is a time scale of years, while the time scale of climate changes is of a time scale of decades, i.e. the time scale for adaptation is smaller than the time scale for climate changes. The modelling carried out therefore indicate that the system will be able to gradually adapt to the impact of climate changes.

The future drainage efficiency will depend on the drainage network inside the polder, the topography of the polder, the intensity of the most severe precipitation event taking place during the monsoon period, the design of the regulators and how they are operated, and the tidal water elevation in the peripheral river. Siltation in front of the regulators (riverside) may also affect the drainage efficiency. Inspection and maintenance dredging (if required) ahead of the monsoon is thereby important to ensure an optimal polder drainage efficiency.

The combination of sea level rise and land subsidence will over time increase the risk for water logging inside the polders. Indicators for the polder drainage level, water logging volume, potential drainage volume were defined to evaluate the impact of sea level rise and subsidence on the drainage potential looking ahead to year 2050 and 2100. The indicators were established from statistical parameters of the tide during the monsoon, where runoff and tidal elevations are increased. The intention of the established indicators is not to provide exact numbers, but rather to document the potential severe impact of sea level rise and subsidence.

The above analyses show that Polder 24 will be severely threathned in the future due to polder subsidence and sea level rise. The polder area is lowlying and very exposed even with nowadays conditions. The gradual lowering of the topography inside the polder and increase of water level in the peripheral Hari River implies that the contained water volume inside the polder increases with time unless 1) drainage improvement measures are implemented, 2) the topography inside the polder is elevated using TRM, 3) dredged material from the Hari River is distributed to selected areas inside the polder to prevent inundation or 4) to lower the polder water levels using pumping. The polder drainage of precipitation can be optimized and controlled using different kind of regulators. This is treated separately and in more detail in the polder drainage models. However, the critical drainage of precipitation is taking place in the monsoon period, where the mean water level in general is increased and drainage efficiency is reduced. On top of this is the risk that climate change will increase precipitation and intensity, and thereby require drainage of an increased rainfall volume.

6.2 Recommendations

Before activating the TRM operation in November 2006 about $0.8 \times 10^6 \text{ m}^3$ was dredged from the peripheral Hari River along a reach of approximately 8 km to amplify the tide. Dredging was not required to achieve a significant exchange with the beel in the simulations. The main reason for this is most likely that the Hari River branch in the model is deeper along the reach from the eastern polder opening and down to the old polder opening at Beel Bhaina. It would have been interesting to use the morphological model for the Hari River to establish a branch, which represent a system with an initial river bathymetry that better corresponds to the conditions back in November 2006 before activating

TRM. Another option could be to test a model based on two sediment fractions. This is however a quite complex task because the sediment entering the polder is eroded from the riverbed. To do so one will need to know how the composition of the two fractions is distributed.

7 References

- /1/ IWM, March 2006: Monitoring the performance of Beel Kedaria TRM and baseline study for Beel Khuksia. Khulna Jessore Drainage Rehabilitation Project. Final Report.
- /2/ IWM, July 2007: Monitoring the Effect of East Beel Khuksia TRM Basin and Dredging of Hari River for Drainage Improvement of Bhabodah Area. Khulna Jessore Drainage Rehabilitation Project. Final Report.